

International Journal of Machine Tools and Manufacture

Energy field assisted metal forming: current status, challenges and prospects

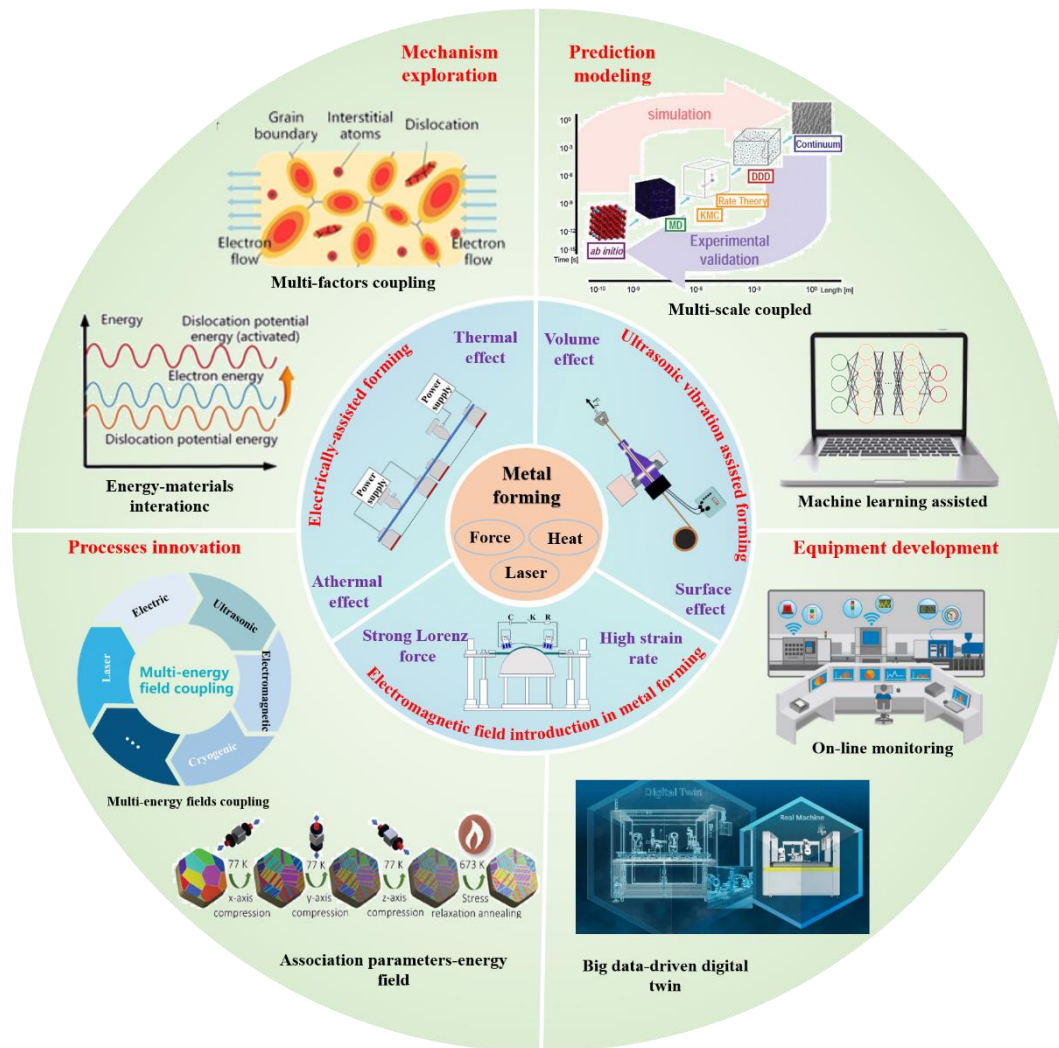
--Manuscript Draft--

| | |
|------------------------------|--|
| Manuscript Number: | IJMACTOOL-D-23-00384R1 |
| Article Type: | Review Article |
| Keywords: | Energy-assisted metal forming; Electrically-assisted forming; Ultrasonic vibration assisted forming; Electromagnetic field supported forming; Microstructure evolution; Process modelling and simulation. |
| Corresponding Author: | Ming Wang Fu, PhD The Hong Kong Polytechnic University HONG KONG |
| First Author: | Ming Wang Fu, PhD |
| Order of Authors: | Ming Wang Fu, PhD Heng li LF Peng B Meng ZT Xu L.L. Wang G. Ngaile |
| Abstract: | <p>To meet the various and critical manufacturing requirements including high precision, low cost, good manufacturability, and more demanding from product service and performance aspects such as high performance, light-weight, less energy consumption and low carbon emissions in today's era of rapid product development with short product life circle, it is crucial to re-innovate and re-invigorate metal forming technologies and enable it to play an even more important role in manufacturing arena. Historically, introducing new kinds of energy fields into the forming process drives the innovative advance and rejuvenating of forming technologies due to the physically interactive mechanisms of energy field and certain material deformation behaviors such as thermal-mechanical coupling effects. In this paper, a classification of energy-aided metal forming processes is orchestrated and presented, and three kinds of energy-assisted metal forming technologies, viz., electrically-assisted forming, ultrasonic vibration assisted forming, and electromagnetic field supported forming, are reviewed and delineated as they are currently receiving a widespread attention with promising application potentials. In this paper, the physical essence and the effects of these introduced energy fields on deformation behavior, process performance, microstructure evolution are elucidated and analyzed. The constitutive modeling of these forming processes is recapitulated, and the newly established energy field assisted metal forming technologies are exemplified and discussed. Based on the advantages and limitations of these unique metal forming processes assisted by additional energy fields, the process capacity and application potentials are unraveled and examined. Finally, from the aspects of exploring physical mechanisms, establishing high-fidelity models, coupling the multiple energy fields, and developing intelligent equipment and realizing these forming processes, the current challenges and future prospects were discussed, summarized and articulated in such a way to present a panorama of the research, development and application of the energy-assisted forming technologies.</p> |

Highlights

1. Three types of energy field-assisted metal forming processes are reviewed
2. The physical mechanisms involved in the three forming processes are elucidated
3. Physically based numerical models for three forming processes are summarized
4. Challenges and prospects of energy field-assisted metal forming are orchestrated

Graphical abstract



Energy field assisted metal forming: current status, challenges and prospects

H. Li ^a, L.F. Peng ^b, B. Meng ^c, Z.T. Xu ^b, L.L. Wang ^d, G. Ngaile ^e, M.W. Fu ^f [#]

^a State Key Laboratory of Solidification Processing, School of Materials Science and Engineering, Northwestern Polytechnical University, Xi'an, 710072, China

^b Shanghai Key Laboratory of Digital Manufacture for Thin-Walled Structures, Shanghai Jiao Tong University, Shanghai, 200240, P. R. China

^c School of Mechanical Engineering and Automation, Beihang University, Beijing 100191, P.R. China

^d Department of Mechanical Engineering, Imperial College London, London, SW7 2AZ, UK

^e Department of Mechanical and Aerospace Engineering
North Carolina State University, USA

^f Department of Mechanical Engineering, Research Institute for Advanced Manufacturing, The Hong Kong Polytechnic University, Hung Hom, Kowloon, Hong Kong, P.R. China

[#] Corresponding author: mmmwfu@polyu.edu.hk

Energy field assisted metal forming: current status, challenges and prospects

Abstract

To meet the various and critical manufacturing requirements including high precision, low cost, good manufacturability, and more demanding from product service and performance aspects such as high performance, light-weight, less energy consumption and low carbon emissions in today's era of rapid product development with short product life circle, it is crucial to re-innovate and re-invigorate metal forming technologies and enable it to play an even more important role in manufacturing arena. Historically, introducing new kinds of energy fields into the forming process drives the innovative advance and rejuvenating of forming technologies due to the physically interactive mechanisms of energy field and certain material deformation behaviors such as thermal-mechanical coupling effects. In this paper, a classification of energy-aided metal forming processes is orchestrated and presented, and three kinds of energy-assisted metal forming technologies, viz., electrically-assisted forming, ultrasonic vibration assisted forming, and electromagnetic field supported forming, are reviewed and delineated as they are currently receiving a widespread attention with promising application potentials. In this paper, the physical essence and the effects of these introduced energy fields on deformation behavior, process performance, microstructure evolution are elucidated and analyzed. The constitutive modeling of these forming processes is recapitulated, and the newly established energy field assisted metal forming technologies are exemplified and discussed. Based on the advantages and limitations of these unique metal forming processes assisted by additional energy fields, the process capacity and application potentials are unraveled and examined. Finally, from the aspects of exploring physical mechanisms, establishing high-fidelity models, coupling the multiple energy fields, and developing intelligent equipment and realizing these forming processes, the current challenges and future prospects were discussed, summarized and articulated in such a way to present a panorama of the research, development and application of the energy-assisted forming technologies.

Keywords: Energy-assisted metal forming; Electrically-assisted forming; Ultrasonic vibration assisted forming; Electromagnetic field supported forming; Microstructure evolution; Process modelling and simulation.

Contents

| | |
|---|----|
| 1. Introduction | 4 |
| 2. Electrically-assisted forming | 7 |
| 2.1 The electroplasticity effect of EAF | 7 |
| 2.2 Mechanical behaviors and properties of materials in EAF | 9 |
| 2.2.1 Mechanical properties | 9 |
| 2.2.2 Micro-structural evolution | 13 |
| 2.3 Model establishment based on the electroplastic effect | 18 |
| 2.3.1 Thermal effect models | 19 |
| 2.3.2 Athermal effect models | 21 |
| 2.4 EAF aided forming process | 24 |
| 2.4.1 Electrically-assisted sheet forming | 24 |
| 2.4.2 Electrically-assisted bulk forming | 26 |
| 2.4.3 Unique electrically-assisted forming process | 27 |
| 3. Ultrasonic vibration assisted forming | 29 |
| 3.1 Working principles of ultrasonic vibration assisted forming | 29 |
| 3.1.1 Surface effects: influence of UVAF on tribological conditions in metal forming | 30 |
| 3.1.2 Volume effects: influence of UVAF on flow stress and forming limit | 31 |
| 3.2 Mechanical behavior and microstructural evolution | 34 |
| 3.2.1 Mechanical properties and constitutive model | 34 |
| 3.2.2 Microstructural evolution | 38 |
| 3.3 Processes of the ultrasonic vibration assisted forming..... | 40 |
| 3.3.1 Ultrasonic vibration assisted sheet metal forming..... | 40 |
| 3.3.2 Ultrasonic vibration assisted wire drawing and tube forming | 42 |
| 3.3.3 Ultrasonic vibration assisted bulk forming | 44 |
| 4. Introduction of electromagnetic field in metal forming | 46 |
| 4.1 Working principle and characteristics of electromagnetic-forming | 47 |
| 4.2 Mechanical behaviors and microstructural evolution | 50 |
| 4.2.1 Macro deformation behaviors and forming limits improvement..... | 50 |
| 4.2.2 Microstructural evolution | 52 |

| | |
|---|----|
| 4.3 Modeling of the electromagnetic forming process..... | 55 |
| 4.3.1 Analytical modeling..... | 55 |
| 4.3.2 Finite element modeling | 55 |
| 4.4 Innovation applications of electromagnetic forming | 58 |
| 4.4.1 Electromagnetic incremental forming | 58 |
| 4.4.2 Calibration and springback control..... | 59 |
| 4.4.3 Combining EMF with conventional forming..... | 60 |
| 5. Summary and outlook | 61 |
| 5.1 Summary | 61 |
| 5.2 Challenges and prospects | 63 |
| 5.2.1 Deeply exploration of the physical mechanism..... | 64 |
| 5.2.2 Establishment of systematic and accurate prediction models..... | 65 |
| 5.2.3 Processes innovation through multi-energy fields coupling..... | 65 |
| 5.2.4 Development of high-efficiency and intelligent equipment | 66 |
| References | 66 |

1. Introduction

Metal forming such as bulk and sheet/tube forming not only plays a crucial role in manufacturing, but also in the development of human civilization and social progress. Metal forming is one of the oldest technologies and can be traced back to 4500 B.C. for manufacturing of copper metal. During the metal forming process, which is generally under the coupling effect of the mechanical and thermal fields, materials are elastic-plastically deformed under loading conditions including certain stress, strain (strain rate) and temperature states, thereby the needed shape and the desirable structure of the workpiece are obtained with the tailored microstructure and properties, in such a way to have the unique advantages of high productivity, low cost, green manufacturing, and good performance of the fabricated parts compared with other materials processing and manufacturing technologies such as machining, casting and welding, etc. It is noted that after the First Industrial Revolution, more and more energy fields were introduced into the metal forming process to assist or directly act on the workpiece for deformation. This has expanded the process potential of metal forming technologies, and driven the innovative advance and rejuvenating of forming technologies [1, 2].

With the increasing demanding from manufacturing industries, high performance, light-weight, high precision, resource conservation and environmental friendliness have always been the goals in development and advanced manufacturing of high-end equipment in different industrial clusters such as aviation and aerospace industries. To meet the needs and the demanding requirements arising from the fast development of various industrial clusters and environmental protection, many difficult-to-form parts and components are increasingly made using hard-to-deform materials. However, the conventional forming technologies have their inherent disadvantages such as high cost, relatively poor forming limits, high energy consumption and serious carbon emissions [3-6]. It is difficult to satisfy the demands and requirements in terms of forming accuracy and forming quality just relying on the optimization of process route, process parameters configuration and die structure alone. To overcome these disadvantages and address the issues, the introduction of energy field into the forming environment and system based on the physically interactive mechanisms of energy field and certain material deformation behaviors is an efficient and promising method to realize the forming under the direct or indirect support with a specific energy source such that the parts and structures can be made with high efficiency and environment-friendly characteristics, etc.

As shown in Fig.1, to tailor microstructure, reduce forming resistance, avoid forming defects, enhance forming formability, improve surface quality and forming environments, etc., different kinds of energy sources, such as conventional force (tension, compression and bending, etc.),

thermal energy, laser energy, electricity, ultrasound and electromagnetic have been introduced into metal forming technologies to develop the energy field assisted metal forming [7, 8]. The mechanical field by force is usually implemented through tooling or pressure-carrying media such as pneumatic and hydraulic in forming process. The thermal field can be generated through directly or indirectly heating approach. The laser assisted forming mainly utilizes the thermal field or shock wave generated by laser to achieve the formation of difficult to deform materials, and the variation of the thermal field affects the properties of materials in laser-assisted forming. The electric fields generally affect the internal behaviors of materials, the effects of the introduced ultrasound vibration are manifested by two aspects, viz., internal behaviors and external loadings, while the introduction of electromagnetic field improves the forming limit mainly through generating the external high energy rate loading. In the energy assisted forming process, the complex interaction between the energy field and the forming of material makes it distinctly different from that of the conventional forming processes, especially for the material excitation response and microstructure evolution mechanism caused by the special energy field. Therefore, in the actual manufacturing process, different energy fields need to be selected based on the requirements of the formed shape of workpiece and material properties, in such a way to maximize the unique advantages of each energy field employed to form the selected materials.

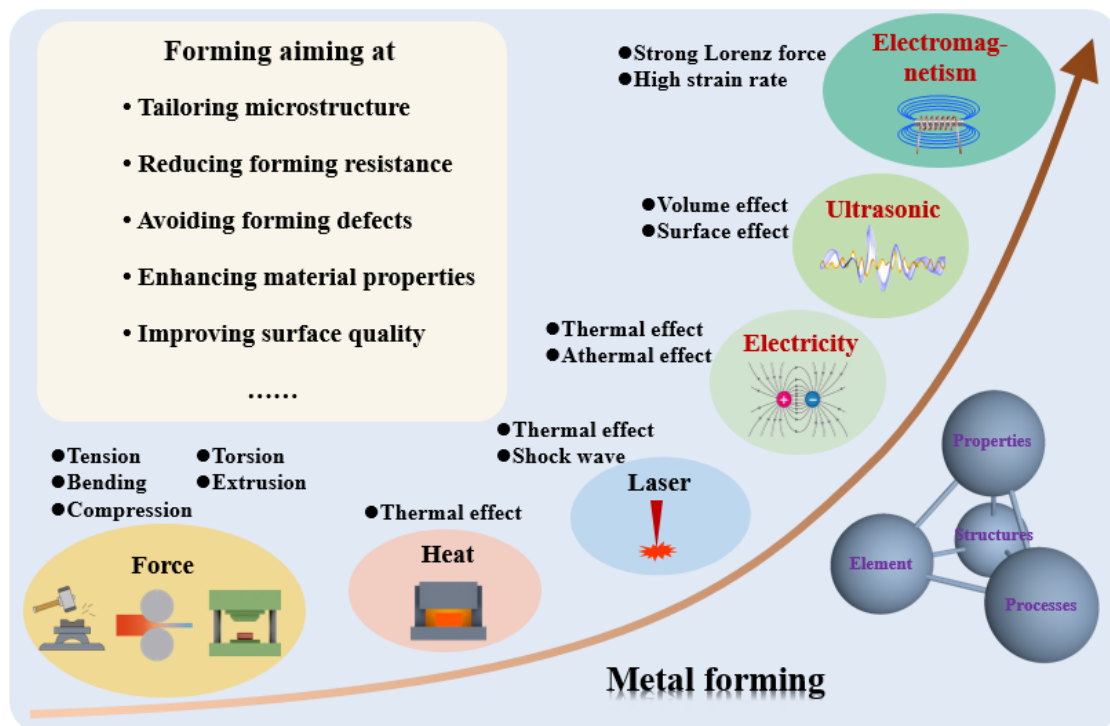


Fig.1. Introduction of energy field into forming environment.

The microstructure evolution and deformation mechanisms of materials under the general thermal-mechanical coupled loading have also been thoroughly understood. The electric,

ultrasonic and electromagnetic fields currently receive a widespread attention with promising application potentials, while the physical mechanisms of these kinds of energy fields are still limited [9-11]:

- Electrically-assisted forming (EAF): The electric fields in EAF allows electric current to flow through the metal workpieces during the plastic deformation of materials. On the one hand, the generated Joule heat leads to higher temperature and further a lower flow stress. On the other hand, many researchers also found an additional athermal effect of electric current contributing to the reduction of flow stress and the increase of formability when passing through metals, viz. the electroplasticity. Many physical theories have been proposed to explain the electroplasticity such as the electron wind, the electromagnetic depinning and the local dislocation activation effects. Utilizing both the thermal and athermal effects in EAF, the forming performance of many hard-to-deform materials can be improved in terms of the flow stress reduction, springback angle elimination, formability improvement, material flow enhancement, etc.
- Ultrasonic vibration assisted forming (UVAF): The ultrasonic vibration with a frequency is imposed on tooling or raw materials during the forming process. The material flow behavior and the microstructure evolution in UVAF are mainly influenced by two aspects, viz., the surface and volume effects. The surface effect refers to the improvement of UV on tribological condition between workpiece and tooling, while the volume effect is caused by stress superposition and the activation of the blocked dislocation.
- Electromagnetic forming (EMF): EMF is a high-speed and contactless impulse forming process that uses a transient pulsed magnetic field to apply a Lorentz force to the workpiece. The forming limit and the dimensional precision of the workpiece can be significantly improved due to the high strain rate employed in the forming process. The electrohydraulic forming and explosive forming also belong to the category of high energy rate forming [12-14].

In this paper, three kinds of energy-assisted metal forming technologies, viz., electrically-assisted forming, ultrasonic vibration assisted forming, and electromagnetic field supported forming, are reviewed and delineated. The working principle and the characteristics of forming process introduced with each energy field are delineated. The research status of the mechanical behaviors and microstructural evolution of materials, modeling methods of material deformation and forming process, process capacity and innovative applications are systematically reviewed. The challenges and prospects in terms of the unraveling and understanding of the forming

mechanisms behind the introduced energy field in forming process, systematic and accurate modelling and simulation, process innovation and the trend of equipment development are discussed, analyzed and articulated. The motivation of the present work is to provide researchers with the complete state-of-the-art information and promote the development and application of the energy-assisted forming processes.

2. Electrically-assisted forming

Electrically-assisted forming (EAF) allows electric current to flow through metallic work-pieces during the plastic deformation process. EAF has been found as a promising technique to improve the formability for a variety of materials. Both thermal and athermal effects brought about by the electric current passing through the metallic materials have been observed as two major factors influencing the plastic deformation of materials in EAF. However, their mechanisms are still far from clear and many contradicting phenomena and analyses exist. In this section, the experimental research and analytical models focusing on the effect of electric current on the plastic deformation of materials are reviewed. The applications of EAF in manufacturing processes are then summarized.

2.1 Electroplastic effect of EAF

The effect of electric current on the mechanical properties of materials was first investigated by Machlin [15]. By applying a voltage to rock salt crystals, the yield stress, flow stress and ductility were found to be sensitive to the voltage amplitude. **The change in the plastic behavior of materials caused by the electric current is collectively referred to as the electroplastic effect, featuring variations in flow stress, yield stress, ductility, springback, etc. with different current parameters. The electroplastic effect is the superposition of multiple sub-effects, which are usually divided into two categories, i.e., thermal and athermal effects. Due to the coupled and complex nature of electroplasticity, how those effects contribute to the change in plastic behaviors of metals remains a challenging and interesting issue with different perspectives.**

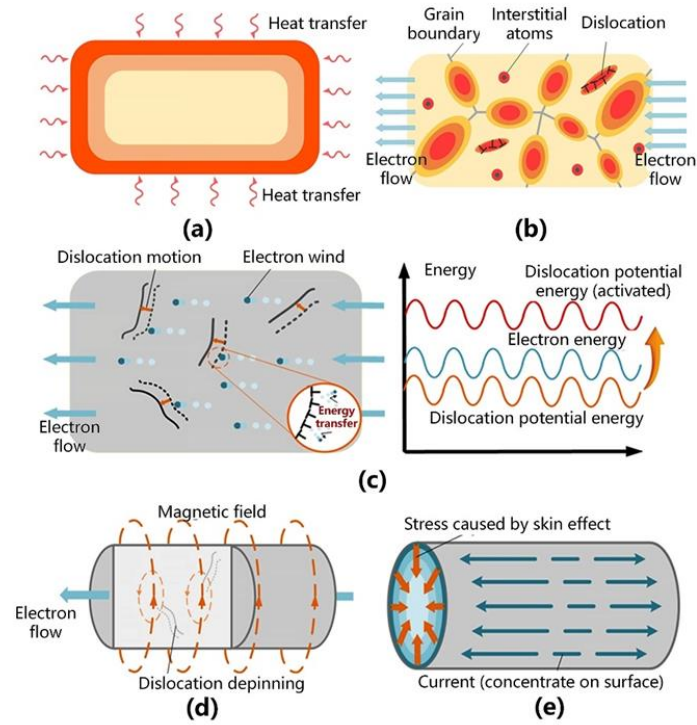


Fig.2. Thermal and athermal effects on the plasticity of materials in EAF. (a) thermal effect by even distribution temperature thermal effect, (b) local heat thermal effect, (c) electron wind athermal effect, (d) electromagnetism athermal effect and (e) skin athermal effect.

The thermal effect arises from resistive heating. It is related to the collision between free electrons and internal obstructions such as grain boundaries, dislocations and interstitial atoms. The characteristics of thermal effect mainly include: (1) even temperature field which is similar to the traditional heat-assisted forming process; (2) uneven thermal field caused by large local overheating near defects. The schematic diagram of thermal effect is shown in Fig. 2(a).

In addition to the thermal effect, the flowing electrons acting on the interstitial atoms or dislocations provide an additional force after scattering near those defects. This interaction is defined as the athermal effect. Many hypotheses have been proposed to explain the athermal effect on the metal flow behavior and microstructure alternation such as the electron wind effect, magnetic field effect, and skin effect. In the electron wind effect, the directional drifting electrons cause additional momentum and energy effects on the dislocations. In comparison, the magnetic field effect is attributed to the athermal effect of the magnetic field generated by the current. Furthermore, the skin effect refers to the state where the current is unevenly distributed inside the material. The above effects are shown in Fig. 2 (b).

Even though both the thermal and the athermal effects of electric current has been extensively discussed, the plastic response of materials in EAF is affected by their coupling influence. For different materials, both these effects are influenced by the composition, microstructure, phases,

etc., leading to various and different deformation behaviors and stress responses. Identifying those effects in different materials is crucial in understanding the electroplasticity mechanism. However, it remains a challenging issue due to the coupled nature of the thermal and athermal effects. The details of the effects will be further discussed in section 2.3.

2.2 Mechanical behaviors and properties of materials in EAF

Owing to the electroplastic effect, the mechanical behaviors of the metals are affected significantly in EAF. The influences of electric current on the mechanical behaviors can be mainly manifested by the variation of three indicators, viz., flow stress, elongation and springback of the working materials. Moreover, the underlying mechanisms of these electroplastic phenomena are attributed to the evolution of the material's microstructure affected by the introduction of electric current. In this section, both the mechanical properties and microstructural evolution under the action of current are summarized to provide a comprehensive understanding of the electroplastic effect in EAF.

2.2.1 Mechanical properties

2.2.1.1 Flow stress

Even though the reduction of flow stress with the introduction of electric current has been reported by numerous researchers, there is an ongoing debate on the mechanisms leading to this effect.

Some researchers suggested that the flow stress reduction is due to the thermal expansion regardless of the influence of the athermal effect. For instance, Kinsey et al. [16] found that the athermal effect is not significant in facilitating the plastic deformation of SS304 and TC4 at a high strain rate, as shown in Fig. 3 (a). The authors suggested that the decrease in flow stress is mainly due to the higher temperature from resistive heating. Magargee et al. [17] found no evident stress reduction in the electrically-assisted tensile tests of CP titanium with forced-air cooling compared to the flow stress obtained in the warm tensile tests at the same temperature (Fig. 3 (b)). This conclusion is also consistent with the study by Wang et al. [18]. By comparing the flow stresses of AZ31 during tensile tests with and without the introduction of electric current, it was revealed that the stress reduction by compared to room-temperature results is due to the thermal softening effect rather than the athermal effect.

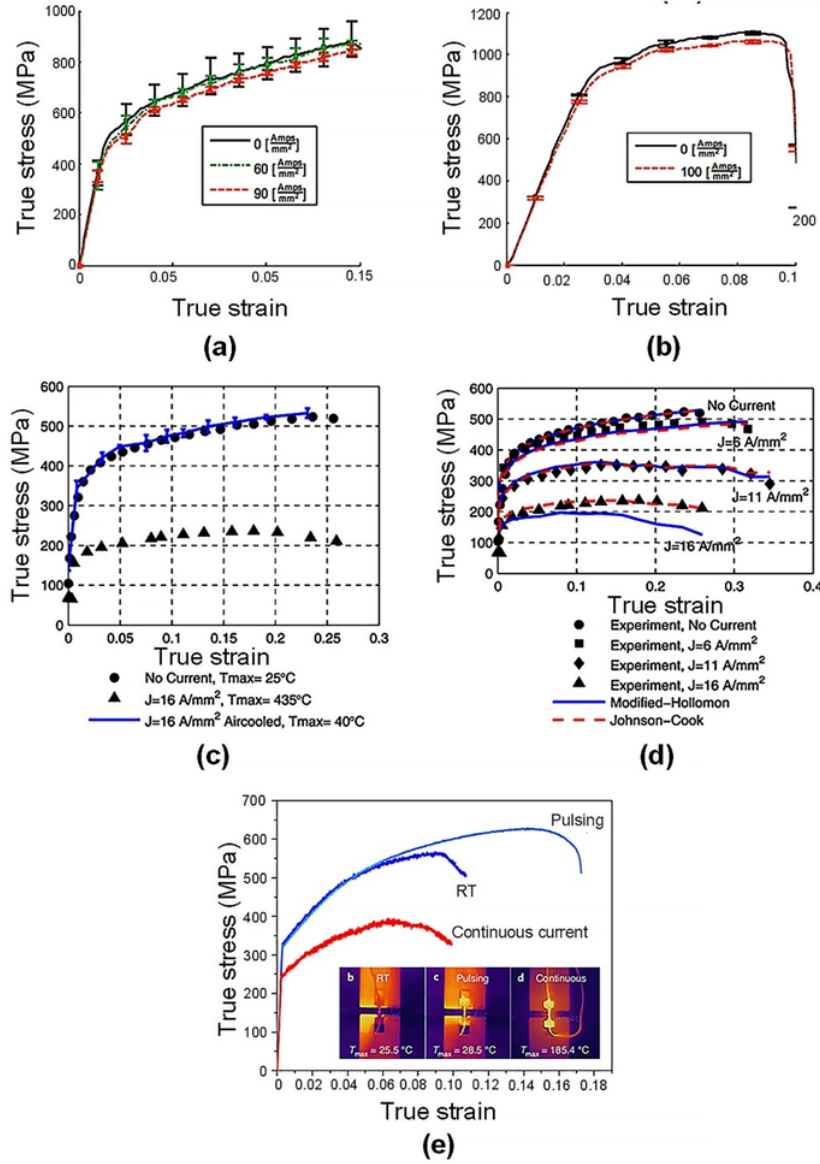


Fig.3. Influence of electric current on flow stress. (a) and (b): True stress-true strain data with varying current densities, (a) 50°C of 304SS and (b) 235°C for TC4 [16]; (c) and (d): Flow behavior of CP titanium in electrically-assisted (EA) tension tests, (c) comparison of “air-cooled” and “non-cooled” tests and (d) predictions of flow stress behavior based on modified-Hollomon and Johnson-Cook model [17]; (e) The tensile results of Ti-Al alloys under different condition [18].

However, other studies have considered alternative causes for the flow stress reduction in EAF. These works revealed that the athermal effect also plays a significant role during the plastic deformation with the introduction of electric current. For example, Heigel et al. [19] used T6511 aluminum, Ross et al. [20] employed TC4, Mai et al. [21] utilized stainless steel and Peng et al. [22] adopted SS316L in their EAF experiments, and they all found that the athermal effect cannot be ignored in EAF. More recently, researchers have revealed additional athermal effects on the

flow stress. Among them, Lee et al. [23] observed that current pulses can change the dynamic strain aging (DSA) behavior of CP-Ti. The same conclusion was also drawn by Xu et al. [24] in EAF of Al-Mg alloy. Considering that DSA is closely related to dislocation motion, the authors inferred that the electric current affects the flow stress of material by influencing the dislocation motion.

In addition to the debate on the flow stress reduction in EAF, Zhao et al. [18] found that the electric current increased the flow stress of the Ti-Al alloy workpieces, as shown in Fig. 3 (e). With the introduction of pulsed current, the flow stress is increased by over 30 MPa with a low temperature rise of 3 °C compared with the tensile results conducted at room-temperature.

2.2.1.2 Ductility

The influence of electric current on the ductility of materials is even more complicated. Many studies have reported that electric current can enhance the ductility of materials. For example, Kim et al. [25] observed that the elongation of 5052-H32 aluminum increased from 6% to 12% in EAF compared to room-temperature tests. Yang et al. [26] introduced pulsed current into the tensile process and successfully increased the ductility of high strength aluminum alloy 2A12 and ultra-high strength aluminum alloy 7A04. Zhu et al. [27] found that pulsed current can improve the ductility of TiNi shape memory alloy during rolling and the superelasticity after annealing. A more significant improvement was reported by Ugurchiev and Stolyarov [28], which enabled the elongation of VT6 and Ti_{49.3}Ni_{50.7} titanium alloys to increase fourfold with the current density of 160 A/mm². Li et al. [29] revealed that the formability of magnesium alloy AZ31, in gas bulging tests was evidently improved with the assistance of current pulse. With the peak current density of 45 A/mm², the limit ratio of height to diameter reached 0.48, which was 20% higher compared to conventional forming. This is because the current pulse can concentrate at the tip of the cavity, leading to crack blunting. Similar conclusions were also obtained by Perkins et al. [30], revealing that the electric current can improve the ductility in compression of titanium alloys.

However, Ross et al. [20] found that the elongation of various metals is decreased with the increase of current density. Similar phenomena were revealed by Zhao et al. [31] in EAF of aluminum alloy 5754 and also by Zhang et al. [32] for Ni-based alloy. Zhu et al. [33] observed that the maximum elongation of ZA22 is increased by 437% with the adoption of electric current at an ambient temperature of 28 °C, as shown in Fig. 4 (a). However, the increase of elongation becomes less significant when the current density is further increased.

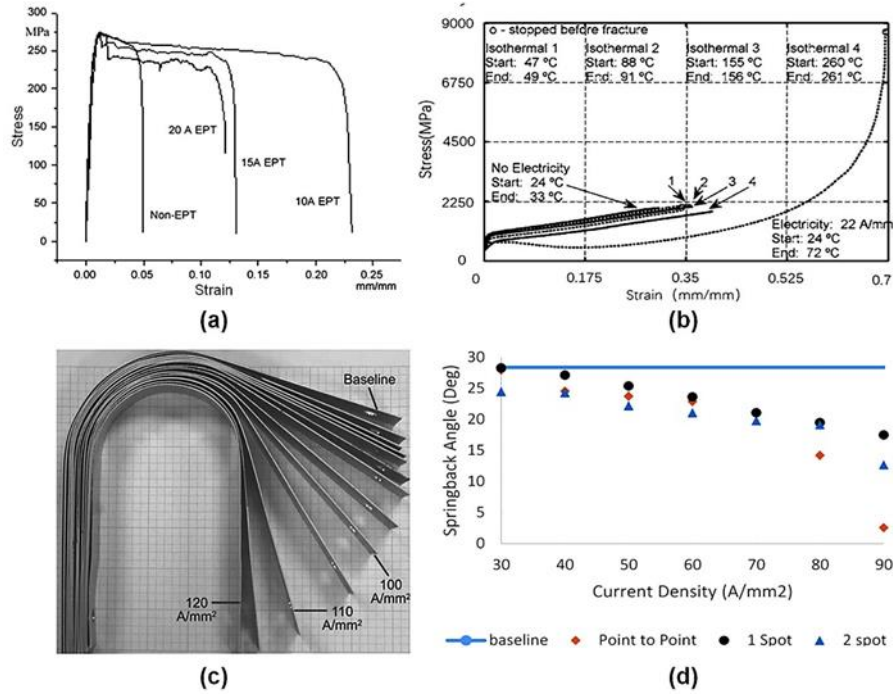


Fig.4. Influence of electric current on the ductility and springback of materials. (a) and (b): Athermal effect on metal's ductility: (a) Stress-strain curves of non-EPT ZA22 alloy specimen and EPT alloy specimen with various current intensities; (b) comparison of “EA compression” and “heated compression” results of titanium alloy under various temperature [30]; (c) Springback elimination in Al 6111 specimens with current pulse treatment after deformation [34]; (d) Springback angle-current density curves for various configurations [35]

2.2.1.3 Springback

In 2009, Green et al. [34] treated Al 6111 alloy with pulse current after U-bending deformation. They observed that the springback angle decreased with the increase in current density until the forming results were constant when the current density reached 120 A/mm^2 (Fig. 4 (b)). Later on, researchers further carried out a series of studies on EA bending process.

Li et al. [36] studied the bending behavior of TC4 alloy with a pulsed current, and found that the stress reduction in electrically-assisted case was no longer evident when the specimens were air-cooled to room temperature. Through observation of the specimen's temperature profile, Jordan et al. [37] also concluded that the electroplastic effect was not significant in the three-point bending process of C260 (brass) with the current density of 40 A/mm^2 . These studies suggested that the springback reduction in EAF was mainly due to the thermal effect.

The athermal effect, however, was reported to be the major factor in springback elimination in some other studies [38]. Among them, Ruszkiewicz et al. [35] examined the effect of locally applied direct current on the springback reduction of aluminum alloy. Three different configurations of current path were applied, which differed in the arrangement of the poles. The results (as shown in Fig. 4 (d)) indicated that the “point to point” case led to the stronger

springback elimination compared with cases 1 and 2. This is because the current was forced to flow across the stress concentration area. Xie et al. [39] employed the control variable method to explore the influence of pulse frequency and peak current density on the springback elimination of AZ31B magnesium alloy in a V-bending process. It was found that the decrease in grain size and twinning grains induced by the pulsed electric current affected the springback elimination significantly.

Some researchers analyzed this process from the perspective of energy. Both athermal and thermal effects provide deformation energy during the bending process. By conducting V-bending experiments on stainless steel, Salandro et al. [40] obtained the relationship between the mechanical forces in the traditional forming and EAF based on the assumption that the total required deformation energy is the same. A notable reduction of springback up to 77% was observed in the experiments. In addition, Kim et al. [41] observed the same phenomenon in single pulse EA U-bending process of advanced high strength steels. The springback was revealed to be effectively suppressed with the increase in current energy density.

2.2.2 Microstructural evolution

It is well known that the mechanical properties of materials are greatly influenced by their microstructures. To explore the physics behind these complicated electroplastic phenomena, studies on the microstructure evolution in EAF were carried out by focusing on its correlation with dislocation, grain, and phase variation.

2.2.2.1 Dislocation behavior

The plastic deformation of metals is closely associated with dislocation motion at micro level. The influence of electric current on dislocations can be reflected by dislocation density, slip conditions and dislocation structures. Zhu et al. provided a comprehensive description of the dislocation motion behavior under electric current, as shown in Fig. 5 (a). In their study [33], electric pulses were applied to ZA22 alloy in tensile tests and it was found that the electric current effectively facilitated the dislocations to move toward and pile up at grain boundaries. This was responsible for the instant stress reduction observed in their experiments.

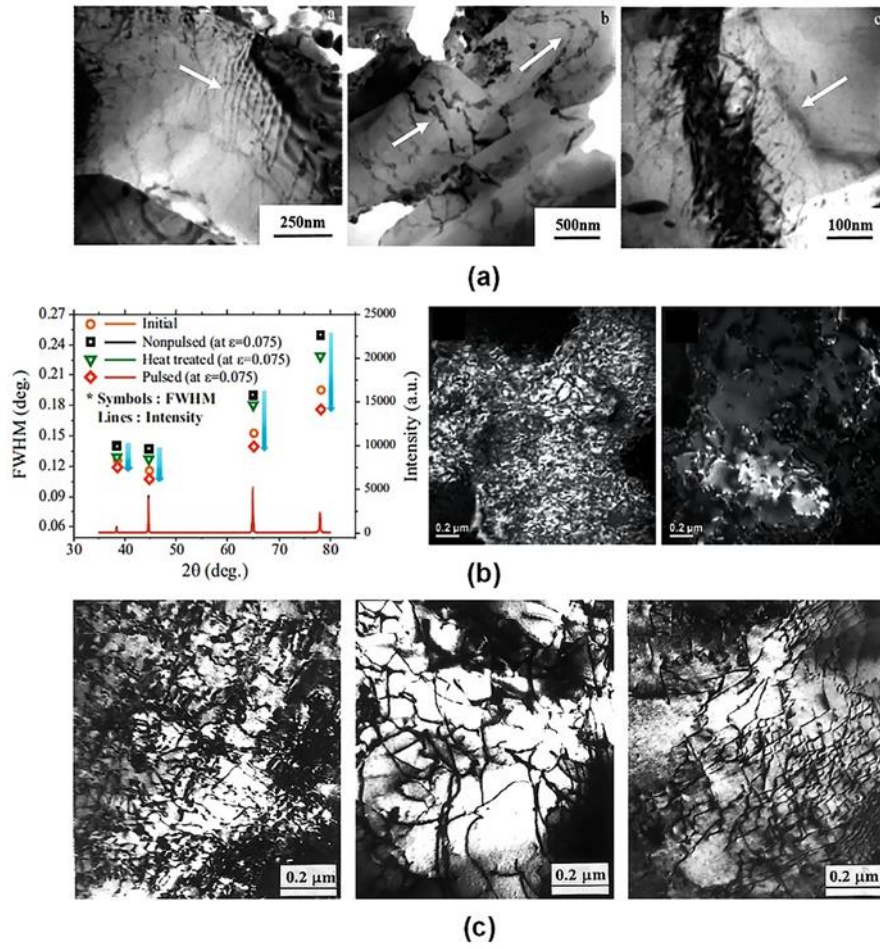


Fig.5. Influence of electric current on dislocation behavior. (a) TEM images of ZA22 alloy of the 10A, 15A and neck zone of the 20A in electro-plastic tensile tests [33]; (b) dislocation density and structure evolution of Aluminum alloy [25]; (c) TEM images of the brass strip with cold-rolled, HDE treatment and annealing treatment [42]

The change in the dislocation motion finally influences the dislocation density and micro-structure. Kim and Lee [25] studied the distribution of dislocations in tensile tests under pulsed-current and no pulsed-current conditions. By analyzing the full width at half maximum of X-ray diffraction peaks [43], it was found that the dislocation density of workpiece with pulsed-current was much lower than that in no pulsed-current condition, and even less than that in the as-received initial workpiece in Fig. 5 (b). This trend was also confirmed via TEM observation. Since the maximum temperature during electrical treatment was considerably lower than the usual annealing temperature for Al alloys and the working time was short, Bertolino et al. [44] believed that the thermal effect induced by resistance heating was negligible. The athermal effect was the major contribution to annihilation of dislocations by enhancing atomic diffusion.

Similar results were also reported by He et al. [42]. They compared the dislocation density in brass strips under cold-rolled treatment, high current density current pulse (HDE) treatment and

annealing treatment (Fig. 5 (c)). The TEM images showed that the dislocation density under the HDE treatment was less than that under annealing treatment as well as cold-rolled treatment. Furthermore, Xu et al. [45] observed the dislocation distribution in the vicinity of grain boundaries for magnesium alloy. They suggested that the dislocations are activated to move towards and pile up at grain boundaries by the athermal effect and are annihilated and rearranged by the coupling of thermal and athermal effects. Liang et al. [46] found that a dislocation density of $7.84 \times 10^{16}/\text{m}^2$ was achievable in brass with $180 \text{ A}/\text{mm}^2$ current density. They explained that the increment may be caused by the instantaneous thermal expansion brought by the high heating rate.

Recently, scholars have attempted to use in-situ methods to measure the dislocation evolution during EAF. Li et al. [47] explored the dislocation density evolution by in-situ XRD method. By analyzing the changes in the full width at half maximum of X-ray diffraction peaks in hot tensile tests and electrically-assisted tensile tests, they found the current can promote the activation of prismatic slip systems and inhibit the increase in dislocation density. More intuitive results were given by Kang et al. [48] by developing an in-situ TEM observation device to explore the dislocation motion in pure Cu under a high density current of $5000 \text{ A}/\text{mm}^2$. The results showed that the current had little effect on promoting the dislocation motion. A similar experiment was also conducted by Kim et al. [49] on Mg alloy. The results indicated that the influence of current on dislocation motion may not fully explain the athermal effect on the flow stress.

2.2.2.2 Recrystallization

Recrystallization, which is a softening mechanism for metals, usually comes into existence at a high working temperature. However, as the electric current flows through metals, recrystallization can take place at a lower temperature. In addition, the recrystallized grains in EAF are also found to be finer than those obtained in the conventional heat treatment. According to Humphreys [50], recrystallization is closely associated with the nucleation rate and growth rate of recrystallized nuclei. With the introduction of electric current, the nucleation rate is remarkably stimulated, and the growth of recrystallized grain is impeded.

Xiao et al. [53] treated copper single crystal after fatigue tests with current pulse and observed two types of finer recrystallized grains. The generation of the finer grains was attributed to the short processing time, high heating rate and accelerated nucleation affected by the pulsed electric current, which did not allow sufficient growth time for the recrystallized grains. Zhou et al. [51] also reported that the recrystallization temperature of Cu-Zn alloys decreased from 650 to 570 °C with the introduction of electric pulses. Finer recrystallized-grains were also obtained as shown in

Fig. 6 (a). The effects of electric current on recrystallization are summarized from three aspects, viz., (a) the high-rate heating; (b) enhanced dislocation mobility and (c) improved atom migration.

Later on, Xu et al. [54] observed the dynamic recrystallization process of AZ31 in EAF. Their study revealed that the flux of diffusion atoms can promote the dislocation climbing in subgrain boundaries. The migration rate of the nuclei boundary as well as the growth rate of recrystallized nuclei were also found to be restrained. With the combination of the above two effects, the dynamic recrystallization was completed at a lower temperature. The mechanism was also verified by the recrystallization processes in other materials [55]. Furthermore, Zhu et al. [56] found that high-frequency electropulsing accelerate atomic diffusion in severely deformed copper, leading to recrystallization within nine seconds. More recently, Liu et al. [57] also compared the recrystallization behavior of aluminum matrix composites under T6 and electropulsing treatment. It was found that the deformed grains were replaced by the recrystallized grains due to the extra driving force of recrystallization induced by current pulse.

For some metallic materials, the thermal effect cannot be ignored during the recrystallization process. Xu et al. [58] explained the recrystallization mechanism in EAF based on the coupling effects. They treated the recrystallization nucleation and growth in magnesium alloy as the motion of low angle boundaries and the motion of high angle boundaries, respectively. The promoted interchange of vacancies and single atoms under thermal and athermal effects accelerated the low and high angle boundary migration, which enhanced the nucleation rate and impeded the growth rate of the recrystallized grains. Furthermore, Jiang et al. [59] deduced the enhanced atomic flux expression based on the assumption that the coupling effects stimulated dislocations to climb into subgrain boundaries, which was closely associated with the recrystallization of magnesium alloys.

2.2.2.3 Phase transformation

According to Zhou et al. [60], apart from the effect on dislocation motion and recrystallization, electric current also has an impact on phase transformation, such as decreasing the thermodynamic barrier and enhancing the nucleation rate during plastic deformation. For instance, Zhang et al. [61] observed the microstructure change of Cu-Zn alloy in deformation process, and found that two nanophases were formed owing to the current pulse treatment. Through further research, the authors [62] suggested that nanostructured transitions were because of the high-rate heating, rapid cooling, and thermal stress affected by the current pulse. Zhang et al. [63] studied the influence of current on precipitation behavior of Al-Mn alloy. Pei et al. [64] investigated the phase transformation of TC6 in EAF, which also had a significant influence on the metal's ductility. Furthermore, Liu et al. [65] revealed that the effects of current pulse on

Fe17Mn5Si8Cr5Ni0.5NbC reduced the critical stress for stress-induced martensite transformation at room temperature, which was ascribed to the enhanced precipitation of NbC particles stimulated by drift electrons. By using a current density over 10^3 A/cm^2 , Conrad [66] identified that solid-state phase transformation was accelerated in some cases and retarded in others. It was suggested that the difference arises from the prior thermal treatment conditions and the specific current parameters.

Recently, more attention has been dedicated to the athermal effect of current pulse on phase transformation. Jiang et al. [67] reported that the phase transformation from β lamellar clusters to spherical β particles was greatly accelerated in AZ91 by applying electric current. In comparison, numerous β lamellar clusters still existed in the sample under conventional heat treatment. They ascribed the enhanced spheroidization of β phase to the athermal effect of electric current. Similarly, Zhang et al. [68] observed that decomposition of the β phase of AZ91 was accelerated by current pulse compared with that after heat treatment at the same temperature.

Due to the different mechanisms of phase transformation in different metals, the athermal effect on phase transformation exhibits a range of behavior. For the displacive phase transition, Liu et al. [69] found that the electric current delayed the transformation from austenite to martensite in TRIP 780/800. During the experiment, the temperature rise was controlled by forced air cooling and had less effect on the phase transformation. The authors suggested that the current impeded the phase transformation by reducing the external mechanical driving force. For the diffusive phase transformation, Jiang et al. [70] and Huang et al. [71] concluded that the current pulse can reduce the temperature and time of phase transition of TC4. The electric current was found to provide additional energy for the diffusion of particles, which enabled the particles to achieve additional diffusion than simply heat diffusion. Similar conclusions were also drawn by Zhao et al. [52], as shown in Fig. 6 (b).

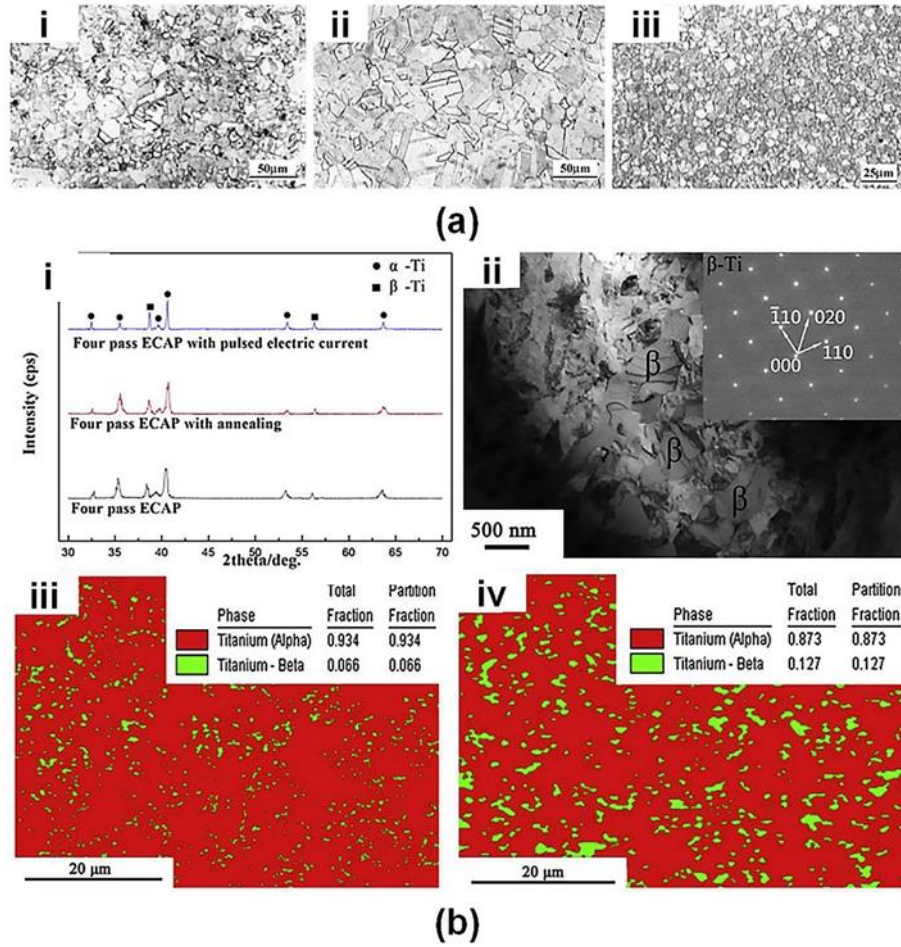


Fig.6. Influence of electric current on recrystallization and phase transformation of materials. (a) optical micrographs of a cold worked brass by an annealing treatment at (i) 570 °C, (ii) 650 °C, and (iii) current pulse treatment [51]; (b) The promotion effect of pulsed current on phase transition of TC4 [52].

Overview of the current researches on the mechanical behaviors and microstructural evolution of materials in EAF, there are some contradictory experimental observations regarding the electroplasticity associated with the flow stress, yield stress, ductility, etc. Some researchers argue that athermal effect plays an important role in EAF while others are convinced that thermal effect is the major factor and athermal effect can be neglected. In view of this, researchers are turning to the microstructure evolution in different materials subjected to electric current to find the essential answer to these contradictory results. The multi-scale connection between the microstructure and the mechanical responses of different materials in EAF is a fundamental issue for the understanding of electroplasticity, which is attracting considerable research attention.

2.3 Model establishment based on the electroplastic effect

Based on the observation described in Section 2.2, numerous models have been proposed to describe the relationship between the mechanical behaviors and current parameters.

2.3.1 Thermal effect models

According to Okazaki et al. [72], the thermal effect, which derives its origins from Joule heating, induces temperature change as a function of electric current flow through the metal. As indicated in Section 2.1, the inhomogeneity of resistivity leads to local heating effect at the microscopic level. Therefore, the thermal effect is the coupling of the uniform heating effect and the local heating effect. Up to now, quantitative models have been developed to focus on the effect of uniform heating.

Salandro et al. [9] found that the “threshold current density” is inversely proportional to the electrical resistivity of materials, showing the importance of thermal effects. In 2017, Wang et al. [73] presented the inverse-S-shaped softening curve of the material and explained the “threshold current” effect successfully. Furthermore, other scholars [74] deduced that the thermal effect is the dominant cause of electroplasticity rather than the direct effect of electrons. He et al. [42] took the thermal expansion into consideration by formulating the instantaneous thermal stress $\sigma(t)$ under rapid heating as follows:

$$\sigma(t) = E\alpha[\Theta(t) - l(t)] \quad (1)$$

where E is the elastic modulus, α is the thermal expansion coefficient, ΔT_{\max} and ΔL_{\max} are the maximum temperature rise and expansion of samples, respectively.

$$\Theta(t) = \Delta T(t) / \Delta T_{\max} \quad (2)$$

$$l(t) = \Delta L(t) / \Delta L_{\max} \quad (3)$$

The study suggested that the instantaneous thermal stress can be treated as the driving force to relieve the tension stress resulting from the cold working of brass strip. Magargee et al. [17] also employed two common plasticity models, specifically the Modified-Hollomon model and the Johnson-Cook model, to analyze the mechanical behavior of CP titanium in EAF.

The Modified-Hollomon model is designated as:

$$\sigma(\varepsilon, T) = K(T)\varepsilon^n \quad (4)$$

The Johnson-Cook model is formulated as:

$$\sigma = B\varepsilon^n \left[1 + C \ln \left(\frac{\dot{\varepsilon}}{\dot{\varepsilon}_0} \right) \right] f(\bar{T}) \quad (5)$$

where σ is the stress, ε is the strain, K is the strength coefficient, n is the strain hardening coefficient, \bar{T} is the homologous temperature, and B and C are material constants. Both models give satisfactory prediction of the measured mechanical behavior in the EA tensile test. The

Johnson-Cook model was also further modified by Kim et al. [75], who considered the Joule heat generated by current. The expression was rewritten as follows:

$$\sigma = [(A + B(\varepsilon)^n) + (1 - \exp(D_1 \varepsilon^{D_2}))]((a\rho_0^2 + 1)\varepsilon^{b\rho_0^2}) \quad (6)$$

where σ is the stress, ε is the flow strain, n is the strain hardening coefficient and ρ_0 is the current density. A , B , a and b are material constants, while D_1 and D_2 are empirical coefficients.

In addition, Magargee et al. [76] proposed empirical equations to describe the relationship between the applied current density (J_{eff}) and the thermal softening parameter ($f(J_{eff})$) based on the resistance heating mechanism for various metals.

For low melting temperature metals, the relationship is represented as:

$$f(J_{eff}) = \frac{c}{c + \exp\left(\frac{d\rho J_{eff}^2}{\rho_m c_p (T_m - T_R)}\right)} \quad (7)$$

For high melting temperature metals, it has the following equation:

$$f(J_{eff}) = \alpha \exp\left(-\frac{\beta\rho J_{eff}^2}{\rho_m c_p (T_m - T_R)}\right) \quad (8)$$

where c , d , α and β are empirical constants. ρ , ρ_m , c_p are electrical resistivity, mass density, and specific heat capacity, respectively. T_m and T_R refer to melting temperature and room temperature respectively. The results suggest that the temperature-dependent deformation mechanism can depict the stress softening during EA deformation. Furthermore, it also provides explanations for the threshold current density.

The models presented above are mainly used to describe the even thermal field effect caused by the current. As presented in Section 2.1, local heat effect is an essential part of the thermal effect. However, as the scale of the local heat point is in nanometers, it is difficult to establish a quantitative analysis model. At present, most studies mainly discuss the local thermal effect through qualitative analysis.

In addition, Salandro et al. [77] suggested that the local resistivity at the dislocation can be up to 7 times the resistivity of the substrate. Therefore, the local temperature at the dislocation is significantly greater than the actual measured temperature. By measuring the element diffusion behavior under the action of current, Li et al. [78] speculated that the dislocation area has a higher temperature, which increases the diffusion rate of the element (as illustrated in Fig. 7). The local heat effect can also explain the influence of electric current on the PLC effect in Ni-based alloys. In general, the experimental results indicate the existence of the local heat effect. Nevertheless,

the creation of a quantitative model poses challenges for researchers.

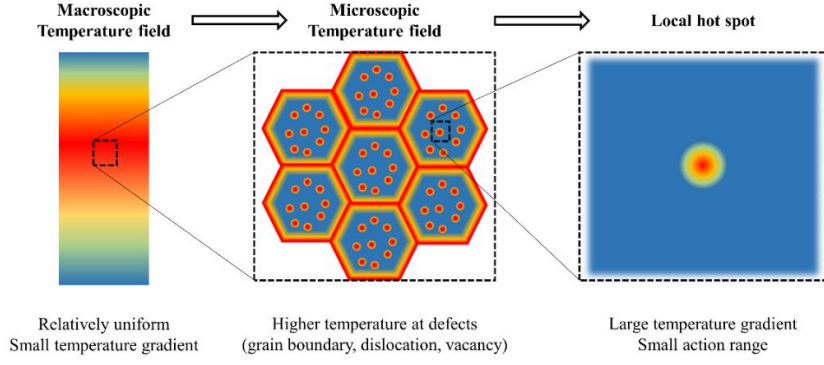


Fig.7. Description of the local heat effect: the local resistivity at microstructural defects is higher than the substrate causing a local hot spot and further affecting the dislocation motion.

2.3.2 Athermal effect models

As elucidated in Section 2.1, the following three categories of athermal effects have been explored in prior research regarding the effect on mechanical behavior: (1) the pinch and skin effect due to the uneven distribution of the electric field; (2) the induced magnetic field effect generated by the alternating electric field, and (3) the electron wind effect caused by the orientation of electrons. These effects are discussed respectively below.

In a previous report [72], the skin effect was defined as the concentration of current near a specimen surface when a high-frequency current is introduced. The depth δ can be evaluated as follows:

$$\delta = \left(\frac{\pi f \mu}{\rho} \right)^{-1/2} \quad (9)$$

where f is the pulse frequency, μ is the permeability, and ρ is the resistivity of the specimen. Experimental results [79] demonstrated that the current was uniformly distributed in the specimen cross-section. Due to the existence of the pinch effect [72], the radial compressive stress is induced and can be estimated by:

$$\Delta\sigma_{pinch} = \frac{1}{2} \nu \mu J^2 r^2 \quad (10)$$

where ν , r and J are the Poisson's ratio, specimen radius, and current density, respectively. However, Okazaki et al. [72] pointed out that the pinch effect only has a small contribution to the load drops.

Regarding the magnetic field effect, Molotskii et al. [80] found that the magnetic field generated by the electric current accounts for the athermal reduction of flow stress in 1997. They suggested that the magnetic field can provide energy to promote the de-pinning of dislocations. Based on this, the study presented the following formula to predict the decrease in flow stress:

$$\Delta\sigma = \sigma^* \frac{J^2}{J^2 + J_0^2} \quad (11)$$

where σ^* is the effective shear stress, J and J_0 are the current density and characteristic current density, respectively. It is worth noting that the magnetic field effect is dependent on the material type and only paramagnetic materials can be influenced by this effect.

In addition to the models described above, recent research efforts have focused on the effect of electron wind. The models established based on the electron wind effect can be further classified into two categories based on force conduction and energy transfer. In either way, researchers agree that the electron wind affects by affecting the dislocation motion and state. The following models were developed to explain the mechanism at the micro level, which makes them difficult to be verified.

For instance, Conrad [81] took the drift electrons into consideration and suggested that they can promote the dislocation motion via exerting an external force during plastic deformation. The expression of electron wind is established as follows:

$$F_{ew} = \frac{b}{4} \left(\frac{v_e}{v_d} - 1 \right) \frac{v_d}{v_F} \frac{\partial n_e}{\partial u} \Delta^2 \quad (12)$$

where v_e is the velocity of the electron, v_d is the velocity of the dislocation, v_F is the Fermi velocity, b is the Burgers vector, n_e is the electron consistency, u is the chemical potential and Δ is the deformation energy constant. Okazaki et al. [72] also reported the similar mechanism of electron wind force. Since the electrons were scattered by the existence of dislocations, Conrad [82] postulated that the force exerted by electron flows on per unit dislocation length is as follows:

$$F_{ew} = (\rho_d / N_d) e n_e J \quad (13)$$

where (ρ_d / N_d) represents the specific resistivity for the unit length of dislocation, N_d is the dislocation density, e is the electron charge, n_e is the electron concentration and J is the current density.

On the other hand, the effect of electron flows on the plastic behavior was captured by describing the energy transfer between drifting electrons and ions [83]. Energy transfer is considered a major factor for the reduction of Gibbs free energy in dislocation motion by Li and Yu [84]. As a result, the dislocation motion as well as the material flow are facilitated by the introduction of electric current. The strain rate with an applied current pulse is modelled as:

$$\dot{\varepsilon}_e = \dot{\varepsilon} \exp[\ln(\dot{\varepsilon}_{0e}/\dot{\varepsilon}_0) + (\frac{x t}{n \gamma k T} J^2)] \quad (14)$$

where $\dot{\varepsilon}_e$ is the plastic strain rate with applied electricity, $\dot{\varepsilon}$ is the plastic strain rate without applied electricity, $\dot{\varepsilon}_{0e}$ is the pre-exponential factor with electricity applied, $\dot{\varepsilon}_0$ is the pre-exponential factor without applied electricity, x is the average number of metallic ions that form a dislocation, t is the acting time of the electric current, n is the number of free electrons in a unit volume of metal, γ is the electrical conductivity, k is the Boltzmann constant, T is the absolute temperature and J is the electric current density. Later on, Li and Yu [83] proposed another formula to calculate the decrease in flow stress in pure copper with applied current pulse. In this study, the free energy exchange capacity of dislocations was obtained by using the quantum theory. The relationship between electric current and strain rate can be established and designated as:

$$\dot{\varepsilon}_e = \dot{\varepsilon} \exp(\frac{x 3 N_e}{4 n E_0} \Delta E \frac{t}{\tau}) \quad (15)$$

where $\dot{\varepsilon}_e$ is the plastic strain rate with applied electricity, $\dot{\varepsilon}$ is the plastic strain rate without applied electricity, x is the average number of metal ions consisting a dislocation, N_e is the number of free electrons in metal, n is the number of metal ions, E_0 is the Fermi energy at absolute zero, ΔE is the increment energy of electrons under the electric field force and t/τ is the function time of electric current.

The size of recrystallized grains affected by electric current has also been explored analytically. In 1990, Conrad et al. [85] proposed an expression to describe the process of grain growth as follows:

$$\left(d\bar{D} / dt \right)^{-1} = K_G^{-1} \left(\Delta F_0^{-1} + K_R t_A \right) \quad (16)$$

where \bar{D} is the grain size, K_G is the grain boundary mobility constant, K_R is the second order kinetics dislocation annihilation constant, t_A is the annealing time and F_0 is the driving force at $t_A = 0$. Based on this equation, Hu et al. [86] explained for the occurrence of finer recrystallized grains under current pulse. Due to the promoted annihilation of dislocations under current pulse, K_R was significantly increased.

To quantitatively estimate the constitutive behaviors of materials in EAF, many physical and phenomenological models have been developed to capture different thermal and athermal effects.

However, due to the existing debate over the various electroplastic phenomena in different materials, a well-accepted methodology is still lacking. Accurate constitutive modeling in EAF relies on the in-depth understanding of the thermal and the athermal physical mechanisms, which requires more detailed and fundamental studies

2.4 EAF-assisted forming process

EAF processes have been widely employed in various manufacturing scenarios, especially for hard-to-deform alloys, via electrically-assisted sheet metal forming, bulk forming, wire/tube drawing, etc. Compared to the commonly employed hot forming technologies, EAF has been proven to be more efficient and energy-saving by directly introducing current to the workpiece. The heating process thus requires much less time and the heat loss during the handling of workpiece is also much lower. In addition, the equipment is also less complicated and more flexible by removing the heating devices, thermal insulation facilities, etc.

2.4.1 *Electrically-assisted sheet forming*

For sheet forming, EAF is mainly used in stamping, rolling, bulging and incremental forming.

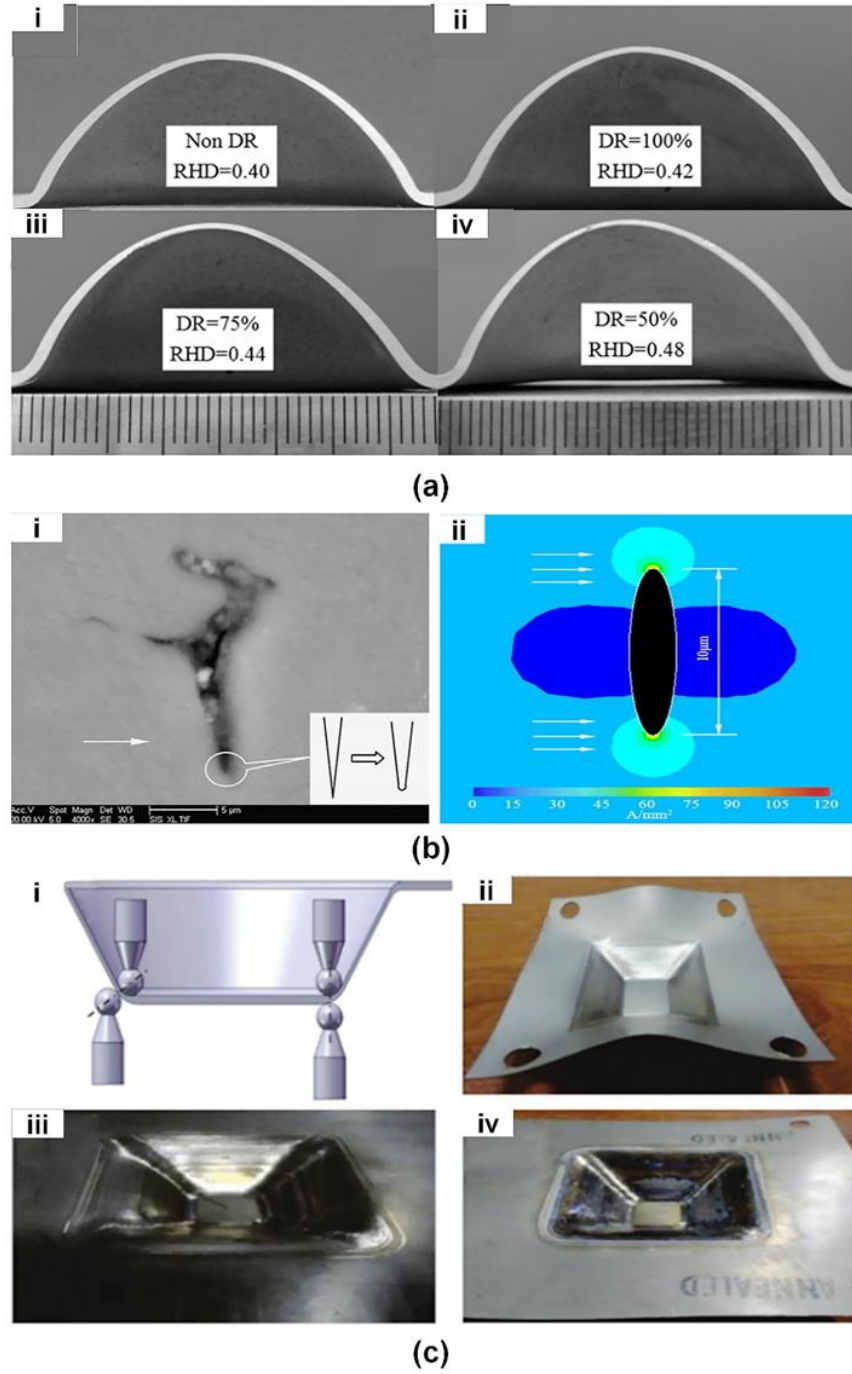


Fig.8. Electrically-assisted sheet forming. (a) cross-section graphs of AZ31 magnesium alloy samples of EA gas bulging forming with varying duty ratios: (i) non-pulse current; (ii) duty ratio of 100%; (iii) duty ratio of 75%; (iv) duty ratio of 50% [29]; (b) Passivation effect of current on the tip of microcrack [29]; (c) Forming tool and formed components of the EA incremental forming: (i) assembly; (ii) no current; (iii) 80A; (iv) 140A [87].

In EA stamping process, Song et al. [88] investigated the feasibility of current pulse treatment (EPT) for enhancing the mechanical properties of TC4 alloy by reducing the yield stress and yield-to-tensile ratio during the plastic deformation. The study found that the introduction of current pulse helped reduce the stamping force and the tendency for springback.

In EA rolling process, Klimov [89] revealed that the strength and plastic properties of Ti, Cu, and Al were enhanced as the degree of deformation increased upon EA rolling. Subsequently, Zhu et al. [90] successfully rolled the NiTiNb strips from 1.89 to 0.5mm aided by current pulse. For cold rolling, cracks were revealed to occur when the total thickness reduction reached 47%. In comparison, the critical thickness reduction was 74% when the electropulse was introduced. More recently, EA rolling was also used in other fields. For instance, Ng et al. [91] joined sheet metals by EA rolling and found the binding force was clearly increased. Moreover, the advantages of EA rolling were utilized to emboss a microtexture onto the surface of sheet metals [92].

In the EA bulging process, Li et al. [29] improved the formability of AZ31 magnesium alloy with the assistance of current pulse during the gas bulging process. With the peak current density of 45 A/mm^2 , the limit ratio of height to diameter reached 0.48, as shown in Fig. 8 (a), which is 20% higher than compared to conventional forming. The current pulse was revealed to be concentrated at the tip of the cavity (Fig. 8 (b)), leading to the crack blunting. Therefore, the stress concentration was substantially reduced contributing to the restrained crack growth.

Incremental sheet metal forming technology combined with current pulse was proposed by Fan et al. [93] to improve the formability of hard-to-form sheet metals. The method was found promising in forming magnesium alloy and titanium alloy parts. The technology was also studied by Xu et al. [94]. A double-sided incremental forming machine with two spherical-ended tools connected to the power source was constructed to form pyramid shaped components, as illustrated in Fig. 9c. By utilizing inner water cooling and rolling ball end tooling, Liu et al. [95] successfully reduced the surface wear and improved the surface quality in electrically-assisted incremental sheet forming. An analytical model for calculating the local temperature in electrically-assisted incremental forming was developed by Magnus [96], and the method was also verified by forming of Ti6Al4V sheets. Compared to the traditional incremental sheet forming, it was found that the introduction of electric current led to lower forming forces, reduced springback and enhanced formability.

2.4.2 *Electrically-assisted bulk forming*

In terms of bulk forming, EAF has been employed in compression and drawing processes. Salandro et al. [97] found that the introduction of electric current in compression processes can transform TC4 alloys with high strength and low ductility into highly formable materials. With the electric current, the compressed part was successfully formed to the desired height without failure (Fig. 9 (a)). Mai et al. [98] introduced electro-pulsing to the micro embossing process to improve the formability of SS316. The channel depth was found to increase with the current density at the same load. The plastic deformation of the workpieces in the EA embossing process

was evidently improved while the residual stress was reduced (Fig. 9 (b)). Subsequently, Peng et al. [22] investigated the effect of various parameters such as current density, die geometric dimension, and grain size of the specimen in micro embossing. They revealed that the application of electric current increased the feature height due to the reduced flow stress and better formability.

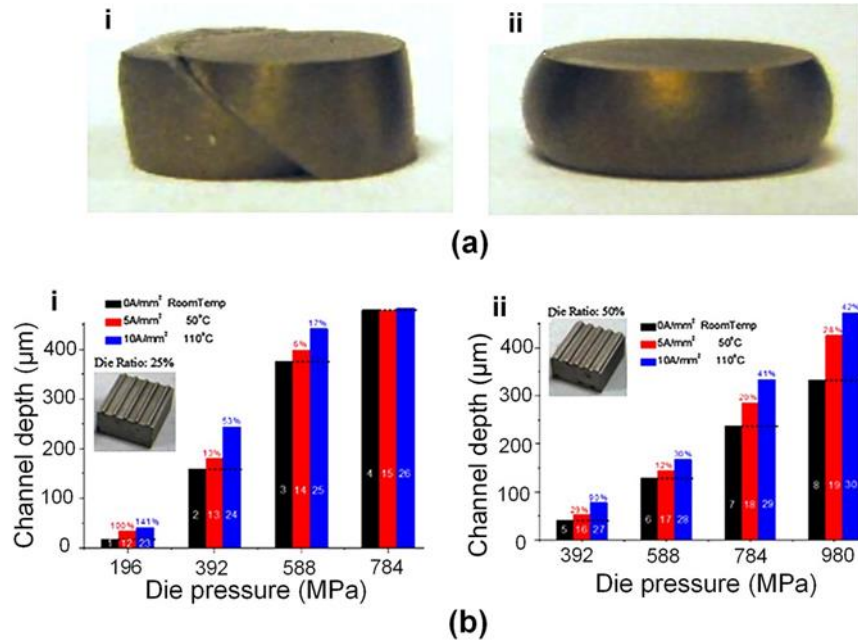


Fig.9. Electrically-assisted bulk forming. (a) TC4 formability improvement with current pulse treatment: (1) Conventional forming; (2) continuous EAF [97]; (b) Channel depth-pressure curves of EA stamping with varying die ratios: (1) die ratio is 25%, (2) die ratio is 50% [98].

In EA drawing processes, the current is mainly employed to decrease the drawing force. For instance, Tang et al. [99] applied current pulse to stainless steels in cold drawing processes and found that the drawing force was remarkably reduced. Furthermore, Zhou et al. [100] investigated the effect of current pulse on the deformation of TC4 workpieces during drawing. Their results showed that high-density current pulse improved the deformability of the alloy grains and led to more homogeneous deformation. Wang et al. [101] took advantage of the thermal effect in the deep drawing of SiCp/2024Al composite sheets. In comparison with the traditional process, better surface quality with less oxidation was achieved due to the high heating rate. Moreover, no microcracks were observed in the workpieces. More recently, Egea et al. [102] introduced current into the drawing of SS308L wire. Compared with the traditional drawing process, they found that the EA process reduced the drawing force and increased the elongation.

2.4.3 Unique electrically-assisted forming process

Due to the scalability of electrically-assisted forming processes, they can be widely applied

to various unique processing technologies. In 2016, Wang et al. [103] introduced pulsed current to the original ultrasonic surface rolling process (USRP) to investigate the effect of current pulses on the surface mechanical properties and microstructures of TC4 (Fig. 10 (a)). It was found that the current pulse effectively facilitated the surface crack healing and improved the surface micro-hardness and wear resistance. In 2013, Potluri et al. [104] studied EA friction stir welding (EAFSW) in order to reduce tool forces involved in the traditional friction stir welding process. They found that EAFSW reduced the feed force by 58% and decreased the torque compared to conventional processes.

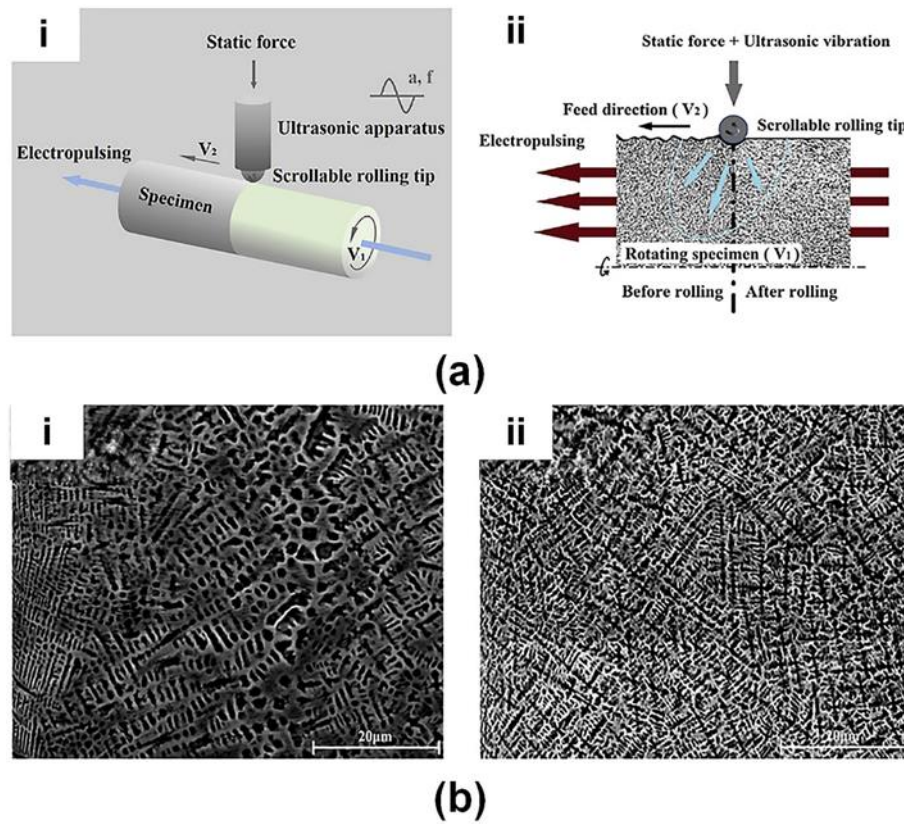


Fig.10. The unique electrically-assisted forming process. (a) Schematic illustration of the electrical-pulsed USRP: (i) setup, (ii) basic mechanism principle [103]; (b) The microstructure of the bionic units processed by laser: (i) processed in water; (ii) processed in water and treated by pulsed current [105].

In addition to surface treatment processes, EAF has also been employed to improve the product performance. For instance, Stepanov et al. [106] investigated the influence of treatment based on direct passage of pulsed electric current (PEC) through the workpiece. The PEC treatment was revealed to be a powerful tool for residual stress reduction and redistribution in the structure elements. Liu et al. [105] applied current pulse treatment on bionic compacted graphite cast iron processed by laser in water. It was found that the current pulse treatment facilitated the

reaction of oversaturated carbon atoms with iron atoms to form Fe_3C . Finally, the microstructures of the bionic units were refined by the electrical pulse treatment (Fig. 10 (b)). In addition, the microcracks on the bionic units were reduced, and the thermal fatigue resistance of bionic CGI was improved.

EAF has been demonstrated as an efficient forming method by reducing flow stress and yield stress, facilitating material flow, reducing springback, tuning microstructure, etc. in various scenarios. With the deeper understanding of electroplasticity, more novel EAF processes will be proposed and developed for different industrial applications

3. Ultrasonic vibration assisted forming

3.1 Working principles

UVAF is a material processing method, in which the ultrasonic vibration with a frequency of 20 kHz or higher is imposed on die tooling or raw material [107]. The main parameters of the ultrasonic-assisted forming technology are the frequency, amplitude and vibration modes which change the material flow behavior during the plastic deformation process, as well as the interfacial conditions between material and die [108,109].

The key components of UVAF system generally include three parts: ultrasonic generator, transducer and concentrator, as shown in Fig. 11(a). Upon receiving the electric power, the ultrasonic generator converts the power into a vibration signal in the transducer, and then transmits the energy to the die through the concentrator. The choice of a proper transducer is determined by the frequency and the required power. There are two types of ultrasonic transducers commonly used, namely, magneto-strictive and piezoelectric transducers. Piezo-electric transducers are much more efficient than the magneto-strictive ones because the losses due to internal friction in the emitter and attachments are smaller and they can also provide a greater amplitude.

Compared with the traditional forming processes, the UVAF technology offers several advantages. First, the material forming resistance is reduced due to the improved lubrication conditions at the die/workpiece interface. Second, the material can be subjected to a greater amount of plastic deformation, and the material formability is enhanced. Furthermore, the surface roughness and the dimensional accuracy of the formed products can also be significantly improved. To clearly explain the improvement effect of UVAF on the properties of materials, the effect of ultrasonic vibration in the tube drawing process is used as an example in Fig. 11(b). Based on the different modes of energy transfer generated by ultrasonic vibration (UV) in the forming processes, the mechanisms of UVAF can be classified into surface effect and volume effect. The surface effect occurs at the boundary between the deformed material and the tool. For example, the UVAF

can alter the frictional state due to the instantaneous separation of the contact between the deformed workpiece and the surface of the forming tools. The volume effect refers to the influence of UV on the flow behavior of the materials as well as the microstructure evolution and behavior such as dislocation slip and texture variation.

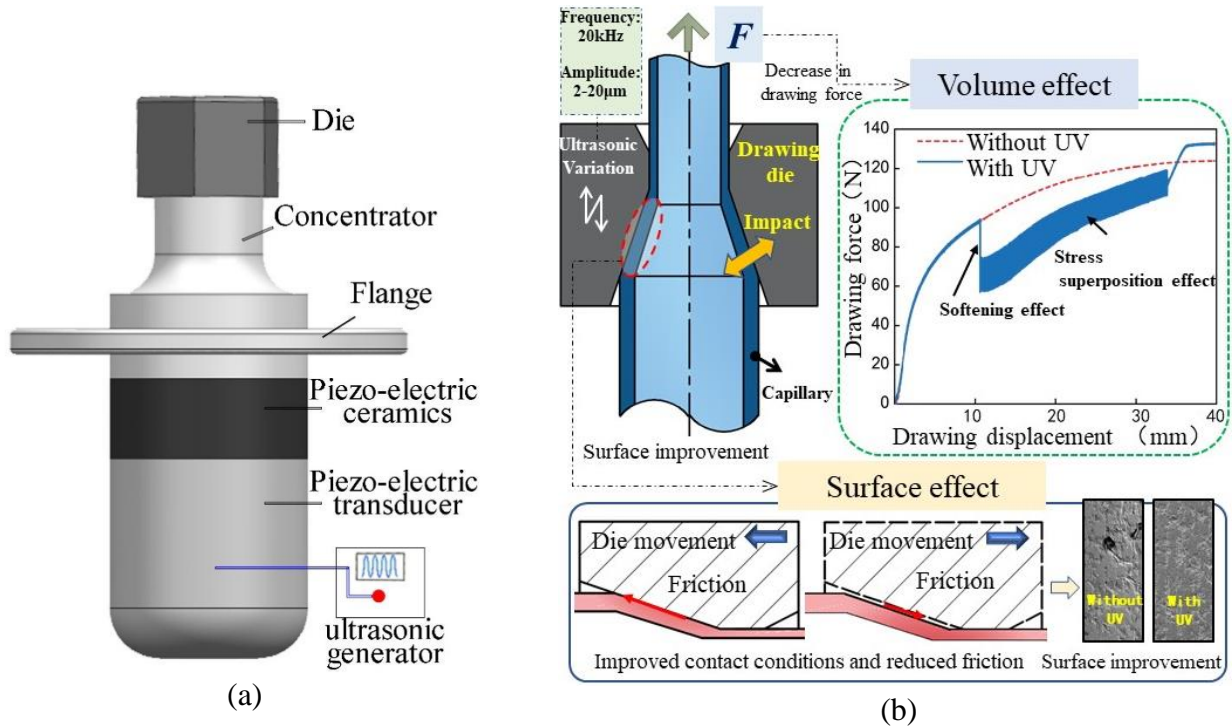


Fig.11. Principle of UVAF: (a) Key components of UVAF system and (b) Effect of UVAF in tube drawing process

3.1.1 Surface effects: influence of UVAF on tribological conditions in metal forming

The surface effect refers to the changes in tribological conditions at the contact interface between die and forming material in the presence of UVAF. These tribological conditions ultimately determine the surface quality and forming limit of the products. Pohlman et al. [110] studied the effect of UVAF on the frictional behavior as early as 1966, revealing that the application of UVAF can reduce the friction. When the direction of UVAF is the same as the direction of the relative motion between the contact interface of the metals, the friction has the minimum value. However, when the relative speed approaches the vibration speed of the contact interface, the frictional force does not decrease further. In addition, Siegert [111,112] pointed out that the friction reduction results from the combined effect of the ultrasonic amplitude and the relative speed between the metals.

The surface quality of the workpiece is also affected by the amplitude and the relative speed of UVAF. Kumar et al. [113] performed a tribological study to determine the influence of UVAF on friction by using the sliding test. Their study showed that vibration in either longitudinal or

transverse directions can be used to reduce the sliding friction between the interfaces, as shown in Fig. 12 (a). Therefore, designing tooling for UVAF should consider how best to propagate the ultrasound at the tool-workpiece interface. To emulate actual process conditions that occur in metal forming processes, Rozner [114] investigated the influence of UV on friction using the strip drawing test. Fig. 12 (b) presents the friction profiles of copper samples with and without ultrasound. For all the samples, a significant drop in friction under the action of UV was observed. The research also reported that the differences in the direction of vibrations and that of friction significantly influenced the effectiveness of ultrasound to reduce friction. For this type of experimental set up, attention should be paid to evaluating the effect of UV on friction due to the fact that the flow stress also changes with ultrasound. In addition, increasing input energy is not the only way to reduce friction, and the friction can be significantly reduced even at lower amplitudes of $0.1\ \mu\text{m}$ [115].

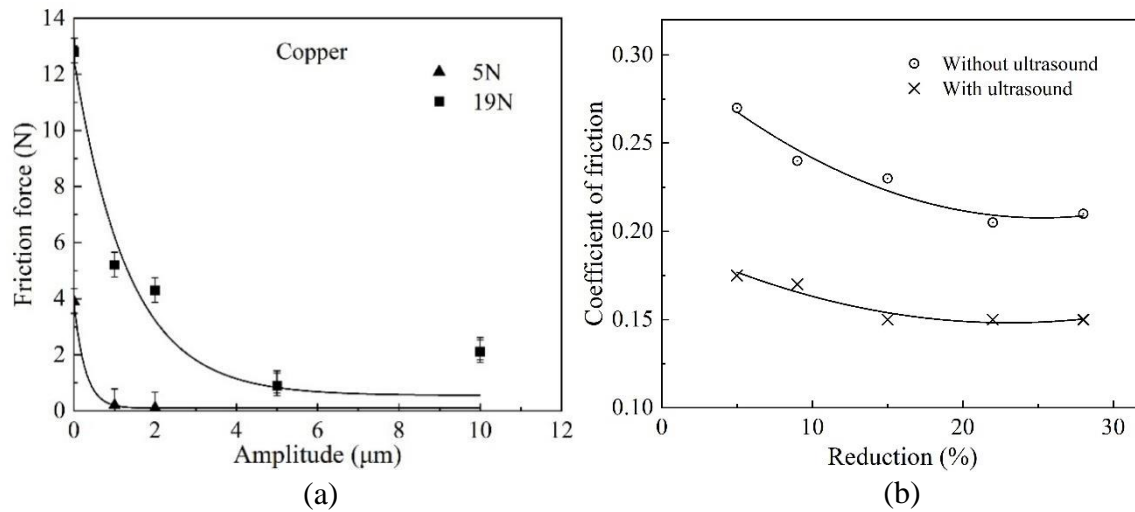


Fig.12. Effect of UV on tribological condition: (a) Friction force versus vibration amplitude for copper [113]; (b) the influence of UVAF on friction [114].

3.1.2 Volume effects: influence of UV on flow stress and forming limit

The volume effect refers to the influence of UV on the stress-strain behavior of the deformed materials in terms of flow stress and forming limit curve. In 1955, Blaha and Langenecker [116] observed a sudden drop in the tensile deformation load when they imposed UVAF on a single crystal zinc rod under tension. In the subsequent research, Langenecker [117] found that the reduction in forming force during plastic deformation under compressive loads was similar to the softening characteristics of materials deformed at high temperature. Even though a number of researchers have experimentally observed the acoustic softening behavior for different materials, the mechanisms underlying this phenomenon are yet to be understood.

Two schools of thought have been proposed and hotly debated over the years to explain the

acoustic softening phenomenon, namely stress superposition and activation of blocked dislocation. The stress superposition effect refers to the application of an ultrasonic vibration field into the plastic forming process to make the forming die resonate. Consequently, the metal is always in a cyclical state of loading and unloading during the plastic deformation, and the stress-strain relationship of the material changes accordingly. In this respect, Kirchner [118] performed compression tests using aluminum alloys assisted by **ultrasonic vibration** with the frequency of 0.5, 1, 10, 50, and 20000 Hz. The results showed that the average load of the material was significantly decreased, and the trajectory of the lowest point of stress and the average stress was parallel to the trajectory when no vibration field was applied. Experimental validation of the stress superposition mechanism has largely been hindered by the lack of measurement of oscillatory force response in ultrasonic experiments. The quantification of acoustic softening in many ultrasonic research studies has been based on the mean stress. In addition, Daud et al. [119] conducted an ultrasonic tensile test using a well-developed test setup capable of accurately capturing the oscillatory force response, as shown in Fig. 13 (a). It can be observed that the maximum path was significantly lower than that of the static stress, suggesting that the acoustic softening was not caused by just stress superposition.

Regarding the activation of the blocked dislocation mechanism, it is assumed that the dislocations, which encounter barriers during deformation can be activated by ultrasound, leading to the decrease in stress. When the metal is formed under UVAF, the peak value of the shear stress required for its plasticity decreases, and it further decreases rapidly when the intensity of the ultrasonic vibration increases within a certain range. Langenecker [117] suggested that the energy of the ultrasonic vibration is concentrated. Consequently, the internal microstructures of the material including dislocations, voids, and grain boundaries, absorb the energy of ultrasonic vibration, thus facilitating the start of dislocation slip. With the increase in accumulation of crystal dislocations, the plastic deformation performance of the metallic materials is enhanced. Schinke [120] studied the softening effect in detail by conducting tensile deformation of stainless steel in UVAF and revealed that the degree of ultrasonic vibration softening was related to the frequency, amplitude, and strain rate.

At present, there are still different views on the physical mechanism of the volume effect. However, many scholars have turned their attention to describing the contribution of different physical mechanisms to the forming process, which helps relate the change of energy in UVAF with the change of dislocation in material, and systematically explain the influence of the volume effect at microscopic level. In the study of UVAF, Lum et al. [121] assumed that the basic plastic deformation behavior of the material remains unchanged, and proposed that ultrasonic softening

is due to pure stress superposition, and that the material deformation resistance is affected by static and high frequency alternating loads [122]. In addition, Daud et al. [123] argued that the softening effect of UV can also be the coupled result of acoustic softening and stress superposition. Sedaghat et al. [124] considered the dislocation dynamics and sound energy conversion mechanism of materials, and accurately described the deformation behavior of metals in UVAF from the perspective of free energy, as shown in Fig. 13 (b). This theory has been applied in incremental forming [125]. To understand the potential mechanism of stress reduction in the UVAF process, Wang et al. [126] established an analytical model that considered both acoustic softening and stress superposition, and expounded the contribution of acoustic softening and stress superposition to the forming process, as shown in Fig. 13 (c). This theory can be well applied to the forming and manufacturing of superalloy capillary (shown in Figure 13 (d)), providing an effective way to coordinate and control the forming quality and mechanical properties of deformed tubular microparts.

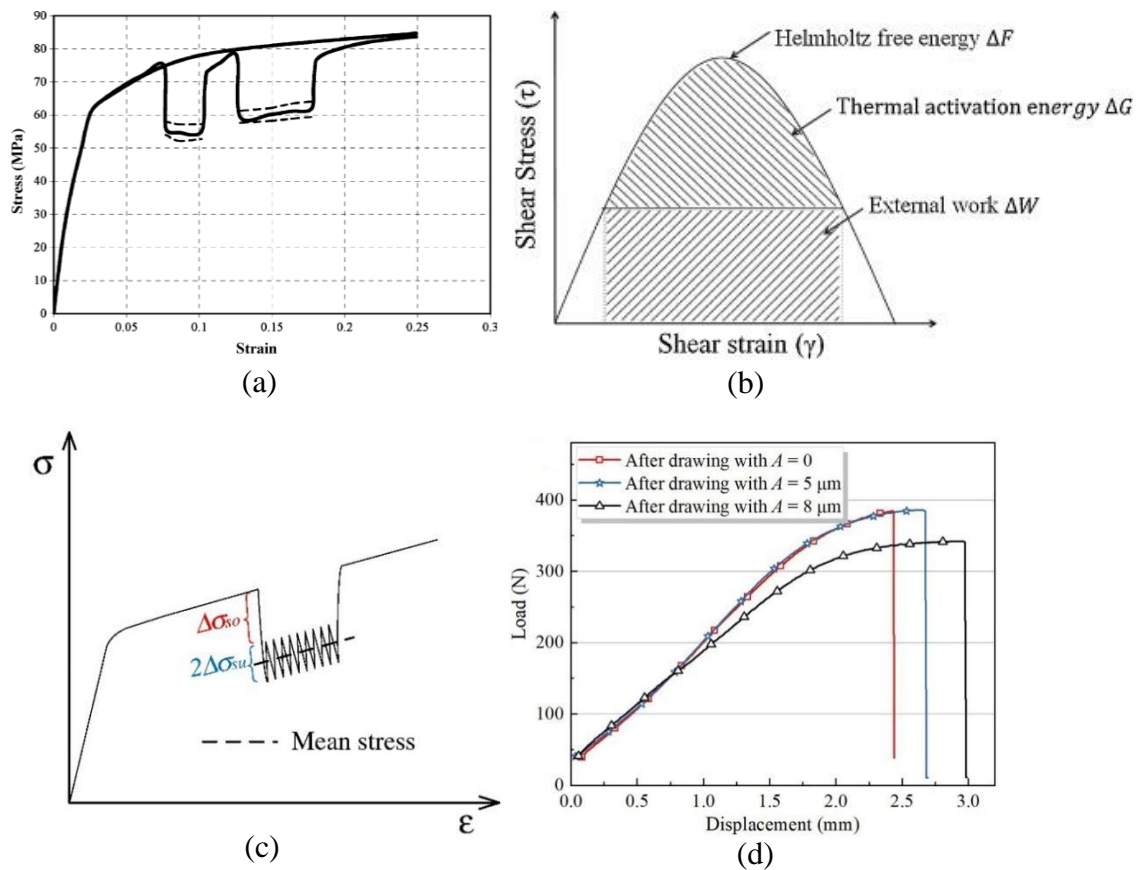


Fig.13. Volume effects of UV: (a) Static-ultrasonic tension test stress-strain curve of aluminum: the solid lines represent the static and mean stress; while the dashed lines denote the maximum and minimum oscillating paths [119]; (b) the relation between Helmholtz free energy, Gibbs free energy and external work [124]; (c) schematic diagram of stress reduction due to ultrasonic excitation: acoustic softening ($\Delta\sigma_{so}$) and stress

superposition ($\Delta\sigma_{su}$) [126]; (d) mechanical property of the fabricated capillaries after UVAF [127].

3.2 Mechanical behavior and microstructural evolution

3.2.1 Mechanical properties and constitutive model

As discussed in Sections 3.1.1 and 3.1.2, the softening effect of UVAF on material crystals improves the material formability and enhances the tribological conditions at the tool-workpiece interface, which is the theoretical basis for the subsequent UVAF. This section further reviews the studies on UVAF from the aspects of mechanical properties and modeling efforts. Several researchers have conducted finite element numerical modeling to investigate the UVAF. Accurate depiction of the process can only be possible after developing reliable constitutive models, which also require better understanding of the mechanisms that cause acoustic softening behavior.

At present, extensive theoretical and experimental studies have been conducted on the "softening effect" of ultrasonic assisted forming, clarifying the deformation characteristics of a variety of materials under ultrasonic fields. For example, Kirchner et al. [118] observed a significant reduction in the forming load by superimposing low-frequency ultrasonic vibration on the static deformation of metal. A low-frequency excitation force was applied in the static compression test during the plastic deformation to verify the oscillating stress superposition effect. Nevertheless, there are also differences in response to the "softening effect" under the superposition of UV stress for different materials [128]. Consequently, although the stress superposition effect can explain part of the softening effect of UVAF on the constitutive behavior of metals, the decrease in the average forming load measured in the ultrasonic vibration assisted process of some metals cannot be explained by this effect. Therefore, the softening mechanism may involve one or several other mechanisms [129,130], including reduction of internal and contact friction [131], dynamic effects of high-frequency vibration tools [132], thermal effects [133,134], and absorption of sound energy at dislocations [135]. For metal forming processes involving contact between the sample and the die, such as upsetting, drawing, and extrusion, numerous researchers have reported the reduction in the average forming load by carrying out experiments (with and without UV) under different lubrication conditions. Perotti [136] conducted upsetting experiments for copper, lead and aluminum billets and demonstrated that the drop in the measured stress was mainly due to the reduction in friction at the interface between die and workpiece. The reduction in the interface friction due to the application of ultrasonic vibration has also been explained by the cyclic reversal of friction [137-139]. Although the influence of UV on tribological conditions can be simply assessed by testing with different lubricants, the actual

quantification of reduction in the forming load associated with the surface effect or volume effect is a challenge. Many research works have shown that the softening effect of UV is closely related to the dislocation movement inside the materials [140]. Yao et al. [141] established a material constitutive model featuring acoustic softening based on the theory of crystal plasticity and the dislocation evolution relationships. This model takes into account the vibration amplitude, time, and ultrasonic residual hardening. Based on this model, Prabhakar et al. [142] integrated the Kocks-Mecking (KM) theory to describe the acoustic softening behavior. The acquired constitutive model can be expressed as follows:

$$\begin{cases} \sigma = \sigma_a + \sigma^* \\ \sigma_a = M\alpha Gb\sqrt{\rho} \\ \dot{\varepsilon} = \dot{\varepsilon}_0 \exp\left(\frac{\sigma}{\sigma_a}\right)^m \\ \frac{d\rho}{d\varepsilon^p} = k_1\sqrt{\rho} - k_2\rho \\ \Delta\sigma = C_1 E^{C_2} \end{cases} \quad (17)$$

where the flow stress σ is composed of the temperature-independent terms σ_a and σ^* affected by heating effect, ρ indicates the average dislocation density, A is the ultrasonic amplitude and ω is the vibration angular frequency. This model can match the above parameters together and can be easily implemented in the commercial finite element code. In addition, the residual hardening can be incorporated into the model as a unit.

The application of UVAF in the forming process of miniaturized parts is becoming increasingly promising. It is well known that when the dimensions of parts and components are millimeter level or below, their mechanical properties and responses change and become more dependent on grain size. This phenomenon is known as size effect [143]. Therefore, in the UVAF of microparts, the combined influence of size effect and ultrasonic vibration should be emphasized and considered. In tandem with this coupled effect, Hung et al. [129] conducted ultrasonic-assisted compression experiments on micro-column parts with different dimensions and several grain sizes. They found that the size effect had a significant impact on the forming force, but little impact on the mechanical properties of material. In addition, Shahrokh [140] conducted the ultrasonic assisted compression test of 316 stainless steel micro-rings and discovered that the friction coefficient at the contact surface increased with the reduction of the sample size. Furthermore, UVAF has a larger effect on the reduction of frictional coefficient than the ultrasonic softening effect. Meng et al. [127] investigated the UVAF of difficult-to-deform superalloy materials at microscale. The study found that the softening effect and the residual effect of UV had a saturation threshold value. The absorption capacity of the ultrasonic energy was found to be the main factor influencing the saturation point. Since the energy produced by UV is absorbed by local defects

such as dislocations, vacancies, and microvoids, the absorbable ultrasonic energy density inside the material eventually tends to a saturation value and reaches a threshold. The material flow stress drop caused by the post-acoustic softening effect tends to be saturated. By inputting ultrasonic energy density as a medium, the logistic function is used to modify the quantitative relationship between the amount of stress drop caused by the softening of sound energy and the ultrasonic amplitude, as shown in Eq. (18) [127].

$$\Delta\sigma = R_1 \frac{E(A/2)}{L_0} + \frac{R_2}{1 + \beta_1 \exp(-\beta_2 \omega^2 \rho_m A^2)} \quad (18)$$

where E is the elastic modulus. A is the ultrasonic amplitude, L_0 is the length of the specimen's reduced section, and R_1 is the parameter describing the amplitude attenuation of the ultrasonic wave in the transmission process. β_1 and β_2 describe the increasing trend of the material flow stress softening when the input ultrasonic energy density continues to rise. $\omega=2\pi f$ is angular frequency. ρ_m represents the material density, and R_2 represents the final stable value of the flow stress reduction caused by the softening of sound energy after that the energy absorbed by the material is saturated. R_2 is affected by grain size D , as shown in Eq. (19):

$$R_2 = a + b \cdot D^{-1} \quad (19)$$

Metallic materials are usually affected by the “residual effect” upon ultrasonic-assisted deformation. After the ultrasound stops, the stress-strain response of the material does not completely return and overlap with the conventional deformation curves. The difference in the flow stress value and the hardening index shown in the stress-strain curve is caused by the residual effect of UV [126]. Numerous scholars have studied the mechanical properties of materials under ultrasonic fields to understand the changes caused by UVAF, as shown in Fig. 14. Zhou et al. [144] discovered that when the ultrasonic energy was sufficient, titanium only showed residual softening effect, while aluminum specimen exhibited the residual hardening phenomenon. Meng et al. [127] found that under different ultrasonic amplitudes, the flow stress of a superalloy reduced at the moment the UV was activated, and the softening profile maintained a parallel relationship with the base stress-strain profile. With the increase in ultrasonic amplitude, the material stress reduction also increased. At the end of the ultrasound process, the stress-strain curves of each group returned to the vicinity of the conventional curves, as shown in Fig 14(a).

Moreover, Wang et al. [126] observed a stress reduction of approximately 14 MPa in the vibration assisted tensile test of a copper foil with an amplitude of 0.89 μm , and the stress continued to decline with the increase in amplitude. Fartashvand et al. [145] demonstrated that the flow stress of TC4 alloy decreased by approximately 10 MPa after applying UV, while the flow stress is increased by 7.2 MPa after turning off the UV. It was found that the TC4 alloy did not

show the phenomenon of acoustic hardening, and its softening effect was obvious. During the UV assisted compression experiment of aluminum alloy conducted by Yao et al. [146], UVAF also caused a significant softening effect. However, the softening effects of UV on diverse materials are different. For example, the softening effect of superalloys is small compared with titanium and aluminum alloys under the same ultrasonic amplitude, as illustrated in Fig. 14 (a), (c) and (d). In addition, the residual effect is apparent in UV assisted deformation of titanium and aluminum alloys, whereas it is absent for superalloys. Furthermore, there is a clear distinction in the residual effects displayed by titanium and aluminum alloys. The residual stress of titanium is lower than the stress without UV when the amplitude exceeds 4.06 μm . However, the residual stress of aluminum alloy is higher than the flow stress deformed without UV. The response of different materials to UV is very different, so the applicability and forming efficiency of UVAF need an in-depth and insightful investigation.

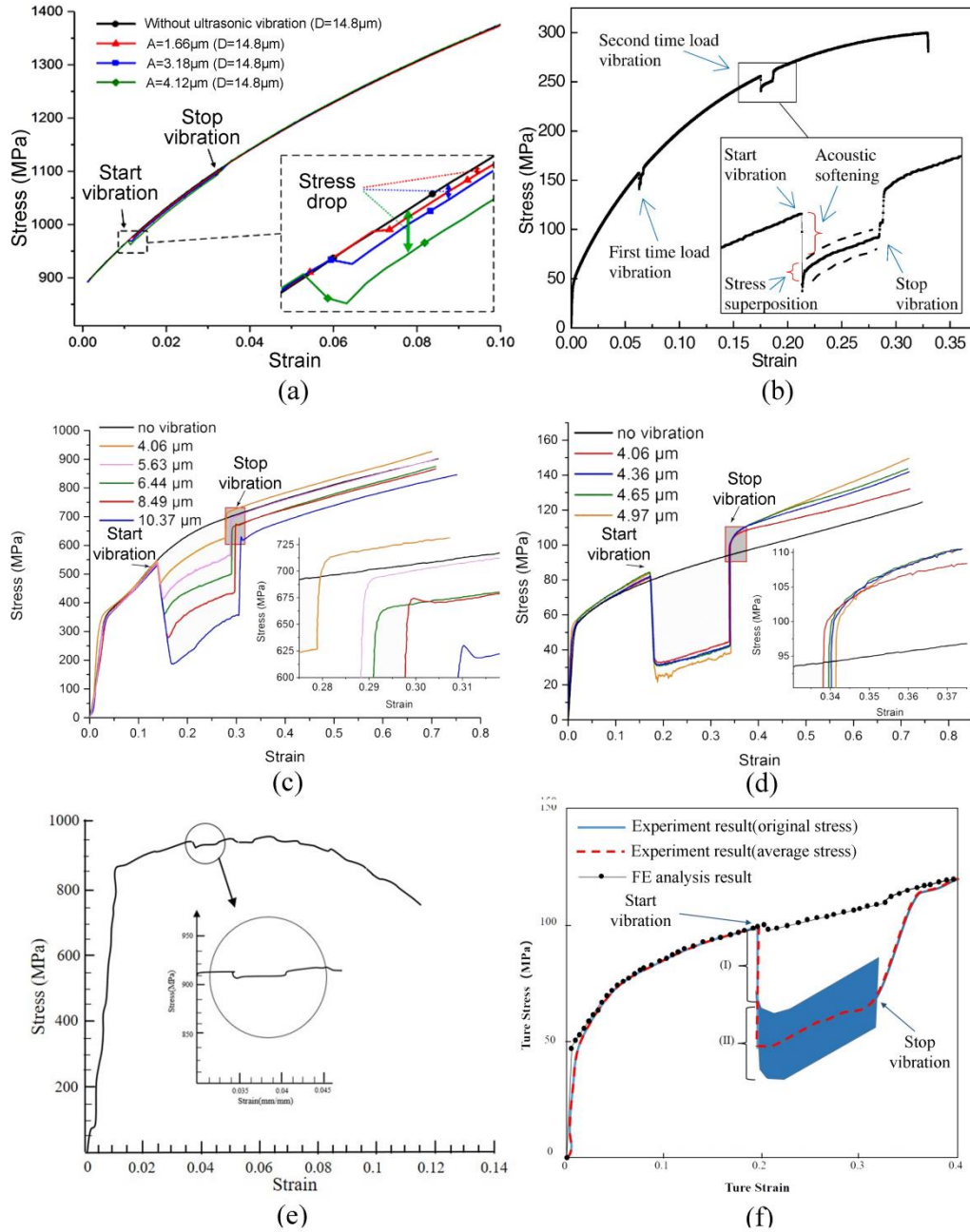


Fig.14. Mechanical properties of different materials under ultrasonic vibration: (a) Inconel 718 [127], (b) Copper foil [126], (c) titanium [144], (d) aluminum [144], (e) Ti-6Al-4V alloy [145] and (f) Titanium alloy [146].

3.2.2 Microstructural evolution

The abundant research studies carried out over the years on UVAF have demonstrated that the forming load can be reduced and the forming quality can be improved. There is potential to further advance the in-depth understanding because recent experiments have demonstrated that the impact of UV on material structure remains worth studying. Research efforts to explore the microstructure evolution in UVAF may be helpful and critical to uncover the physical essence and mechanisms behind the phenomena.

The effect of ultrasonic vibration on the mechanical behavior of metals is essentially related to

the microstructure. Siu et al. [147] observed that a large number of subgrains were formed in the ultrasonic assisted micro-indentation test of aluminum. The dislocation dynamic simulations revealed that the enhancement of dipole annihilation is one of the potential mechanisms. Furthermore, Dutta et al. [148] conducted an UV assisted tensile test on low-carbon steel, and revealed that the dislocation density and the proportion of low-angle grain boundaries all decreased. This was because the energy of ultrasonic vibration is more likely to be selectively absorbed by local areas such as dislocations, vacancies, and grain boundaries inside the material, and the energy required to achieve the same softening effect as thermal assistance is smaller [149]. The internal microstructures of materials, such as dislocations, voids, and grain boundaries, absorb the energy of ultrasonic vibration and increase the activity of materials. This facilitates the start of dislocation slip increases the accumulation of crystal dislocations, and enhances the plastic deformation performance of metallic materials.

In addition, UV is conducive to the initiation of the twinning mechanism [150]. Compared with the slipping mechanism, the twinning mechanism requires large shear stress, and it mostly occurs at the locations where the slipping motion is obstructed and the stress concentration appears. These stress concentration locations are mostly manifested as the intertwining of dislocations. Ultrasonic vibration wave can be transmitted almost without energy loss at the location with favorable structural consistency in the crystal grain, especially in the forming process of meso/micro-scaled parts. However, this high-frequency vibration cannot continue to transmit due to the structure formed by the dislocations at the stress concentration area. The energy is absorbed easily by the dislocation structure, activating the twinning mechanism. On the other hand, UV promotes the twinning mechanism to refine the grains. The excitation effect of ultrasonic vibration on the formation of twins is mainly attributed to the material being in a deformed state similar to a high strain rate under the ultrasonic field. Under this scenario, the local area in the material is more likely to produce stress greater than the critical twin stress in the high-speed plastic deformation process [151]. Furthermore, Meng et al. [152] found that when the propagation process of ultrasonic vibration energy was hindered by twins in ultrasonic-assisted forming of Inconel 718 sheet, the ultrasonic vibration energy was transformed into the kinetic energy for twinning excitation and movement, as shown in Fig. 15 (a) and (b). The fraction of twin boundary was altered when ultrasonic vibration was superimposed, and the proportion exhibited an upward trend with the increase in amplitude. The increased twin crystal planes promoted the dislocation multiplication and the grain refinement speed.

The influence of UV on microstructure evolution is also reflected in the elimination of microstructure defects, which is beneficial for the processes such as additive manufacturing,

because the parts with fewer pores and cracks can be produced, as shown in Figs. 15 (c) and (d) [153]. UV provides radiation pressure to change the interface between the metal and the internal gas, leading to the collapse of the precipitated pores, thereby refining the microstructure; the average grain size produced is smaller at the scale of 2~5 μm . The increase in thermal gradient caused by the additional ultrasonic energy accelerates the solidification, which in turn promotes the reduction of grain size. Moreover, the dynamic behavior of acoustic flow and cavitation creates a large instantaneous pressure in the liquid material [154, 155]. The pressure in the sound field breaks the tip of the columnar grains, resulting in a transformation from columnar to equiaxed grains. With the increase in ultrasonic frequency, the grain size is further reduced due to more ultrasonic waves [156]. The refinement of microstructure enhances the tensile properties and microhardness. These findings clearly indicate that the application of UV is an effective strategy to improve the mechanical properties and microstructural performance of the deformed workpieces.

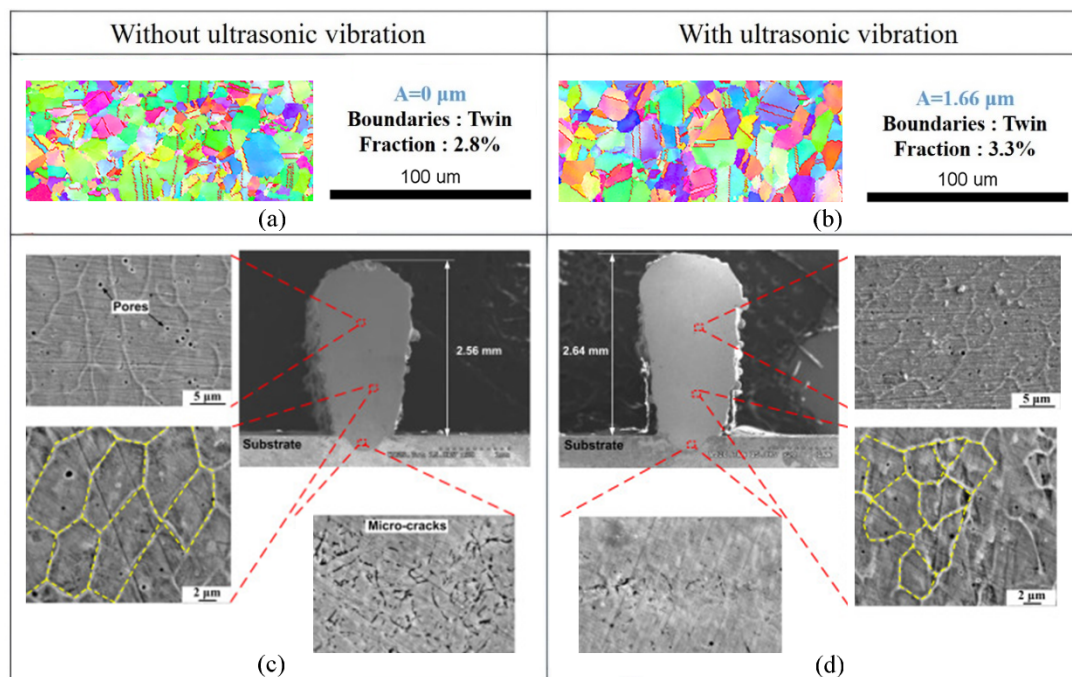


Fig.15. Tensile test of Inconel 718 with (a) and without (b) UV [152], and additive manufacturing with (c) and without (d) UV [153].

3.3 Processes of ultrasonic vibration-assisted forming

3.3.1 Ultrasonic vibration-assisted sheet metal forming

At present, industrial production of components from sheet metals at either macro, meso or micro scale generally employs the traditional forming methods. The prospects for transforming UVAF technologies from research laboratories to industrial application are promising, particularly for making miniature products (meso-micro scale). This is largely because ultrasonic power

needed for ultrasonic vibration system is relatively small for making the meso/micro-scaled parts. Sheet metal forming processes at macro-scale, which do not require large forming load such as incremental sheet forming processes, are also ideal and promising application scenarios for UVAF technologies.

Considering the effects of different materials and vibration frequencies, the limiting draw ratio (LDR) of cup-shaped parts with UV was increased by 15-25%, using an oscillation frequency of 20 to 28 kHz [157]. The changes in LDR and the punch force are shown in Fig. 16 (a) and (b). In ultrasonic vibration assisted micro-drawing of sheet metals, the forming force decreased with the increase in oscillation amplitude [158]. It was also observed that LDR increased with the increase in wall thickness. For sheet metals with thicknesses of 50, 75 and 100 μm , the LDR increased to 0.6, 0.7 and 0.7, respectively. Studies on sheet forming have also shown that UVAF can reduce the coefficient of friction between sheet metal and die, thus preventing wrinkling and crack defects [159-161].

Recently, the demand for complex curved parts has gradually increased, and their forming technologies have also gained more attention. Incremental sheet forming (ISF) is a sheet manufacturing technology that can produce free-form surfaces without die. The complex stress state generated during ISF stabilizes the material and suppresses necking. Compared with the traditional forming processes such as stamping and hydroforming, the sheet forming limit in ISF is significantly higher. In this respect, Li et al. [162] introduced UVAF into ISF based on the advantages of ultrasonic vibration in plastic forming. In the resulting method named US-ISF, ultrasonic source was employed to apply a regular vibration load to the tool and enable the tool to periodically squeeze the metal sheet along the axial direction. Fig. 16 (c) and (d) illustrate the effect of US-ISF, where the increase in frequency caused a decrease in contact time between the tool and the sheet when the frequency was less than 40 kHz, which was contrary to the trend of the frequency greater than 40 kHz. Therefore, the surface curvature can be controlled to improve the surface quality of the sheet by adjusting the amplitude. In addition, Cheng et al. [163] applied UVAF during the single-point (UA-SPIF) and double-point incremental sheet metal forming (UA-TPIF). Longitudinal UV was applied to a hemispherical single-point incremental sheet metal forming tool at an oscillating frequency of 20 kHz, through which a variety of conical shapes were formed. In the UA-TPIF, a 45° conical backing die was used. Studies have shown that there is a positive correlation between the oscillation amplitude and the reduction in forming force as shown in Fig. 16 (e) and (f). The axial forming force dropped when UA was turned on and reached a steady state value. The area where the ultrasonic vibration was applied had a local thickness reduction.

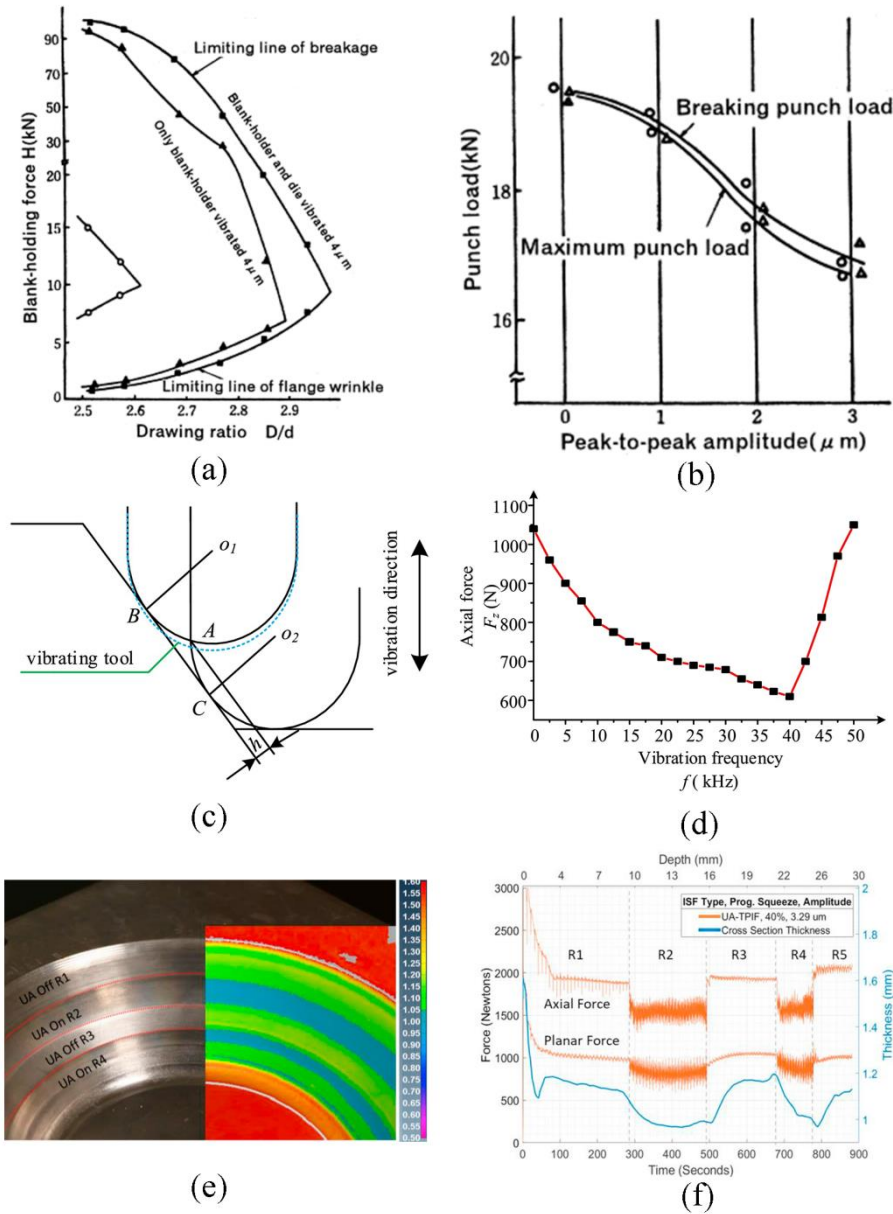


Fig.16. UV assisted sheet forming: Effect of 28 kHz oscillation on the LDR (a) and punch load curve (b) in ultrasonic vibration assisted deep drawing [157], Sheet metal deformation map (c) and relationship curve of forming force and ultrasonic frequency (d) in US-ISF [162], Macro image of part and 3D thickness color plot in mm (e) and relationship curve of forming force and time in US-SPIF & US-TPIF (f) [163]

3.3.2 Ultrasonic vibration assisted wire drawing and tube forming

UV is widely used in wire/tube drawing because the ultrasonic vibration can reduce the forming load and improve tribological conditions. The influence of UV on friction and forming load was studied by Winsper et al. [164] in 1969. After superimposing ultrasonic oscillation on wire drawing, the drawing force was reduced by 50%. Although ultrasonic vibration has multiple loading modes, the mechanisms underlying load reduction are not fully understood. To obtain a greater benefit from oscillatory energy, the length of the wire to be drawn must be equal to an

integer number of the half wavelength of the drawn material. Generally, the reduction in force is attributed to a combination of three mechanisms, i.e., localized heating generated by superposition of the ultrasonic oscillations, stress superposition mechanism, and decrease in the friction force at the die/workpiece (wire) interface.

After the early work of Winsper et al. [164], numerous researchers have investigated different aspects of UV assisted wire drawing. The major findings are the decrease in drawing forces as well as the possibility of reducing wire drawing pass [165,166]. The different loading directions of ultrasonic vibration also have an important influence on the forming process. The vibration signal can be applied either parallel or perpendicular to the drawing direction. Experimental studies have shown that when the vibration direction is perpendicular to the drawing direction, a strong resonance effect occurs and vice versa [167-169].

As the tension changes periodically, the surface of the drawn tube becomes uneven. Applying ultrasonic vibration parallel to the drawing direction has a substantial influence on the surface roughness of the workpiece [170]. Fig. 17 describes how UV can improve the surface of a drawn wire; the larger the amplitude, the smoother the surface of the drawn wire. In addition, during the tube drawing process, applying UV to the mandrel can significantly reduce the drawing force, thus reducing the friction between the mandrel and the tube. This phenomenon increases the accuracy of the inner surface of the drawn tube. Meng et al. [127] studied the UVAF of Inconel 718 thin-walled capillary with an outer diameter of 1.5 mm and a wall thickness of 50 μm through finite element simulation and experimentation. A substantial reduction in the drawing force was observed. With the increase in the ultrasonic amplitude, the dimensional accuracy, surface roughness, and uniformity of the capillary tube after each pass were enhanced. Furthermore, the peeling off of material and other microscopic defects were also restrained. Therefore, the application of UV in forming processes not only requires less energy, but also concentrates ultrasonic energy in a small range of deformation area, achieving an accurate control of dimensional accuracy and microstructural performance.

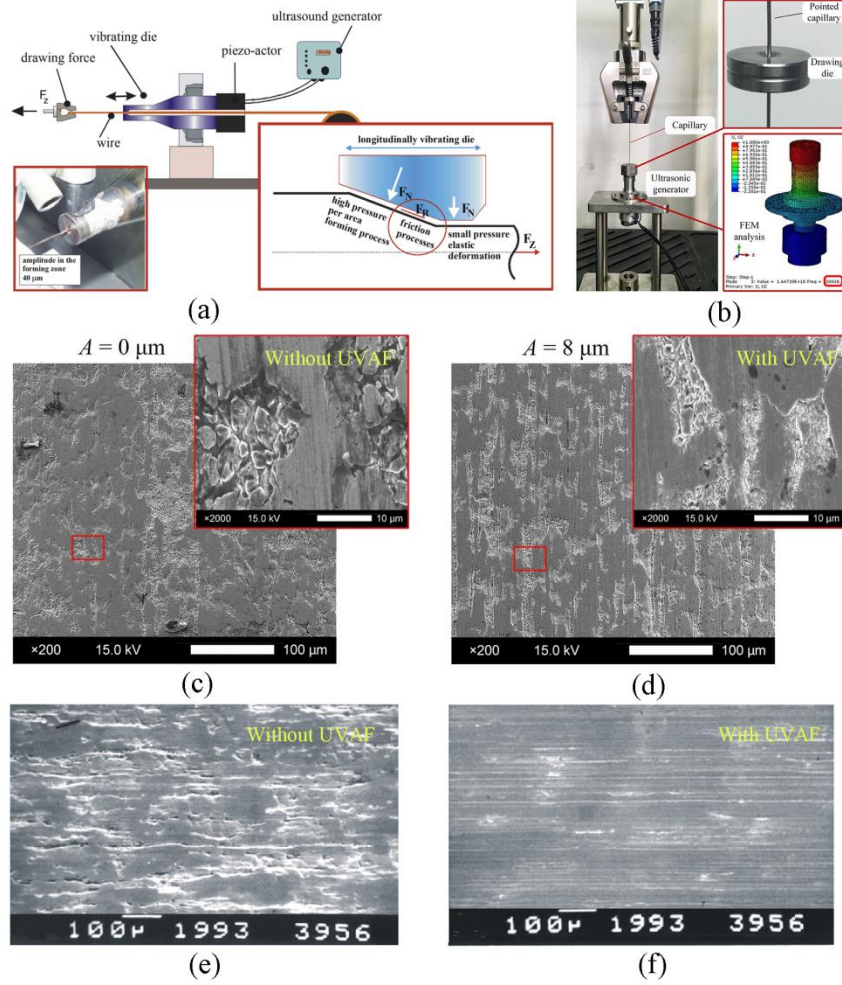


Fig.17. UV assisted tube drawing: Experimental setup (a) for Ref. [170], (b) for Ref. [127]; Surface morphology without ultrasonic variation (c) for Ref. [127], (e) for Ref. [170]; Surface morphology with ultrasonic variation (d) for Ref. [127], (f) for Ref. [170].

3.3.3 Ultrasonic vibration assisted bulk forming

Bunget and Ngaile [171] carried out ultrasonic extrusion experiments, and found that the forming load was reduced by 23% and the surface quality of the sample was also significantly enhanced. The maximum extrusion load for brass samples without UVAF was 8000 N, which was reduced to 6000 N when UVAF was applied. For a billet size of 1.93 mm in diameter, the extrusion load of 8000 N resulted in the compressive stress of 2700 MPa at the punch. This stress exceeded the yield stress of most hardened tool steels. In other words, the cold extrusion of the part would not be practical using the conventional forming methods, which clearly demonstrates the benefits of UVAF. **Different from other forming methods, the impact caused by high frequency vibration on the surface effect in bulk forming needs to be considered.** Zhuang et al. [172] used a 25 kHz high-frequency ultrasonic vibration device to perform compression tests on 1050 aluminum and found that UVAF reduced the flow resistance and improved the surface morphology, as shown in

Fig. 18 (a), (d), (g) and (j). The force reduction level was proportional to the amplitude. The stress superposition and interface effects were considered to be the two main reasons for force reduction. Wang et al. [173] developed a transverse UVAF apparatus and used it for cylinder upsetting of Ti-45Nb alloy, as shown in Fig. 18 (b) and (e). The increase in vibration amplitude enhanced the acoustic residual hardening effect. In addition, when the vibration unit stopped, the stress and strain displayed a linear relationship, and the slope increased with the increase in vibration amplitude. With the increase in amplitude (Fig. 18 (h) and (k)), the grain refinement became more obvious, and the high angle grain boundary decreased from 81.3% to 43.3%. The increase in dislocation density promoted the formation of low angle grain boundaries. Therefore, UVAF can promote the increase in dislocation ring number and dislocation density.

High frequency vibration can also provide considerable heat for the forming process. This is at the cost of consuming ultrasonic vibration energy, which makes it difficult to evaluate the exact contribution of UV to the forming process. Jäckisch et al. [174] performed UVAF compression experiments with steel C35E at oscillation frequency of 20 kHz. To separate the thermal softening effect from the acoustic softening effect, thermal compression tests were performed at the same temperature slope. It was found that the processing force decreased by less than 5.4% due to thermal softening, while the ultrasonic assisted processing force decreased by 40.9% on average at the same temperature. The control of temperature was also realized in the UV assisted compression experiment of 6061 aluminum alloy [175]. It was concluded that the relatively low dislocation density of the annealed aluminum alloy caused material hardening after turning off the UVAF, as shown in Fig. 18 (f). In addition, by comparing the microstructures given in Fig. 18 (i) and (l), it can be seen that the number of subgrains in the particles was significantly increased.

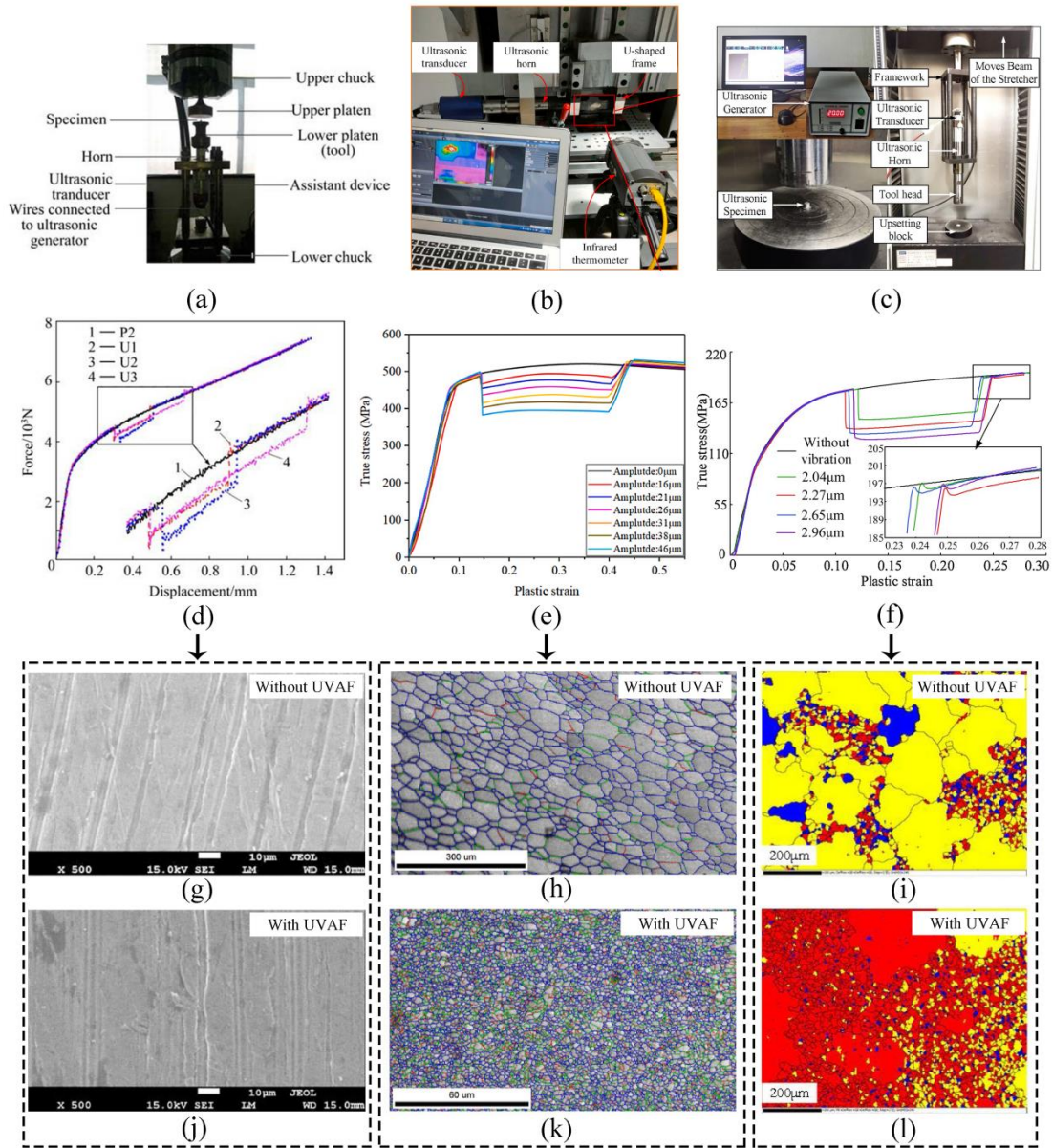


Fig.18. UV assisted bulk forming: Experimental setup (a) [172], (b) [173] and (c) [175]; Drawing force curve (d) [172] and (e) [173] and (f) [175]; Microstructure without ultrasonic vibration (g) [172], (h) [173], and (i) [175]; Microstructure with ultrasonic vibration (j) [172], (k) [173], and (l) [175].

4. Introduction of electromagnetic field in metal forming

Electromagnetic forming (EMF) is a high-speed and contactless impulse forming process which uses a transient pulsed magnetic field to apply Lorentz force to the workpiece to deform. EMF was patented in 1959, followed by years of theoretical and experimental researches. Compared with the quasi-static plastic deformation, the forming limit of materials and the dimensional precision of the workpiece deformed by EMF are significantly improved due to the high forming strain rate. As an environmental-friendly and high-efficiency forming technology, EMF has been

widely used for forming of lightweight and poor formability materials, such as aluminum alloy and magnesium alloy. Thus, EMF technology is a promising manufacturing technology with a wide range of potential applications in aviation, aerospace and automotive fields [11][176-178].

4.1 Working principle and characteristics of electromagnetic forming

The force application in EMF is contactless and no working medium is required. The principle is based on the physical effects described by Maxwell and the mathematical expressions are shown in Eq. (19). Maxwell explained that a temporarily varying magnetic field induces electrical currents in nearby conductors and additionally exerts forces (the so-called Lorentz forces) to these conductors. Subsequent researchers found that the magnetic field strength is sufficient to deform solid conductors, which forms the basis of EMF.

$$\left\{ \begin{array}{l} \oint_S D \cdot dS = q_0 \\ \oint_S B \cdot dS = 0 \\ \oint_S E \cdot dl = - \iint_S \frac{\partial B}{\partial t} \cdot dS \\ \oint_S H \cdot dl = I_0 + \iint_S \frac{\partial D}{\partial t} \cdot dS \end{array} \right. \quad (19)$$

An EMF system mainly consists of a pulse power generator, an exchangeable tool coil, and the workpiece to be deformed. As shown in Fig. 19(a), the core components represent an equivalent resonant circuit including the energy storage with capacitance C , a high current switch, and the energy conduction system (resistance R_{rC} , and inductance L_{rC}) as well as the consumer load consisting of both tool coil and workpiece, with resistance R_{rC} and inductance L_{rC} . The arrangement of tool coil and workpiece defines the process type. The plastic deformation of metallic parts can be achieved through a transient pulse electromagnetic field in the electromagnetic forming. During charging stage, the switch of the charging system is on and the gas switch is off, then the capacitor bank is charged; when the charging stage is finished, the switch of the charging system is turned off and the gas switch is turned on. Then a R - L - C oscillating circuit is formed composed of the inductance, capacitor and discharging circuit. The transient electric current pulse generates a pulsed electromagnetic field around the inductance which can induce a reversed current in the workpiece and generate an induced electromagnetic field. The interaction between the two electromagnetic fields generates a strong time-varying repulsive electromagnetic force between the inductance and the workpiece, which can result in high-velocity deformation of the workpiece [179-181].

The charging energy E_C of this capacitor battery is calculated from the charging voltage $U(t)$ and the capacity C , as follows:

$$E_c(t) = \frac{1}{2} C U(t)^2 \quad (20)$$

The description of damped oscillations can be applied in the following equation:

$$L_{rc} \frac{dI(t)}{dt} + R_{rc} I(t) + \frac{1}{C} \int I(t) dt = 0 \quad (21)$$

The EMF technologies can be classified into three classes depending on the shape of the workpiece, namely, electromagnetic sheet metal forming, electromagnetic tube compression and electromagnetic tube expansion, as shown in Fig. 19(b) and (c). In EMF, sheet metals can be formed by flat tool coils. Tubular workpieces can be compressed by a tool coil located around the workpiece or expanded by a tool coil inside the workpiece [182,183].

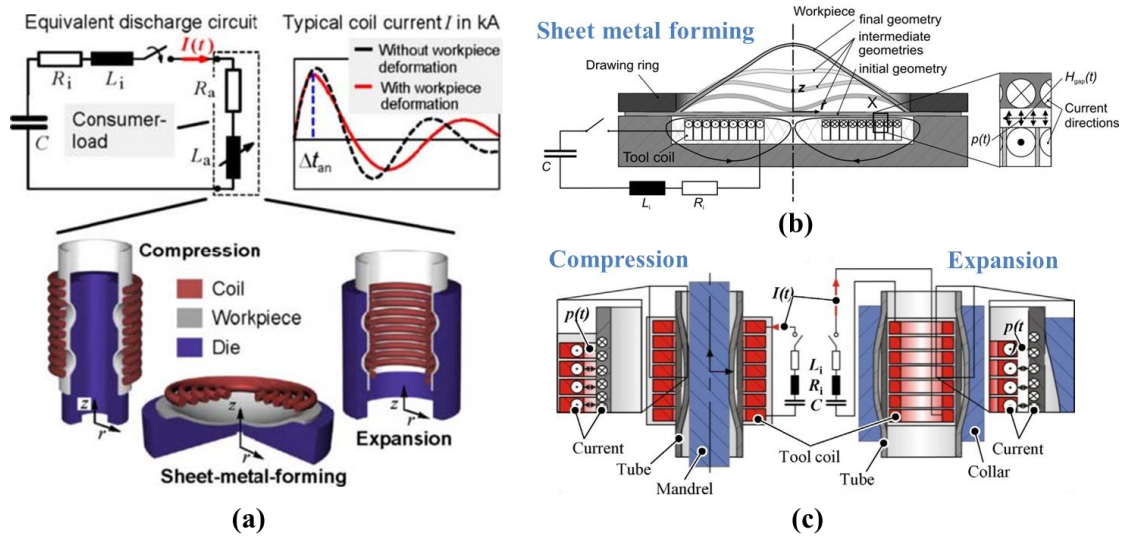


Fig.19. Classification and principle of electromagnetic forming: (a) typical EMF systems and coils types [182], (b) electromagnetic sheet metal forming [11], (c) electromagnetic compression and expansion [183].

During the EMF process, the workpiece is deformed under the influence of multiple factors including electromagnetic pulse, structure and temperature. The deformation velocity can thus reach up to 300 m/s and the strain rate can be in the range between 10^3 to 10^4 s^{-1} . Hence, due to the high-speed impact between the workpiece and die in EMF process, a huge impact force is produced, which can improve the forming limit and formability of materials compared with quasi-static processes. As a result, some problems and issues inherited from the traditional forming processes no longer exist in EMF, which include difficult-to-control material plastic flow, forming failures such as instability, wrinkling, fracture and thickness reduction, uneven stress and strain distributions, and the large and difficult-to control springback. The tooling cost, energy consumption, and pollution emissions during the forming process are also greatly reduced. The

issues of conventional forming processes limit the workability of materials and the capability for making large components and parts, especially for large sheet metal parts, due to their inability to meet the property and quality requirements in fields such as aviation and aerospace industries. However, in EMF, materials exhibit high formability, less wrinkles and reduced springback [184,185]. The typical EMFed components are summarized in Fig.20, including die-less sheet free bulging, sheet stamping, circular hole flanging, tube bulging, tube compression, and tube joining [186-191].

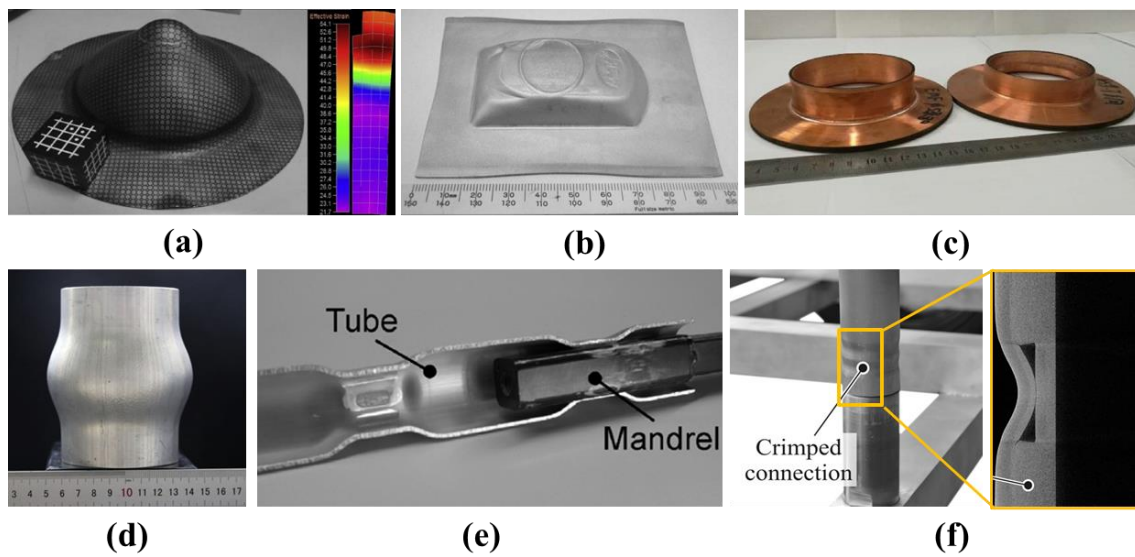


Fig.20. Components processed by electromagnetic forming: (a) die-less sheet free bulging [186], (b) sheet stamping [187],(ASEM Digital Collection)(c) circular hole flanging [188], (d) tube bulging [189], (e) tube compression [190], (f) tube joining [191].

EMF has several unique advantages compared to the conventional quasi-static forming processes. First, the mechanical properties and forming limits of the workpiece material can be improved at high strain rate. Fig. 21 shows the enhanced formability of AA2195-T6 aluminum alloy sheet in electromagnetic bulging and the electromagnetic drawing of EN AW-5083 aluminum alloy cylindrical cup, respectively [192,193]. Due to the contactless force application, it is possible to form covered semi-finished parts without destroying the layer and with improved surface quality. Moreover, high repeatability can be achieved by adjusting the setting of forming machine and the process can be precisely controlled through the adjustment of the applied forces via the charging energy and the voltage. Finally, springback is significantly reduced which simplifies the die design significantly [194, 195]. However, there are some disadvantages of EMF. It is only suitable for materials with high electrical conductivity and low flow stress; only a small part of the charging energy is used for the plastic deformation, resulting in a comparably low

efficiency. Another main limitation for EMF process is the mechanical and thermal loadings of the tool coil [196, 197]. In EMF forming process, the coil wires are subjected to a considerable electromagnetic force, which can lead to the unexpected deformations to destroy the insulation layer and further result in coil failure.

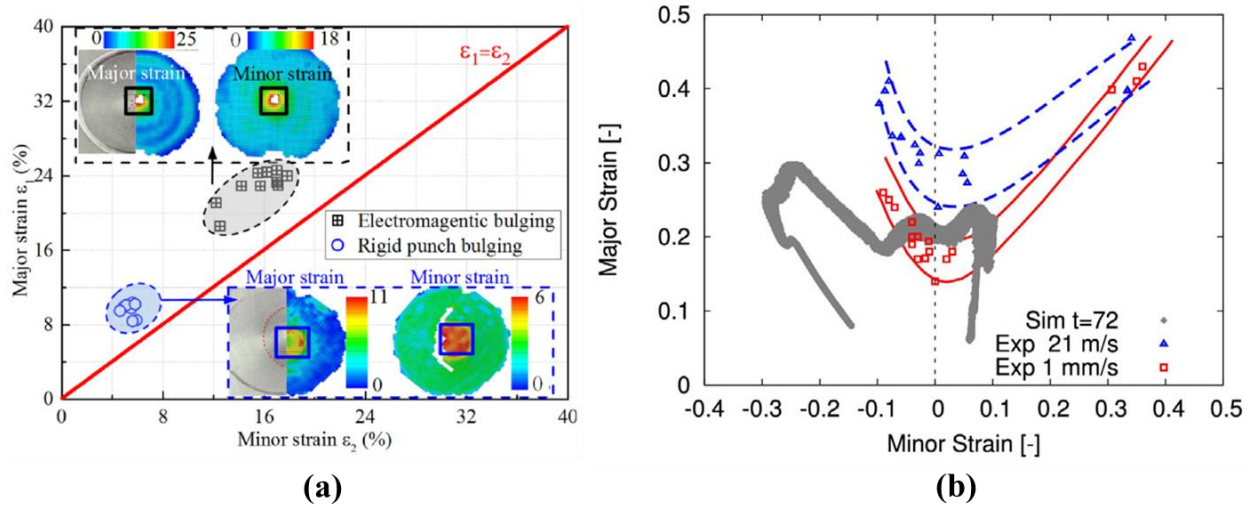


Fig.21. Enhanced formability of materials in electromagnetic-forming: (a) electromagnetic bulging of AA2195-T6 aluminum alloy sheet [192], (b) electromagnetic drawing of EN AW-5083 aluminum alloy cylindrical cup [193].

4.2 Mechanical behaviors and microstructural evolution

4.2.1 Macro deformation behaviors and forming limits improvement

Due to the complex temporal-spatial distribution of the electromagnetic force field and the effects of transient pulsed current, a dynamic non-uniform deformation of material occurs under large strain and large strain rate. This could result in the complicated deformation behavior and mechanism at the macro and micro levels. For the objectives of design optimization and innovation applications of EMF, it is essential to clarify the macro deformation behavior, mechanical response, microstructure evolution and effects of acting loads on the forming quality of the EMFed parts [198]. Compared with quasi-static deformation, the inertial effect is attributed to the increase in strain rate and the rapid loading/unloading of electromagnetic force, leading to the delay of necking development [199,200]. As shown in Fig.22, Su et al. [201] investigated the deformation behaviors of the workpiece in a two-step EMF by combining electromagnetic forming with electromagnetic calibration through simulations and experiments. The results showed that for the two-step EMF, the biaxial tension and plane strain areas are beneficial to forming of the local feature while the uniaxial tension area is detrimental. During the

electromagnetic calibration, the stress distribution in the workpiece is ameliorated, the bending moment is reduced, and the rebound is restricted due to the electromagnetic pulse.

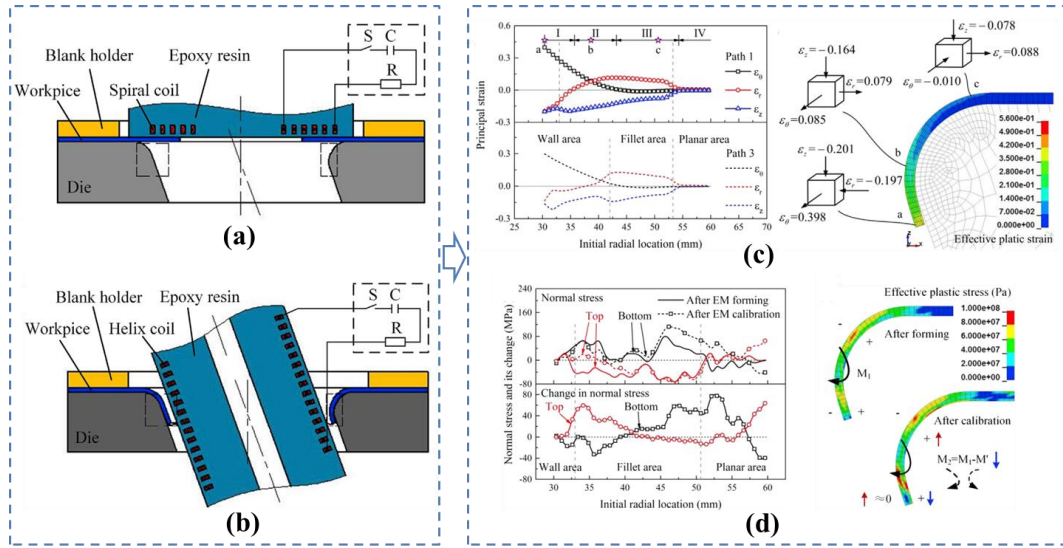


Fig.22. Deformation behaviors of two-step electromagnetic hole-flanging of large-size sheet metal: (a) schematic diagram of electromagnetic hole-flanging, (b) schematic diagram of electromagnetic calibration, (c) strain distribution of workpiece, (d) stress distribution of workpiece [201].

The acting loads depend on many different parameters, mainly classified as machine parameters and tool parameters [202-204], which significantly affect the deformation behavior of the workpiece during EMF process. The key parameters include the capacity, inner inductance, inner resistance, ringing frequency and charging energy. These parameters involve the geometry and the material of the coil, the field shaper properties, and the shape of die/mandrel [205, 206]. Paese et al. explored the effects of discharge energy on the forming height of A1050 aluminum sheet in EMF, as shown in Fig. 23(a). They found that forming limits were enhanced with the increase in discharge energy [207]. In the electromagnetic bulging of AA6061-O aluminum alloy tube, Ouyang et al. found that the tube deformation can be significantly facilitated by multiple discharges using the attractive forming process (Fig. 23(b)) [208]. Thibaudeau et al. optimized the magnetic pressure mode and coil form based on analytical and FE methods, and the deformation uniformity and the final shape of the workpiece were significantly improved (Fig. 23(c)) [209].

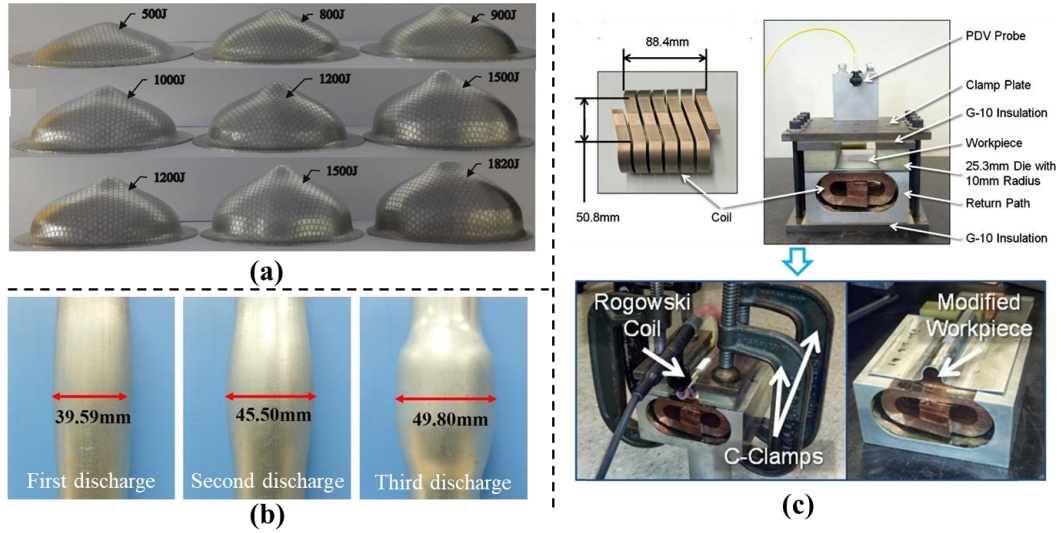


Fig.23. Effects of process parameters on forming limits and accuracy in electromagnetic forming: (a) forming height of A1050 aluminum with different discharge energies [207], (b) deformed AA6061-O aluminum alloy tubes with multiple discharges [208], (c) modified workpiece through optimization design of coils [209].

4.2.2 Microstructural evolution

It is well known that the deformation behaviors of most metals are significantly affected by the strain rate and the strain rate sensitivity of materials is increased with strain rate. In addition, the microstructure evolution, especially for dislocation evolution, is remarkably different from that in the quasi-static deformation [210-213]. To clarify the interaction effect of temperature and strain rate on workpiece behavior in forming process, a deformation mechanism map was proposed by Zhou et al. [214], as shown in Fig. 24. In addition, the rate type deformation equations were also proposed and developed, which can be used to comprehensively model the effect of temperature and strain rate on deformation mechanism characteristics.

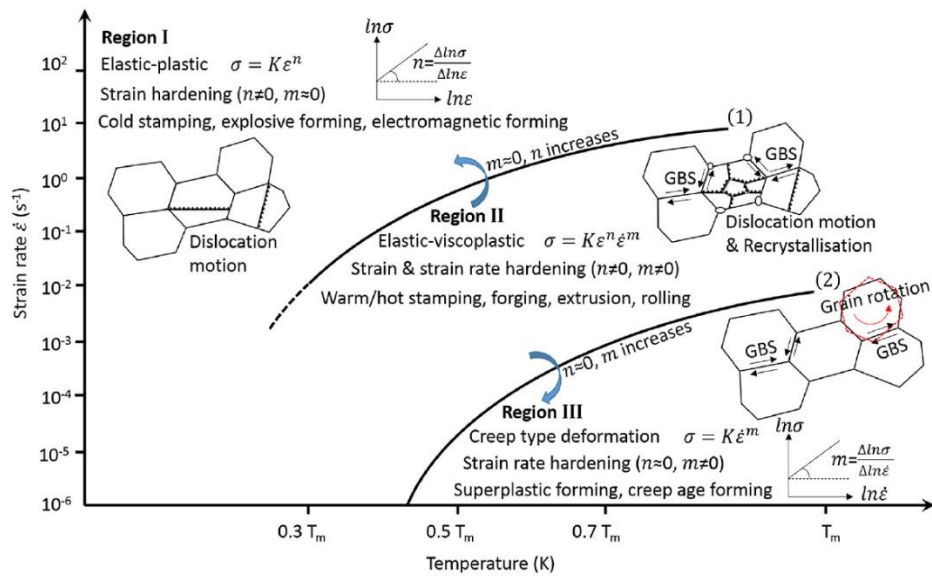


Fig.24. Schematic of the effect of temperature and strain rate on the deformation mechanism [214].

Fang et al. introduced electromagnetic incremental drawing to improve the forming limit of aluminum alloy cylindrical cup. The microstructures at different deformation zones in the components formed by the conventional drawing process and the electromagnetic incremental drawing process were also observed and compared [215]. As shown in Fig. 25, the grain shape was significantly changed during the forming process, and the internal substructure and dislocations of the grains also changed markedly. It can be found that the higher the degree of grain fragmentation, the greater the amount of sub-grain boundary and the higher the dislocation density. In addition, the dislocation density increased notably while the distribution was quite uniform in EMF. Jin and Yu [192] concluded that the forming limit of AA2195-T6 aluminum alloy sheet was obviously enhanced by EMF compared to the conventional rigid punch bulging. In addition, the results showed that the small and equiaxed grains were increased and distributed more uniformly with the increase of the effective strain. The dislocation density and low-angle grain boundaries were increased with strain. Helical dislocations were formed during electromagnetic bulging, which was another reason for the improved hardness of the specimen with the increase in strain. Xie et al [216] proposed the thermo-electromagnetic forming process (TEP), which includes solution treatment, electromagnetic forming (EMF) and aging, to solve the problem of poor formability and avoid quenching distortion of Al-Li alloy at room temperature. The microstructure evolution and strengthening mechanism of Al-Li alloy during TEP were also investigated. As seen from Fig. 26, the results showed that TEP can provide higher density and aspect ratio of T_1 phases compared with conventional thermo-mechanical process. The dislocations formed by EMF were different from quasistatic tensile case in terms of both configuration and density, which further increased the nucleation site of T_1 phase and improved the aging kinetics. Moreover, EMF enhanced the thermal stability of T_1 and effectively inhibited the coarsening of grains.

On the other hand, extensive research has been conducted on material constitutive behavior accompanied by complex microstructure evolution under high strain rate condition in EMF. However, EMF is a complex process with highly coupled multi-physical fields. An in-depth understanding of the coupling effects of the electric, magnetic, and temperature fields with the structural design of the forming workpiece and EMF system on the deformation behaviors, damage mechanics and microstructure evolution of the materials should be taken into consideration.

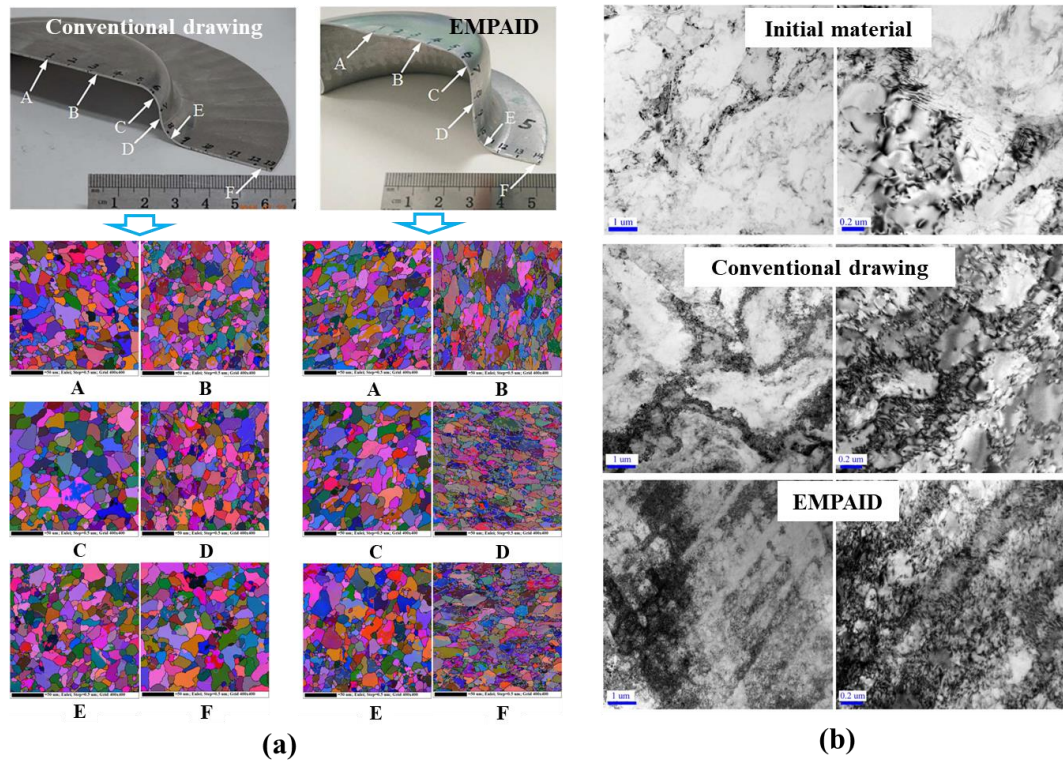


Fig.25. Microstructure difference between the conventional drawing and the electromagnetic pulse incremental drawing (EMPAID) of 5052 aluminum alloys: (a) comparison of the grain morphology in different regions of the workpiece, (b) dislocation distribution from different deformation modes [215].

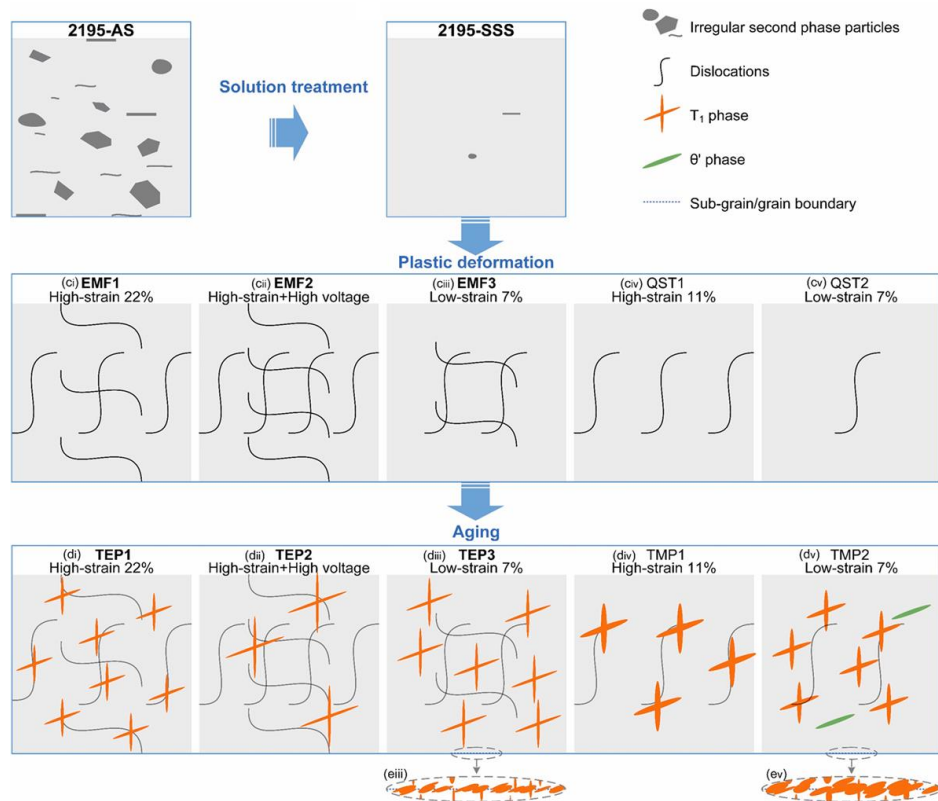


Fig.26. Schematic of microstructure evolution of the materials during the thermo-electromagnetic forming [216].

4.3 Modeling of the electromagnetic forming process

EMF is a complex forming process with highly coupled multi-physical fields including magnetic and temperature fields. The dynamic deformation of the workpiece is a nonlinear process in which the inertia effect, material nonlinearity, geometric nonlinearity and contact nonlinearity should all be considered. It is worth establishing suitable models to reproduce the forming process and investigate the deformation behavior of materials. Generally, the effect of temperature on specimen deformation is neglected because of the limited magnitude of temperature rise. The modeling strategy can be simplified into three analysis steps, viz., the current analysis of R-L-C oscillating circuit, the alternating electromagnetic field and Lorentz force analysis of coil discharge process, and the dynamic deformation analysis of sheet metal under Lorentz force loading [217-219].

4.3.1 Analytical modeling

The analytical model has been considered as a concise and effective method for determining and optimizing the process parameters of EMF. In tandem with this, Weddeling et al. [220] established an analytical model of the electromagnetic form fit joining process to predict the dynamic response of the material and determine the characteristics of the RLC circuit and the charging energy. A pure analytical model was developed by Kinsey and Nassiri for a multi-turn, axisymmetric coil with field shaper to predict the magnetic pressure and velocity during electromagnetic tube compression. The model was electro-magnetic-mechanically coupled with tube position, which affected the magnetic field generated at each time increment [221]. Furthermore, Maloberti et al. [222] proposed an analytical model of the one-turn bulk coil used in EMF process. The pseudo-harmonic solution to the 1D-problem was expanded with the help of Bessel basis functions, including some specific limit conditions and constraints. Compared with the numerical 2-D and 3-D computations, the proposed model gave the numerical value of each parameter, and also provided analytical formulae with explicit dependences upon some key geometrical and physical variables.

4.3.2 Finite element modeling

According to the physical quantities considered in FE simulation, the modeling procedures can be classified as full coupling, loose coupling and sequential coupling [223, 224]. For full coupling, all the coupling field effects are calculated in each element for every time step (all the degrees of freedom are resolved at the same time). The main drawback of this strategy is that it is very time-consuming. Cao et al. presented a full coupling model of electromagnetic sheet forming process which considers the thermal and velocity effects theoretically. Although this approach leads to

higher accuracy than the sequential and loose coupling, the application is limited because it is only available for 2D models and is also time-consuming at present [225].

In the case of loose coupling, the Lorentz forces are calculated without considering the workpiece deformation. These forces are the input loads of the mechanical simulation, which is carried out in one step. This strategy neglects the force evolution during the process due to the geometry change. Hence, it is a less accurate strategy in some cases, but it requires lower computation time [226, 227].

For the sequential coupling, in each time interval, the induced Lorentz forces in the workpiece are calculated with the electromagnetic model, and then automatically transferred as input loads to the mechanical model [228]. In this model, the workpiece deformation is calculated and the geometry is updated in order to transfer it to the electromagnetic model. The Lorentz forces are again calculated and the iterative process is repeated until the forces are negligible. Oliveira et al. [229] proposed a three-dimensional model coupled with electromagnetic field and structure field to study the material plastic flow behavior and sheet die collision behavior in the process of electromagnetic sheet metal forming. The construction of near-field and far-field air units and the interaction between electromagnetic field and structural design of the forming workpiece and the EMF system laid a good foundation for the subsequent mature sequential coupling modeling. Long et al. [230] proposed modeling strategies for simulation of electromagnetic tube and sheet forming processes, as shown in Fig. 27. The results showed that the strategies were valid and time-saving in simulating the forming process. The relative deviation between simulation and experiment was less than 5% and the decrease in computational time-cost was approximately equal to 90%. Sequential coupling has been widely applied in the prediction of EMF process as it realizes the coupling between magnetic field and structural design of the forming workpiece and the EMF system. It also has high calculation accuracy and low time-cost. Fig. 28 shows the comparison of the workpiece profiles between simulations utilizing sequential coupling and experimental results. These profiles include the electromagnetic partition forming of curved parts, coil-less electromagnetic forming of shaping sheet, electromagnetic expansion joining between tubular and flat sheet component, and electromagnetic hemming [231-234].

The current modeling methods mainly focus on the prediction of macroscopic deformation behaviors of materials. Establishing accurate material constitutive models and developing multi-scale modeling approaches are crucial for an in-depth understanding of the microstructure evolution and the physical mechanisms during the forming process, which is also a bottleneck issue which needs to be addressed.

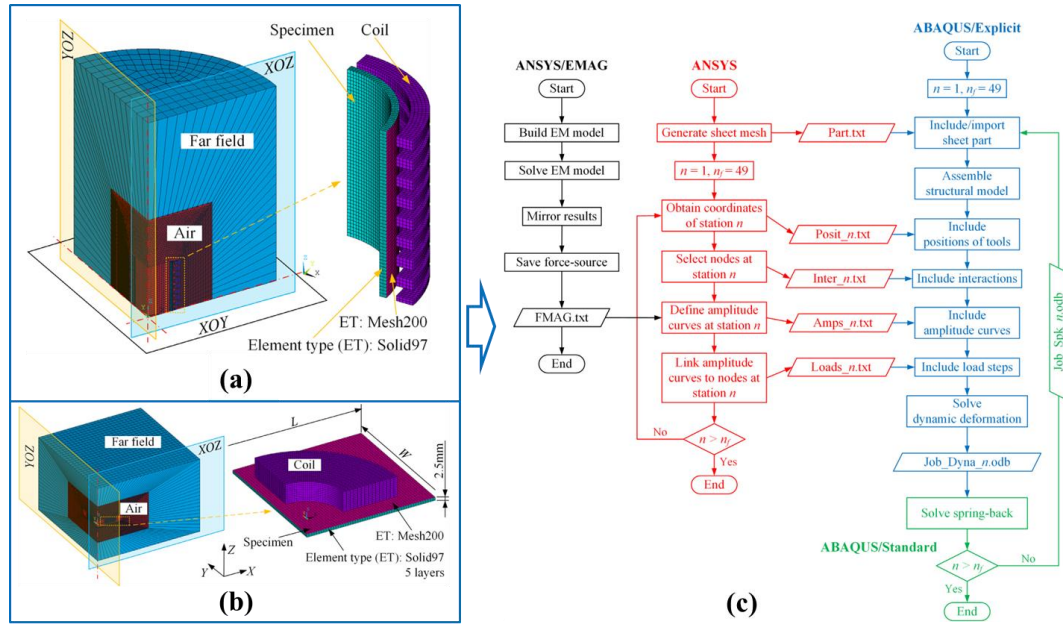


Fig.27. Modeling strategies of electromagnetic forming process: (a) FE model of tube compression, (b) FE model of sheet bulging, (c) Flowchart of the modeling strategies [230].

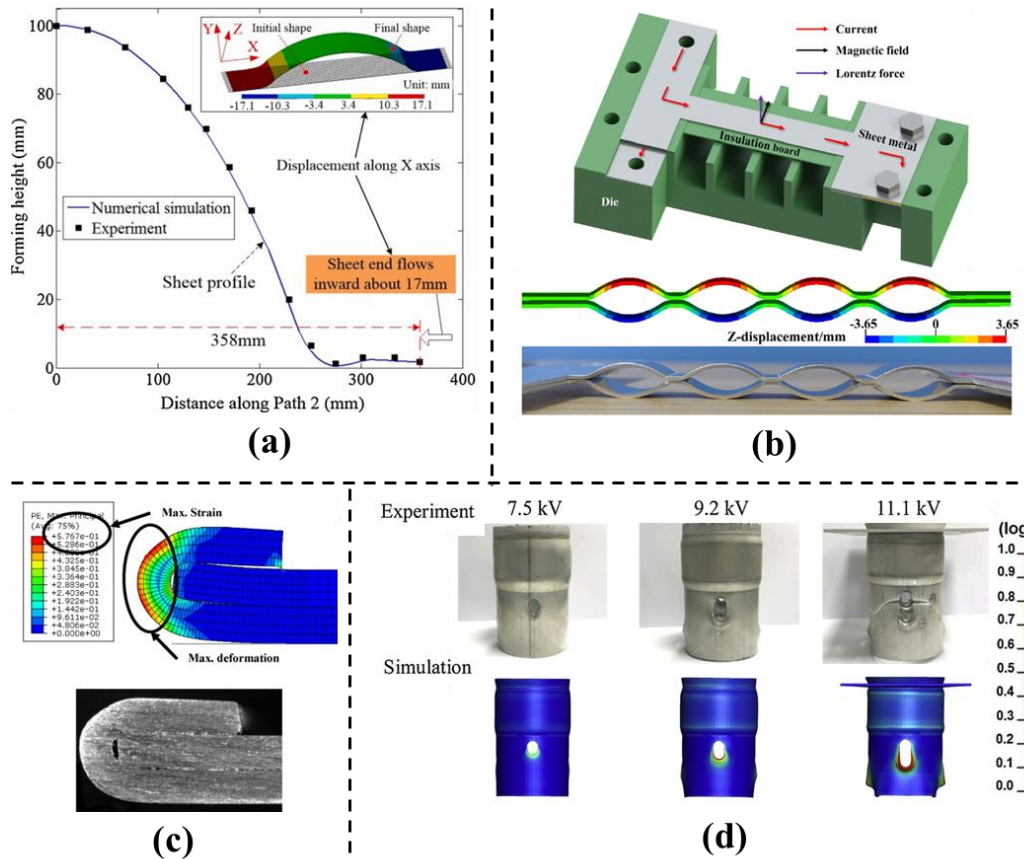


Fig.28. Comparison of the workpiece profiles between simulation and experiment results: (a) electromagnetic partitioning forming of curved parts [231], (b) coil-less electromagnetic forming for shaping sheet [232], (c) electromagnetic expansion joining between tubular and flat sheet component [233], (d) electromagnetic hemming [234].

4.4 Innovative applications of electromagnetic forming

4.4.1 Electromagnetic incremental forming

For conventional electromagnetic sheet forming processes, the coil stays in a fixed position and the sheet metal deforms during an electric discharge. As the electromagnetic force decreases significantly with the increase in distance between the workpiece and the coil, and the electromagnetic force acting time is short, electromagnetic forming is only generally applicable to small workpieces with local deformation [235, 236].

To produce large and complex parts for industrial applications, multi-step EMF technology may be needed. Kamal et al. utilized electromagnetic forces in a two-step method to fabricate a phone face [187]. In the first step, a uniform pressure electromagnetic actuator was used to obtain fine surface details in the part according to the features in the forming die. In the second step, electromagnetic flanging was used to achieve greater depth. Fan et al. [237] proposed an electromagnetic cladding process for manufacturing bimetal tubes. During the multi-step EMF process, the joining cycle is controlled by a sequence of electromagnetic tube bulging steps. The working coil moves to a particular position and the clad tube deforms through many charge and discharge cycles of the capacitor through the working coil. A defining feature of the MPC process is the progressive application of magnetic force on the deformation zone. Based on the principle of single point incremental forming, Cui et al. [238] proposed a new technology named electromagnetic incremental forming, which was proved feasible to form a large aluminum alloy sheet using small working coil and small discharge energy. As shown in Fig. 29 (a), the forming system consists of the energy storage device, working coil, holding device, cables, sheet metal and forming die. During the electromagnetic incremental forming process, the working coil moves and the sheet deforms in many cycles of charging and dis-charging, and finally the local deformation accumulates into the final deformation. The multi-point die electromagnetic incremental forming was proposed for the forming of a large-sized workpiece by Feng et al. [239] which combines electromagnetic incremental forming with multi-point die, as shown in Fig. 29 (b). The multi-point die can be transformed into a surface of different shapes, which can improve the plastic deformation ability and forming efficiency of difficult-to-form workpiece.

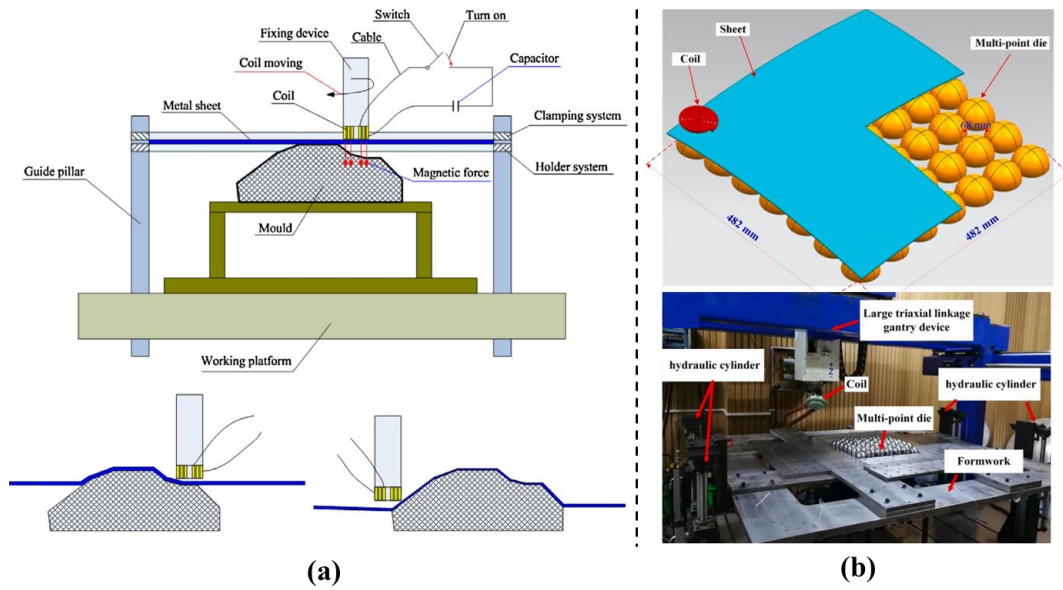


Fig.29. Electromagnetic incremental forming: (a) electromagnetic incremental forming using single coil and convex die [238], (b) electromagnetic incremental forming using single coil and multi-point die [239].

4.4.2 Calibration and springback control

Springback control using traditional stamping often needs many debugging processes as well as tooling repair, which increases manufacturing costs and reduces production efficiency. Applying electromagnetic forming to reduce or eliminate springback has been suggested by many research works [240, 241]. The basic idea is to use electromagnetic forces to introduce an elastic wave that propagates through the blank multiple times and thereby eliminates elastic residual stresses without significant deformation of the part. Experimental results have demonstrated that the magnetic force can contribute to the reduction of springback. Cui et al. [242] revealed the springback decrease mechanism following EMF. It was found that the vibration effect induced an alternating phenomenon of tension and compression that occurred repeatedly in the inner and outer layers of the bent sheet region. As a result, the residual stress was significantly reduced, and the springback was decreased or even eliminated. Cui et al. [243] further introduced electromagnetic stamping with magnetic-force reverse loading to control springback of 5052-O aluminum alloy sheet, as shown in Fig. 30 (a). Du et al. [244] proposed a novel method of electromagnetic partitioning forming with elastic cushion, as shown in Fig. 30 (b). The main principle was based on the fact that the parts vibrate at high speed under the action of the electromagnetic force and the rebound force of the elastic pad. The state of the elastic parts inside the workpiece changes into plastic state, and springback is then eliminated through vibration. A common spiral coil was used to generate the magnetic field.

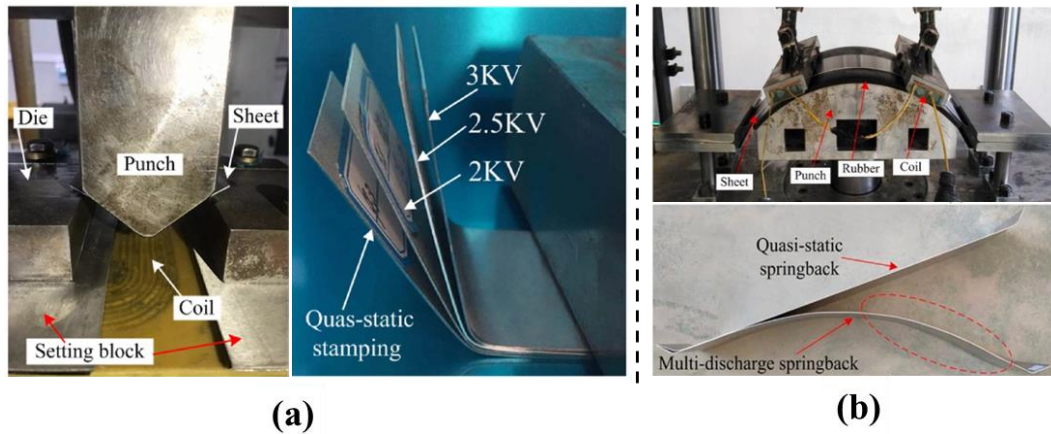


Fig.30. Calibration and springback control of the workpiece through electromagnetic-forming technologies: (a) incremental forming of AA3003-H14 aluminum alloy sheet [243], (b) inverse bending of 5052-O aluminum alloy sheet [244].

4.4.3 Combining EMF with conventional forming

The development and industrial use of EMF do not aim at to compete with but to supplement the conventional forming methods. Innovative approaches combining electromagnetic and conventional forming operations have been developed to exploit the process specific advantages [245-249]. Cui et al. proposed a new method denoted as electromagnetic incremental forming combined with stretch forming, which was adopted for manufacturing large-size and thin-walled ellipsoidal parts [245]. As shown in Fig. 31(a), the sheet with a large local region was formed at a very high speed in a comparatively short time, which improved the material flow. Consequently, sheet thinning was inhibited, the forming limit was enhanced and the forming time was decreased. Imbert and Worswick [246, 247] combined the conventional stamping and electromagnetic forming technologies to reduce the forming radius of AA 5754 aluminum alloy sheet. As shown in Fig. 31(b), a large 20 mm radius sheet was pre-formed from flat sheet using conventional stamping, and the radius was reduced to 5 mm by die-less electromagnetic forming. The results showed that the hybrid electromagnetic corner fill process can achieve corner radius reductions, which is not achievable using conventional stamping operations. In addition, Psyk et al. combined the electromagnetic technology to enhance the forming limits of the conventional hydroforming process [248]. As shown in Fig. 31(c), the electromagnetic tube compression process can be applied to realize an optimized contoured preform for subsequent hydroforming. Starting with a semi-finished part of a medium diameter, the cross-section is locally reduced by electromagnetic compression. This pre-contoured semi-finished part is then used in a hydroforming process to enlarge the cross-section locally and calibrate the preformed regions. Thus, the achievable spectrum of cross section geometries within one and the same part can be increased. Furthermore,

Fang et al. proposed a new approach combined with incremental electromagnetic forming and drawing to enhance the forming height of large size sheets (Fig. 31(d)) [249]. The results showed that the radial electromagnetic force generated by the auxiliary coil reduced the radial tensile stress, which mitigated the crack of the workpiece.

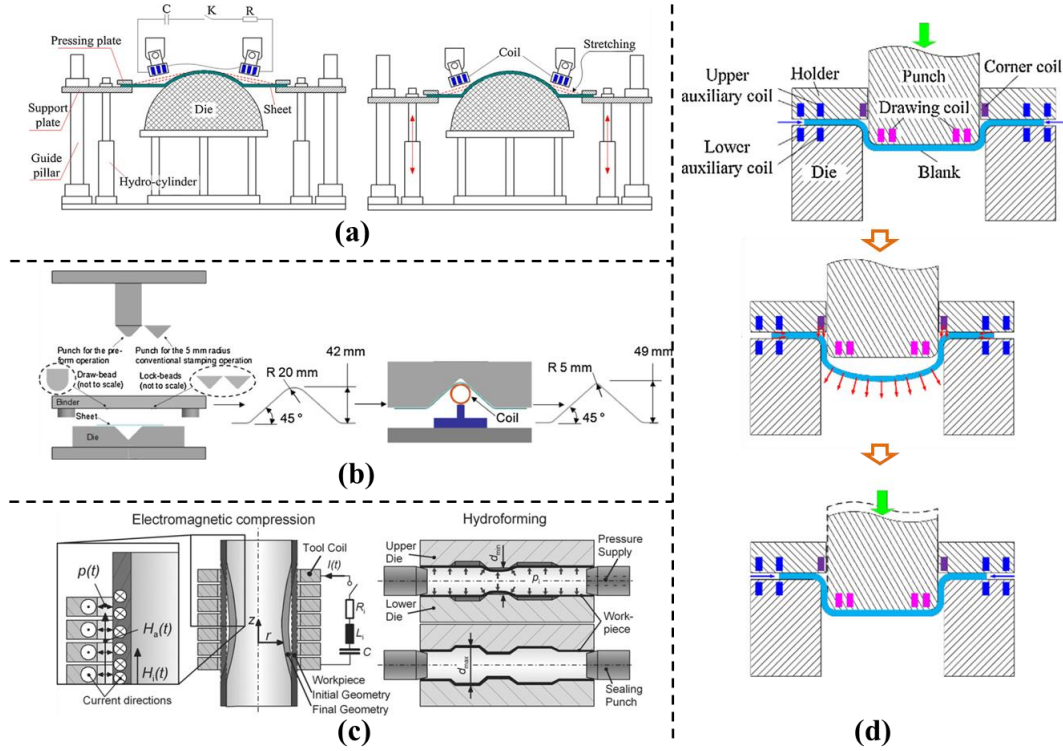


Fig.31. Combined electromagnetic forming with (a) stretch forming [245], (b) stamping [247], (c) hydroforming [248], (d) incremental drawing [249].

The present EMF methods focus on the forming of materials with high conductivity and low strength. For the forming of hard-to-deform materials such as Ti-alloy, the coupling of multi-energy fields (e.g., thermal-electromagnetic, electric-electromagnetic, ultrasonic-electromagnetic) with deformation process can improve the forming limits and forming quality. In addition, EMF can be considered as an effective approach for fabricating workpieces with complex structures made of difficult-to-form materials, which cannot be made by the conventional manufacturing and forming processes. Hence, EMF should be further developed and innovated.

5. Summary and outlook

5.1 Summary

In this paper, the typical energy fields introduced in metal forming processes including EAF, UVAF, and EMF, are reviewed. The working principle and characteristics, mechanical behaviors

and microstructure evolution of materials, advantages and limitations of each process as well as the process capacity and application potential are discussed and summarized (as illustrated in Fig. 32). Compared with the conventional forming processes, the energy field-assisted forming technologies have attracted considerable attention. They have been applied in different industrial clusters for making parts, structures and high-end equipment owing to their advantages, including reduced forming force, improved forming limit, the enhanced dimensional precision, and the reducing of forming defects.

Regarding mechanical response and behavior of the working materials in EAF, the decrease in flow stress, increase in elongation and elimination of springback are the major benefits compared to the traditional forming methods. The thermal and athermal effects induced by the electric current are the two major factors influencing the mechanical behaviors of metallic materials in the forming process. Observation of the microstructure evolution provides unique insights into the influence of the applied current. The unique process features can be summarized as follows: dislocation motion is promoted when the current is applied; recrystallization and phase transformation occur at a lower temperature; and the electric current can lead to unique texture variation and micro-crack healing. The current analysis models based on the thermal effect are mainly focused on the even thermal field effect and local heat effect. For the latter, a quantitative model can be employed to reveal the physical mechanism, which is currently not fully understood.

It is concluded that the UVAF process possesses unique advantages, including improved material formability, reduced interfacial friction and deformation resistance, and enhanced performance of the fabricated parts and structures. The surface effect in the plastic forming process is essentially caused by the friction variation at the contact interface between die and workpiece, which determines the surface quality and forming limit of the formed products. The volume effect, on the other hand, is another key issue to be considered and addressed in UVAF process. Currently, the core mechanism of the volume effect is considered to involve the stress superposition effect and the acoustic softening effect. Due to its substantial benefits, UVAF is expected to gradually become a promising process to play a leading role in manufacturing of super-hard, super-brittle, ultra-thin, and difficult-to-process materials.

EMF is an environmentally-friendly and high-efficiency forming technology, which has been widely used for forming of lightweight and difficult-to-deform materials such as Al- and Mg-alloys. The interaction between the two electromagnetic fields can generate a strong time-varying repulsive electromagnetic force between the inductance and the workpiece, which can cause a high-rate plastic deformation of the workpiece. Many prior works have shown that the forming limit and accuracy of metal sheet and tube can be significantly improved by EMF. Applying

electromagnetic forming as a supplement to the conventional processing technologies could be an effective approach for forming of complex parts and structures.


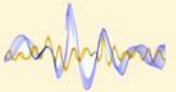
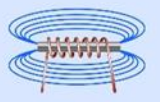
| Energy field | Working principles | Advantages | Limitations | Applications |
|--|--|--|---|--|
| Electric field  | <ul style="list-style-type: none"> • Thermal effect • Athermal effect: <ul style="list-style-type: none"> ➢ Electron wind effect ➢ Magnetic field effect ➢ Skin effect | <ul style="list-style-type: none"> • Reduce deformation resistance • High efficiency heating • Improve plasticity • Reduce springback • Defect heal | <ul style="list-style-type: none"> • Large workpiece requires high power supply to meet current density threshold conditions • Local temperature may not be uniform | <ul style="list-style-type: none"> • Heat treatment. • Rolling, forging, bending, deep drawing, blanking • Incremental forming, creep age forming |
| Ultrasonic field  | <ul style="list-style-type: none"> • Surface effect • Volume effect: <ul style="list-style-type: none"> ➢ Stress superposition ➢ Acoustic softening | <ul style="list-style-type: none"> • Reduce forming force • Reduce friction • Improve surface quality • Avoid forming defects | <ul style="list-style-type: none"> • Complex equipment and relatively low stability • Hard to form workpiece with high strength and complex structures | <ul style="list-style-type: none"> • Wire and tube drawing • Sheet forming and blanking • Surface strengthening |
| Electromagnetic field  | <ul style="list-style-type: none"> • High strain rate • Strong time-varying repulsive Lorentz force | <ul style="list-style-type: none"> • Improve forming limit • Reduce springback • High repeatability • Low die costs | <ul style="list-style-type: none"> • Applicable only for electrically conducting materials | <ul style="list-style-type: none"> • Sheet bulging, stamping and flanging. • Tube bulging/compression • tubular joints fabrication • Cutting, punching, and riveting |

Fig.32. Summaries of the characteristics of metal forming process with the introduced energy field.

5.2 Challenges and prospects

The introduction of energy field into metal forming system/environment has garnered increasing attention in recent years and demonstrated significant advantages and potentials including the improvements of forming limit, forming accuracy and forming efficiency. However, due to the insufficient in-depth understanding of the mechanisms, lack of prediction models, limited process capability and equipment stability, there are still challenges to be overcome and many non-trivial issues to be addressed for the wide applications of introduction of energy field in metal forming process. The challenges and future prospects include in-depth exploration of the physical mechanism, establishment of systematic and accurate prediction models, process innovation through multi-energy fields coupling, and development of high-efficiency and intelligent equipment. These aspects are described in the following and summarized in Fig. 33.

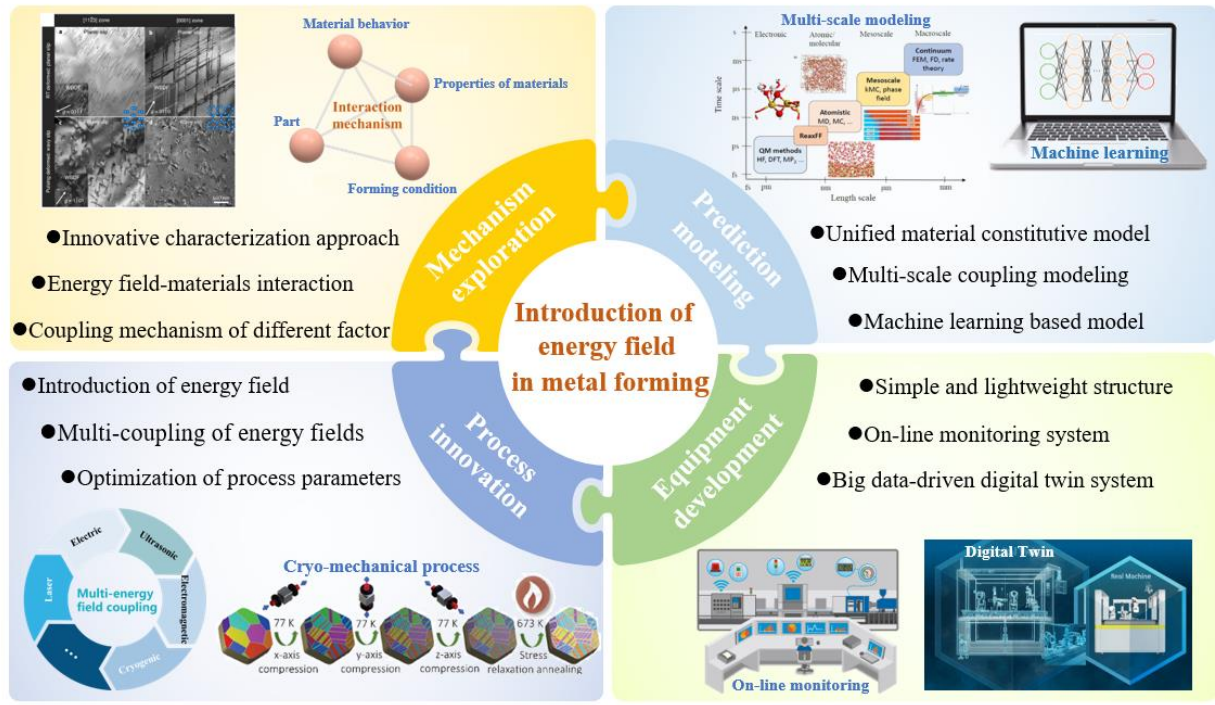


Fig.33. Future prospects for introduction of energy-field into metal forming. Image sources from Refs. [18][250-253]

5.2.1 In-depth exploration of the physical mechanism

To support the product development by using the energy field assisted forming process, a series of solution generations need to be conducted, which include design of formed parts, innovation of forming process route, determination and optimization of process parameters, product quality assurance and control, and the properties tailoring and performance enhancement. In tandem with these, a complete set of theories and knowledge, which describe and unravel the scientific nature of forming mechanisms behind the energy field assisted forming and provide the theoretical fundamentals to support those solution generations, need to be systematically established and tailor-developed for each energy field assisted forming process. To this end, an in-depth exploration of the physical mechanisms behind the energy field assisted forming process needs to be conducted via innovative characterization of forming process and understanding of the interaction among the energy field, materials, part design and deformation of materials, which is affected by the multi-coupling of different factors. On the other hand, energy field assisted forming is generally affected by the multi-coupling of different factors and their corresponding effects, such as the thermal and athermal effects in EAF, the surface and volume effects in UVAF, and the electromagnetic force, thermal effect, and structural characteristics in EMF. All of these effects and their interactions must be decoupled and explored in such a way to form a solid and theoretical

basis for developing the efficient methods to improve the dimensional precision, quality, properties, and eventually the performance of the fabricated parts.

5.2.2 Development of systematic and high-fidelity prediction models

Development of systematic and high-fidelity prediction models is of great significance for in-depth understanding of microstructure evolution, deformation mechanisms, defect prediction, and process optimization in forming process as they are very difficult, if not impossible, to be revealed and understood by traditional experiment approaches. To realize this goal, the current constitutive models may not be able to provide the full solutions as they are mainly developed based on physical measurement and observation, which are more phenomenological nature, rather than more physical essence. On the other hand, the coupling effects of multiple mechanisms have not been fully considered. Therefore, constructing unified constitutive models considering the physical nature is also of importance and has become a crucial issue to be addressed. Moreover, the current available prediction models include the first principles (DFT)-based model, molecular dynamics (MD)-based model, dislocation dynamics (DD)-based model, crystal plasticity (CP)-based model and finite element model (FEM). In view of the complexity of the coupling effects of multi-factors and the interactions between multi-scale deformations, the multi-scale coupling modeling and simulation is a powerful approach to investigating the forming process supported by energy fields. In addition, machine learning (ML) is an alternative potential approach to predicting the mechanical properties and forming quality, if sufficient data is available. Considering the complexity of the energy field assisted forming process compared with the conventional forming processes, the development of ML algorithms based on the sufficient data collection become promising and useful.

5.2.3 Process innovation via employing multi-coupling of energy fields

Introducing energy field into metal forming as a supplement to the conventional processing technologies presents an effective approach for forming of high-performance components. However, considering the limitations of the introduction of single energy field, the employing of multi-energy fields coupling forming technologies would be promising for manufacturing of unique and complex parts and structures. Due to the possible mechanisms involving coupling effects, stacking effects, and the interaction effects, the multi-energy fields coupling technology facilitate microstructure tuning and performance optimization of the deformed parts. Furthermore, new energy fields need to be explored and developed for tailoring the microstructure and properties of materials. For instance, introduction of cryogenic field in forging of titanium alloys

enhanced the strength and ductility simultaneously with the generation of nanotwins [254, 255]. Hence, a deep understanding of the effect of process parameters on energy field distribution, microstructure evolution, and deformation behavior is also crucial for the improvement of forming quality and efficiency.

5.2.4 Development of high-efficiency and intelligent equipment

High-efficiency and customized equipment with simple and lightweight structure via fully employing the advantages and the unique characteristics of the energy field, would be crucial for promoting and facilitating the industrial application of the energy field assisted forming process. Therefore, the development of such high-end equipment is crucial. In terms of the difficulty of precise control of energy field distribution in forming process, development of the tailor-made forming systems and equipment with on-line monitoring to achieve the accurate tailoring of loading conditions, microstructure and properties during the forming process is another important trend. Based on the accurate prediction modeling of the forming process and the on-line monitoring of the forming process, developing big data-driven digital twin system and intelligent equipment is of great significance to accurately ensure the forming quality and achieve high-efficiency forming.

Acknowledgements

The authors acknowledge the funded project of 1-ZE1W and 1-WZ4W from The Hong Kong Polytechnic University, the project of 51835011, 52375385 from National Natural Science Foundation of China, and the project of 15223520 from the General Research Fund of Hong Kong Government.

References

- [1] J. Jeswiet, M. Geiger, U. Engel, M. Kleiner, M. Schikorra, J. Duflou, R. Neugebauer, P. Bariani f, S. Bruschi, Metal forming progress since 2000, *CIRP Journal of Manufacturing Science and Technology*. 1 (2008) 2-17.
- [2] Z. Gronostajski, Z. Pater, L. Madej, A. Gontarz, L. Lisiecki, A. Lukaszek-Solek, J. Luksza, S. Mróz, Z. Muskalski, W. Muzykiewicz, M. Pietrzyk, R.E. Sliwa, J. Tomczak, S. Wiewiórowska, G. Winiarski, J. Zasadzinski, S. Ziółkiewicz. Recent development trends in metal forming, *Archives of Civil and Mechanical Engineering*. 19 (2019) 898-941.
- [3] H. Li, M.W Fu. *Deformation-based processing of materials: behavior, performance, modeling, and control*, Elsevier, 2019.

- [4] K. Zheng, J.H. Zheng, Z. He, G. Liu, D.J. Politis, L. Wang, Fundamentals, processes and equipment for hot medium pressure forming of light material tubular components, *International Journal of Lightweight Materials and Manufacture*. 3 (2020) 1-19.
- [5] W. Zhou, J. Lin, D.S. Balint, T.A. Dean, Clarification of the effect of temperature and strain rate on workpiece deformation behaviour in metal forming processes, *International Journal of Machine Tools and Manufacture*. 171 (2021) 103815.
- [6] S. Toros, F. Ozturk, I. Kacar, Review of warm forming of aluminum-magnesium alloys, *Journal of Materials Processing Technology*. 207 (2008) 1-12.
- [7] H. Krishnaswamy, P. Carlone, Energy-assisted forming: theory and applications, in: *Handbooks in Advanced Manufacturing*, Elsevier, 2021.
- [8] C.L. Tan, R.S. Li, J.L. Su, D.F. Du, Y. Du, B. Attard, Y.X. Chew, H.O. Zhang, E.J. Lavernia, Y. Fautrelle, J. Teng, AP. Dong, Review on field assisted metal additive manufacturing, *International Journal of Machine Tools and Manufacture*. 189 (2023) 104032.
- [9] W.A. Salandro, J.J. Jones, C. Bunget, L. Mears, J.T. Roth, *Electrically assisted forming: Modeling and control*, Springer, 2014.
- [10] G.D. Shao, H.W. Li, M. Zhan, A Review on Ultrasonic-Assisted Forming: Mechanism, Model, and Process, *Chinese Journal of Mechanical Engineering*, 34 (2021) 99.
- [11] V. Psyk, D. Risch, B.L. Kinsey, A.E. Tekkaya, M. Kleiner, Electromagnetic forming-a review, *Journal of Materials Processing Technology*, 211 (2011) 787-829.
- [12] Q. Zheng, H. Yu, Hyperplasticity mechanism in DP600 sheets during electrohydraulic free forming, *Journal of Materials Processing Technology*, 279 (2020) 116582.
- [13] H. Iyama, M. Nishi, S. Tanaka, Explosive forming, Explosion, Shock-wave and High-strain-rate Phenomena of Advanced Materials, Elsevier, *Multiphysics: Advances and Applications*, 2021.
- [14] W.W. Deng, C.Y. Wang, H.F. Lu, X.K. Meng, Z. Wang, J.M. Lv, K.Y. Luo, J.Z. Lu, Progressive developments, challenges and future trends in laser shock peening of metallic materials and alloys: A comprehensive review, *International Journal of Machine Tools and Manufacture*, 191 (2023) 104061.
- [15] E.S. Machlin, Applied voltage and the plastic properties of "Brittle" rock salt, *Journal of Applied Physics*, 30 (1959) 1109-1110.
- [16] B. Kinsey, G. Cullen, A. Jordan, S. Mates, Investigation of electroplastic effect at high deformation rates for 304SS and Ti-6Al-4V, *CIRP Annals*. 62 (2013) 279-282.
- [17] J. Magargee, F. Morestin, J. Cao, Characterization of flow stress for commercially pure titanium subjected to electrically assisted deformation, *Journal of Engineering Materials and*

- Technology, 135 (2013).
- [18] X.W. Wang, J. Xu, D.B. Shan, B. Guo, J. Cao, Modeling of thermal and mechanical behavior of a magnesium alloy AZ31 during electrically-assisted micro-tension, *International Journal of Plasticity*. 85 (2016) 230-257.
 - [19] J.C. Heigel, J.S. Andrawes, J.T. Roth, M.E. Hoque, R.M. Ford, Viability of electrically treating 6061 T6511 aluminum for use in manufacturing processes, *Transactions of the North American Manufacturing Research Institute of SME*. 33 (2000) 145-152.
 - [20] C.D. Ross, D.B. Irvin, J.T. Roth, Manufacturing aspects relating to the effects of direct current on the tensile properties of metals, *Journal of Engineering Materials & Technology*. 129 (2007) 342-347.
 - [21] J.M. Mai, L.F. Peng, Z.Q. Lin, X.M. Lai, Experimental study of electrical resistivity and flow stress of stainless steel 316L in electroplastic deformation, *Materials Science and Engineering: A*. 528 (2011) 3539-3544.
 - [22] L.F. Peng, J.M. Mai, T.H. Jiang, X.M. Lai, Z.Q. Lin, Experimental investigation of tensile properties of SS316L and fabrication of micro/mesochannel features by electrical-assisted embossing process, *Journal of Micro and Nano-Manufacturing*. 2 (2014).
 - [23] T. Lee, J. Magargee, M.K. Ng, J. Cao, Constitutive analysis of electrically-assisted tensile deformation of CP-Ti based on non-uniform thermal expansion, plastic softening and dynamic strain aging, *International Journal of Plasticity*. 94 (2017) 44-56.
 - [24] H. Xu, X.B. Liu, D. Zhang, X.F. Zhang, Minimizing serrated flow in Al-Mg alloys by electroplasticity, *Journal of Materials Science & Technology*. 35 (2019) 1108-1112.
 - [25] M.J. Kim, K. Lee, K.H. Oh, I.S. Choi, H.H. Yu, S.T. Hong, H.N. Han, Electric current-induced annealing during uniaxial tension of aluminum alloy, *Scripta Materialia*. 75 (2014) 58-61.
 - [26] J.J. Yang, Y. Li, P. Xue, W.X. Yu, Effects of impulse current on plastic behavior of 2A12 and 7A04 aluminum alloys, in: *Advanced Materials Research*, 2013, pp. 320-324.
 - [27] R.F. Zhu, G.Y. Tang, S.Q. Shi, M.W. Fu, Effect of electroplastic rolling on the ductility and superelasticity of TiNi shape memory alloy, *Materials & Design*. 44 (2013) 606-611.
 - [28] U.K. Ugurchiev, V.V. Stolyarov, Deformability and microhardness of large-grain titanium alloys in rolling with pulsed current, *Journal of Machinery Manufacture and Reliability*. 41 (2012) 404-406.
 - [29] C. Li, K.F. Zhang, S.S. Jiang, Z.P. Zhao, Pulse current auxiliary bulging and deformation mechanism of AZ31 magnesium alloy, *Materials & Design*. 34 (2012) 170-178.
 - [30] T.A. Perkins, T.J. Kronenberger, J.T. Roth, Metallic forging using electrical flow as an alternative to warm/hot working, *Journal of Manufacturing Science and Engineering*. 129

- (2007) 84-94.
- [31] K.M. Zhao, R. Fan, L.M. Wang, The effect of electric current and strain rate on serrated flow of sheet aluminum alloy 5754, *Journal of Materials Engineering and Performance*. 25 (2016) 781-789.
 - [32] X. Zhang, H.W. Li, M. Zhan, Mechanism for the macro and micro behaviors of the Ni-based superalloy during electrically-assisted tension: Local Joule heating effect, *Journal of Alloys and Compounds*. 742 (2018) 480-489.
 - [33] Y.H. Zhu, S. To, W.B. Lee, X.M. Liu, Y.B. Jiang, G.Y. Tang, Effects of dynamic electropulsing on microstructure and elongation of a Zn–Al alloy, *Materials Science and Engineering: A*. 501 (2009) 125-132.
 - [34] C.R. Green, T.A. McNeal, J.T. Roth, Springback elimination for Al-6111 alloys using electrically assisted manufacturing (EAM), *Transactions of the North American Manufacturing Research Institution of SME*. 37 (2009) 403-410.
 - [35] B.J. Ruszkiewicz, C. Scriva, Z.C. Reese, C.P. Nikhare, J.T. Roth, I. Ragai, Direct electric current spot treatment's effect on springback of 90 degree bent 2024-T3 aluminum, in: *International Manufacturing Science and Engineering Conference*, American Society of Mechanical Engineers, 2015, pp. V001T002A109.
 - [36] X.F. Li, Q. Zhou, S.J. Zhao, J. Chen, Effect of pulse current on bending behavior of Ti6Al4V alloy, *Procedia Engineering*. 81 (2014) 1799-1804.
 - [37] A. Jordan, B.L. Kinsey, Investigation of thermal and mechanical effects during electrically-assisted microbending, *Journal of Materials Processing Technology*. 221 (2015) 1-12.
 - [38] Y.X. Zhao, L.F. Peng, X.M. Lai, Influence of the electric pulse on springback during stretch U-bending of Ti6Al4V titanium alloy sheets, *Journal of Materials Processing Technology*. 261 (2018) 12-23.
 - [39] H.Y. Xie, Q. Wang, K. Liu, F. Peng, X.H. Dong, J.F. Wang, Investigation of influence of direct-current pulses on springback during V-bending of AZ31B magnesium alloy sheet, *Journal of Materials Processing Technology*. 219 (2015) 321-327.
 - [40] W.A. Salandro, C. Bunget, L. Mears, Modeling and quantification of the electroplastic effect when bending stainless steel sheet metal, in: *International Manufacturing Science and Engineering Conference*, 2010, pp. 581-590.
 - [41] M.S. Kim, N.T. Vinh, H.H. Yu, S.T. Hong, H.W. Lee, M.J. Kim, H.N. Han, J.T. Roth, Effect of electric current density on the mechanical property of advanced high strength steels under quasi-static tensile loads, *International Journal of Precision Engineering and Manufacturing*. 15 (2014) 1207-1213.

- [42]G.H. He, B.Q. Wang, X.N. Guo, F. Yang, J.D. Guo, B.L. Zhou, Investigation of thermal expansion measurement of brass strip H62 after high current density electropulsing by the CCD technique, *Materials Science and Engineering: A*. 292 (2000) 183-188.
- [43]T. Ungar, Microstructural parameters from X-ray diffraction peak broadening, *Scripta Materialia*. 51 (2004) 777-781.
- [44]N. Bertolino, J. Garay, U. Anselmi-Tamburini, Z.A. Munir, Electromigration effects in Al-Au multilayers, *Scripta Materialia*. 44 (2001) 737-742.
- [45]Q. Xu, G.Y. Tang, Y.B. Jiang, G.L. Hu, Y.H. Zhu, Accumulation and annihilation effects of electropulsing on dynamic recrystallization in magnesium alloy, *Materials Science and Engineering: A*. 528 (2011) 3249-3252.
- [46]P.C. Liang, K.L. Lin, Non-deformation recrystallization of metal with electric current stressing, *Journal of Alloys and Compounds*. 722 (2017) 690-697.
- [47]X.N. Li, Z.T. Xu, J.H. Huang, L.F. Peng, X.M. Lai, In situ observation of deformation behavior of Ti6Al4V subjected to electrically-assisted forming process, *Procedia Manufacturing*. 50 (2020) 647-651.
- [48]W. Kang, I. Beniam, S.M. Qidwai, In situ electron microscopy studies of electromechanical behavior in metals at the nanoscale using a novel microdevice-based system, *Review of Scientific Instruments*. 87 (2016) 095001.
- [49]S.J. Kim, S.D. Kim, D. Yoo, J. Lee, Y. Rhyim, D. Kim, Evaluation of the athermal effect of electric pulsing on the recovery behavior of magnesium alloy, *Metallurgical and Materials Transactions A*. 47 (2016) 6368-6373.
- [50]F.J. Humphreys, M. Hatherly, *Recrystallization and related annealing phenomena* (Second Edition), Elsevier, 2004.
- [51]Y.Z. Zhou, S.H. Xiao, J.D. Guo, Recrystallized microstructure in cold worked brass produced by electropulsing treatment, *Materials Letters*. 58 (2004) 1948-1951.
- [52]Z.Y. Zhao, G.F. Wang, Y.L. Zhang, Y.Q. Wang, H.L. Hou, Fast recrystallization and phase transformation in ECAP deformed Ti-6Al-4V alloy induced by pulsed electric current, *Journal of Alloys and Compounds*. 786 (2019) 733-741.
- [53]S.H. Xiao, J.D. Guo, S.D. Wu, G.H. He, S.X. Li, Recrystallization in fatigued copper single crystals under electropulsing, *Scripta Materialia*. 46 (2002) 1-6.
- [54]Z.H. Xu, G.Y. Tang, S.Q. Tian, F. Ding, H.Y. Tian, Research of electroplastic rolling of AZ31 Mg alloy strip, *Journal of Materials Processing Technology*. 182 (2007) 128-133.
- [55]Y.R. Ma, H.J. Yang, Y.Z. Tian, J.C. Pang, Z.F. Zhang, Hardening and softening mechanisms in a nano-lamellar austenitic steel induced by electropulsing treatment, *Materials Science and*

- Engineering: A. 713 (2018) 146-150.
- [56] R.F. Zhu, J.N. Liu, G.Y. Tang, S.Q. Shi, M.W. Fu, Properties, microstructure and texture evolution of cold rolled Cu strips under electropulsing treatment, *Journal of Alloys and Compounds*. 544 (2012) 203-208.
- [57] R.F. Liu, W.X. Wang, H.S. Chen, S.P. Wan, Y.Y. Zhang, R.H. Yao, Comparative study of recrystallization behaviour and nanoindentation properties of micro-/nano-bimodal size B4C particle-reinforced aluminium matrix composites under T6 and electropulsing treatment, *Journal of Alloys and Compounds*. 788 (2019) 1056-1065.
- [58] Z.H. Xu, G.Y. Tang, S.Q. Tian, J.C. He, Research on the engineering application of multiple pulses treatment for recrystallization of fine copper wire, *Materials Science and Engineering: A*. 424 (2006) 300-306.
- [59] Y.B. Jiang, G.Y. Tang, L. Guan, S.N. Wang, Z.H. Xu, C.H. Shek, Y.H. Zhu, Effect of electropulsing treatment on solid solution behavior of an aged Mg alloy AZ61 strip, *Journal of Materials Research*. 23 (2008) 2685-2691.
- [60] Y.Z. Zhou, W. Zhang, B.Q. Wang, G.H. He, J.D. Guo, Grain refinement and formation of ultrafine-grained microstructure in a low-carbon steel under electropulsing, *Journal of Materials Research*. 17 (2002) 2105-2111.
- [61] W. Zhang, M.L. Sui, K.Y. Hu, D.X. Li, X.N. Guo, G.H. He, B.L. Zhou, Formation of nanophases in a Cu–Zn alloy under high current density electropulsing, *Journal of Materials Research*. 15 (2000) 2065-2068.
- [62] W. Zhang, M.L. Sui, Y.Z. Zhou, D.X. Li, Evolution of microstructures in materials induced by electropulsing, *Micron*. 34 (2003) 189-198.
- [63] H.K. Zhang, H. Xiao, K. Huang, Precipitation behavior of aluminum-manganese alloy under different heating methods, *Materials Transactions*. 63 (2022) 128-132.
- [64] C.H. Pei, Q.B. Fan, H.N. Cai, J.C. Li, High temperature deformation behavior of the TC6 titanium alloy under the uniform DC electric field, *Journal of Alloys and Compounds*. 489 (2010) 401-407.
- [65] W.B. Liu, Y.H. Wen, N. Li, S.Z. Yang, Effects of electropulsing treatment on stress-induced ϵ martensite transformation of a pre-deformed Fe₁₇Mn₅Si₈Cr₅Ni_{0.5}NbC alloy, *Materials Science and Engineering: A*. 507 (2009) 114-116.
- [66] H. Conrad, Effects of electric current on solid state phase transformations in metals, *Materials Science and Engineering: A*. 287 (2000) 227-237.
- [67] Y.B. Jiang, G.Y. Tang, C.H. Shek, Y.H. Zhu, L. Guan, S.N. Wang, Z.H. Xu, Improved ductility of aged Mg-9Al-1Zn alloy strip by electropulsing treatment, *Journal of Materials Research*.

24 (2009) 1810-1814.

- [68]D. Zhang, S. To, Y.H. Zhu, H. Wang, G.Y. Tang, Dynamic electropulsing induced phase transformations and their effects on single point diamond turning of AZ91 alloy, *Journal of Surface Engineered Materials and Advanced Technology*. 2 (2012) 16-21.
- [69]X. Liu, S.H. Lan, J. Ni, Experimental study of electro-plastic effect on advanced high strength steels, *Materials Science and Engineering: A*. 582 (2013) 211-218.
- [70]T.H. Jiang, L.F. Peng, P.Y. Yi, X.M. Lai, Flow behavior and plasticity of Ti–6Al–4V under different electrically assisted treatments, *Materials Research Express*. 3 (2016) 126505.
- [71]J.H. Huang, Z.T. Xu, Y.J. Deng, L.F. Peng, Electropulsing-induced α to β phase transformation of Ti–6Al–4V, *Journal of Manufacturing Science and Engineering*. 141 (2019) 111012.
- [72]K. Okazaki, M. Kagawa, H. Conrad, An evaluation of the contributions of skin, pinch and heating effects to the electroplastic effect in titanium, *Materials Science & Engineering*. 45 (1980) 109-116.
- [73]X.W. Wang, J. Xu, D.B. Shan, B. Guo, J. Cao, Effects of specimen and grain size on electrically-induced softening behavior in uniaxial micro-tension of AZ31 magnesium alloy: Experiment and modeling, *Materials & design*. 127 (2017) 134-143.
- [74]P.D. Goldman, L.R. Motowidlo, J.M. Galligan, The absence of an electroplastic effect in lead at 4.2K, *Scripta Metallurgica*. 15 (1981) 353-356.
- [75]M.J. Kim, H.J. Jeong, J.W. Park, S.T. Hong, H.N. Han, Modified Johnson-Cook model incorporated with electroplasticity for uniaxial tension under a pulsed electric current, *Metals and Materials International*. 24 (2018) 42-50.
- [76]J. Magargee, R. Fan, J. Cao, Analysis and Observations of Current Density Sensitivity and Thermally Activated Mechanical Behavior in Electrically-Assisted Deformation, *Journal of Manufacturing Science and Engineering*. 135 (2013) 61022.
- [77]W.A. Salandro, J.J. Jones, C. Bunget, L. Mears, J.T. Roth, *Electrically Assisted Forming*, Springer, 2015, pp. 40-41.
- [78]X.N. Li, Z.T. Xu, J.H. Huang, L.F. Peng, P. Guo, Effects of Electropulsing Treatment on the Element Diffusion Between Ti6Al4V and Commercially Pure Titanium, *Journal of Manufacturing Science and Engineering*. 142 (2020).
- [79]A.F. Sprecher, S.L. Mannan, H. Conrad, On the mechanisms for the electroplastic effect in metals, *Acta Metallurgica*. 34 (1986) 1145-1162.
- [80]M. Molotskii, V. Fleurov, Magnetic effects in electroplasticity of metals, *Physical Review B (Condens Matter)*. 52 (1995) 15829-15834.

- [81]H. Conrad, A.F. Sprecher, Dislocations in solids: Basic problems and applications, Elsevier Science, 1989.
- [82]H. Conrad, Thermally activated plastic flow of metals and ceramics with an electric field or current, *Materials Science and Engineering: A*. 322 (2002) 100-107.
- [83]D.L. Li, E.L. Yu, Z.T. Liu, Microscopic mechanism and numerical calculation of electroplastic effect on metal's flow stress, *Materials Science and Engineering: A*. 580 (2013) 410-413.
- [84]D.L. Li, E.L. Yu, An approach based on the classical free-electron theory to study electroplastic effect, in: *Advanced Materials Research*, 2011, pp. 71-74.
- [85]H. Conrad, Z. Guo, A.F. Sprecher, Effects of electropulse duration and frequency on grain growth in Cu, *Scripta Metallurgica et Materialia*. 24 (1990) 359-362.
- [86]G.L. Hu, Y.H. Zhu, G.Y. Tang, C.H. Shek, J.N. Liu, Effect of electropulsing on recrystallization and mechanical properties of silicon steel strips, *Journal of Materials Science & Technology*. 27 (2011) 1034-1038.
- [87]J. Asghar, N.V. Reddy, Importance of tool configuration in incremental sheet metal forming of difficult to form materials using electro-plasticity, in: *Proceedings of the world congress on engineering*, 2013, pp. 1734-1738.
- [88]H. Song , Z.J. Wang, T.J. Gao, Effect of high density electropulsing treatment on formability of TC4 titanium alloy sheet, *Transactions of Nonferrous Metals Society of China*. 17 (2007) 87-92.
- [89]K.M. Klimov, I.I. Novikov, Absence of strain hardening upon electrostimulated rolling of metals under cold conditions, in: *Doklady Physics*, 2007, pp. 359-360.
- [90]R.F. Zhu, G.Y. Tang, S.Q. Shi, M.W. Fu, Effect of electroplastic rolling on deformability and oxidation of NiTiNb shape memory alloy, *Journal of Materials Processing Technology*. 213 (2013) 30-35.
- [91]M.K. Ng, L.Y. Li, Z.Y. Fan, R.X. Gao, E.F. Smith, K.F. Ehmann, J. Cao, Joining sheet metals by electrically-assisted roll bonding, *CIRP Annals*. 64 (2015) 273-276.
- [92]M.K. Ng, Z.Y. Fan, R.X. Gao, E.F. Smith, J. Cao, Characterization of electrically-assisted micro-rolling for surface texturing using embedded sensor, *CIRP Annals*. 63 (2014) 269-272.
- [93]G.Q. Fan, L. Gao, G. Hussain, Z.L. Wu, Electric hot incremental forming: A novel technique, *International Journal of Machine Tools and Manufacture*. 48(2008) 1688-1692.
- [94]D.K. Xu, B. Lu, T.T. Cao, H. Zhang, J. Chen, H. Long, J. Cao, Enhancement of process capabilities in electrically-assisted double sided incremental forming, *Materials & Design*. 92 (2016) 268-280.

- [95] R.Z. Liu, L.B. D.K. Xu, J. C. F. Chen. H.G. Ou, H. Long, Development of novel tools for electricity-assisted incremental sheet forming of titanium alloy, *The International Journal of Advanced Manufacturing Technology*. 85 (2016) 1137-1144.
- [96] C.S. Magnus, Joule heating of the forming zone in incremental sheet metal forming: part 1: state of the art and thermal process modelling, *The International Journal of Advanced Manufacturing Technology*. 91 (2017) 1309-1319.
- [97] W.A. Salandro, C. Bunget, L. Mears, Thermo-mechanical investigations of the electroplastic effect, in: *International Manufacturing Science and Engineering Conference*, 2011, pp. 573-582.
- [98] J.M. Mai, L.F. Peng, X.M. Lai, Z.Q. Lin, Electrical-assisted embossing process for fabrication of micro-channels on 316L stainless steel plate, *Journal of Materials Processing Technology*. 213 (2013) 314-321.
- [99] G.Y. Tang, J. Zhang, Y.J. Yan, H.H. Zhou, W. Fang, The engineering application of the electroplastic effect in the cold-drawing of stainless steel wire, *Journal of Materials Processing Technology*. 137 (2003) 96-99.
- [100] Y. Zhou, G.Q. Chen, X.S. Fu, W.L. Zhou, Effect of electropulsing on deformation behavior of Ti-6Al-4V alloy during cold drawing, *Transactions of Nonferrous Metals Society of China*. 24 (2014) 1012-1021.
- [101] B. Wang, G.F. Wang, S.S. Jiang, K.F. Zhang, Effect of pulse current on thermal performance and deep drawing of SiCp/2024Al composite sheet, *The International Journal of Advanced Manufacturing Technology*. 67 (2013) 623-627.
- [102] A.J.S. Egea, H.A.G. Rojas, D.J. Celentano, J.J. Perió, J. Cao, Thermomechanical analysis of an electrically assisted wire drawing process, *Journal of Manufacturing Science and Engineering*. 139 (2017) 111017.
- [103] H.B. Wang, G.L. Song, G.Y. Tang, Evolution of surface mechanical properties and microstructure of Ti6Al4V alloy induced by electropulsing-assisted ultrasonic surface rolling process, *Journal of Alloys and Compounds*. 681 (2016) 146-156.
- [104] H. Potluri, J.J. Jones, L. Mears, Comparison of electrically-assisted and conventional friction stir welding processes by feed force and torque, in: *International Manufacturing Science and Engineering Conference*, 2013.
- [105] Y. Liu, H. Zhou, H. Su, C.Y. Yang, J.Y. Cheng, P. Zhang, L.Q. Ren, Effect of electrical pulse treatment on the thermal fatigue resistance of bionic compacted graphite cast iron processed in water, *Materials & Design*. 39 (2012) 344-349.
- [106] G. Stepanov, A. Babutsky, L. Kruszka, Residual stresses relaxation caused by pulsed

- electric current, in: Materials Science Forum, 2010, pp. 2429-2433.
- [107] F. Honarvar, A. Varvani-Farahani, A review of ultrasonic testing applications in additive manufacturing: Defect evaluation, material characterization, and process control, *Ultrasonics*. 108 (2020) 106227.
 - [108] K.K. Lu, Y.L. Tian, C.F. Liu, Z.Y. Guo, F.J. Wang, D.W. Zhang, B. Shirinzadeh, Experimental investigation of the effects of vibration parameters on ultrasonic vibration-assisted tip-based nanofabrication, *International Journal of Mechanical Sciences*. 198 (2021) 106387.
 - [109] K. Uchino, Piezoelectric ultrasonic motors: overview, *Smart Materials and Structures*. 7 (1998) 273-285.
 - [110] R. Pohlman, E. Lehfeltdt, Influence of ultrasonic vibration on metallic friction, *Ultrasonics*. 4 (1966) 178-185.
 - [111] K. Siegert, J. Ulmer, Influencing the friction in metal forming processes by superimposing ultrasonic waves, *CIRP Annals*. 50 (2001) 195-200.
 - [112] K. Siegert, A. Möck, Wire drawing with ultrasonically oscillating dies, *Journal of Materials Processing Technology*. 60 (1996) 657-660.
 - [113] V.C. Kumar, I.M. Hutchings, Reduction of the sliding friction of metals by the application of longitudinal or transverse ultrasonic vibration, *Tribology International*. 37 (2004) 833-840.
 - [114] A.G. Rozner, Effect of ultrasonic vibration on coefficient of friction during strip drawing, *The Journal of the Acoustical Society of America*. 49 (1971) 1368-1371.
 - [115] E. Teidelt, J. Starcevic, V.L. Popov, Influence of ultrasonic oscillation on static and sliding friction, *Tribology Letters*. 48 (2012) 51-62.
 - [116] F. Blaha, B. Langenecker, Tensile deformation of zinc crystal under ultrasonic vibration, *Science of Nature*. 42 (1955) 1-10.
 - [117] B. Langenecker, Effects of ultrasound on deformation characteristics of metals, *IEEE Transactions on Sonics and Ultrasonics*. 13 (1966) 1-8.
 - [118] H.O.K. Kirchner, W.K. Kromp, F.B. Prinz, et al., Plastic deformation under simultaneous cyclic and unidirectional loading at low and ultrasonic frequencies, *Materials Science and Engineering*. 68 (1985) 197-206.
 - [119] Y. Daud, M. Lucas, Z.H. Huang. Modelling the effects of superimposed ultrasonic vibrations on tension and compression tests of aluminium[J]. *Journal of Materials Processing Technology*. 2007, 186(1-3):179-190.
 - [120] B. Schinke, T. Malmberg, Dynamic tensile tests with superimposed ultrasonic oscillations for stainless steel type 321 at room temperature, *Nuclear Engineering and Design*.

- 100 (1987) 281-296.
- [121] I. Lum, H. Huang, B.H. Chang, et al., Effects of superimposed ultrasound on deformation of gold, *Journal of Applied Physics*. 105 (2009) 024905.
 - [122] G.A. Malygin, Acoustoplastic effect and the stress superimposition mechanism, *Physics of the Solid State*. 42 (2000) 72-78.
 - [123] Y. Daud, M. Lucas, Z. Huang, Modelling the effects of superimposed ultrasonic vibrations on tension and compression tests of aluminium, *Journal of Materials Processing Technology*. 186 (2007) 179-190.
 - [124] H. Sedaghat, W.X. Xu, L.C. Zhang, Ultrasonic vibration-assisted metal forming: Constitutive modelling of acoustoplasticity and applications, *Journal of Materials Processing Technology*. 265 (2019) 122-129.
 - [125] LC Zhang, CH Wu, H Sedaghat. Ultrasonic vibration–assisted incremental sheet metal forming, *The International Journal of Advanced Manufacturing Technology*. 114 (2021) 3311–3323.
 - [126] C.J. Wang, Y. Liu, B. Guo, et al., Acoustic softening and stress superposition in ultrasonic vibration assisted uniaxial tension of copper foil: Experiments and modeling, *Materials & Design*. 112 (2016) 246-253.
 - [127] B. Meng, B.N. Cao, M. Wan, et al., Ultrasonic-assisted microforming of superalloy capillary: Modeling and experimental investigation, *Journal of Manufacturing Processes*. 57 (2020) 589-599.
 - [128] Z.H. Huang, M. Lucas, M.J. Adams, Influence of ultrasonics on upsetting of a model paste, *Ultrasonics*. 40 (2002) 43-48.
 - [129] J.C. Hung, Y.C. Tsai, C.H. Hung, Frictional effect of ultrasonic-vibration on upsetting, *Ultrasonics*. 46 (2007) 277-284.
 - [130] M. Lotfi, S.A. Sajjadi, S. Amini, Wettability analysis of titanium alloy in 3D elliptical ultrasonic assisted turning, *International Journal of Lightweight Materials and Manufacture*. 2 (2019) 235-240.
 - [131] M. Zhang, D. Zhang, D. Geng, et al., Effects of tool vibration on surface integrity in rotary ultrasonic elliptical end milling of Ti–6Al–4V, *Journal of Alloys and Compounds*. 821 (2020) 153266.
 - [132] S.J. Zhang, S. To, G.Q. Zhang, Z.W. Zhu, A review of machine-tool vibration and its influence upon surface generation in ultra-precision machining, *International Journal of Machine Tools and Manufacture*. 91 (2015) 34-42.
 - [133] O. Izumi, K. Oyama, Y. Suzuki, Effects of superimposed ultrasonic vibration on

- compressive deformation of metals, Transactions of the Japan Institute of Metals. 7 (1966) 162-167.
- [134] O. Izumi, K. Oyama, Y. Suzuki, On the superimposing of ultrasonic vibration during compressive deformation of metals, Transactions of the Japan Institute of Metals. 7 (1966) 158-161.
- [135] Z. Yao, G.Y. Kim, L. Faidley, et al., Effects of superimposed high-frequency vibration on deformation of aluminum in micro/meso-scale upsetting, Journal of Materials Processing Technology. 212 (2012) 640-646.
- [136] G. Perotti, An experiment on the use of ultrasonic vibrations in cold upsetting, CIRP Annales. 27 (1978) 195-197.
- [137] M. Susan, L.G. Bujoreanu, The metal-tool contact friction at the ultrasonic vibration drawing of ball-bearing steel wires, Revista de Metalurgia. 35 (1999) 379-383.
- [138] R.K. Dutta, R.H. Petrov, R. Delhez, et al., The effect of tensile deformation by in situ ultrasonic treatment on the microstructure of low-carbon steel, Acta Materialia. 61 (2013) 1592-1602.
- [139] J.C. Hung, Y.C. Tsai, Investigation of the effects of ultrasonic vibration-assisted micro-upsetting on brass, Materials Science and Engineering: A. 580 (2013) 125-132.
- [140] R. Shahrokh, A. Ghaei, M. Farzin, et al., Experimental and numerical investigation of ultrasonically assisted micro-ring compression test, The International Journal of Advanced Manufacturing Technology. 95 (2018) 3487-3495.
- [141] Z.H. Yao, G.Y. Kim, Z.H. Wang, et al., Acoustic softening and residual hardening in aluminum: modeling and experiments, International Journal of Plasticity. 39 (2012) 75-87.
- [142] A. Prabhakar, G.C. Verma, H. Krishnasamy, et al., Dislocation density based constitutive model for ultrasonic assisted deformation, Mechanics Research Communications. 85 (2017) 76-80.
- [143] J.H. Zhang, H. Li, M. Zhang, et al., Study on force modeling considering size effect in ultrasonic-assisted micro-end grinding of silica glass and Al₂O₃ ceramic, The International Journal of Advanced Manufacturing Technology. 89 (2017) 1173-1192.
- [144] H.Y. Zhou, H.Z. Cui, Q.H. Qin, Influence of ultrasonic vibration on the plasticity of metals during compression process, Journal of Materials Processing Technology. 251 (2018) 146-159.
- [145] V. Fartashvand, A. Abdullah, S.A. Sadough Vanini, Investigation of Ti-6Al-4V alloy acoustic softening, Ultrasonics Sonochemistry. 38 (2017) 744-749.
- [146] Z.H. Yao, G.Y. Kim, L. Faidley, et al., Acoustic softening and hardening of aluminum in

- high-frequency vibration-assisted micro/meso forming, *Materials and Manufacturing Processes*. 28 (2013) 584-588.
- [147] K.W. Siu, A.H.W. Ngan, I.P. Jones, New insight on acoustoplasticity–ultrasonic irradiation enhances subgrain formation during deformation, *International Journal of Plasticity*. 27 (2011) 788-800.
- [148] R.K. Dutta, R.H. Petrov, R. Delhez, et al., The effect of tensile deformation by in situ ultrasonic treatment on the microstructure of low-carbon steel, *Acta Materialia*. 61 (2013) 1592-1602.
- [149] A. Siddiq, T.E. Sayed, A thermomechanical crystal plasticity constitutive model for ultrasonic consolidation, *Computational Materials Science*. 51 (2012) 241-251.
- [150] H.Y. Zhou, H.Z. Cui, Q.H. Qin, et al., A comparative study of mechanical and microstructural characteristics of aluminium and titanium undergoing ultrasonic assisted compression testing, *Materials Science and Engineering: A*. 682 (2017) 376-388.
- [151] X. Wu, Y.T. Zhu, M.W. Chen, et al., Twinning and stacking fault formation during tensile deformation of nanocrystalline Ni, *Scripta Materialia*. 54 (2006) 1685-1690.
- [152] B. Meng, B.N. Cao, M. Wan, et al., Constitutive behavior and microstructural evolution in ultrasonic vibration assisted deformation of ultrathin superalloy sheet, *International Journal of Mechanical Sciences*. 157 (2019) 609-618.
- [153] F.D. Ning, W.L. Cong, Microstructures and mechanical properties of Fe-Cr stainless steel parts fabricated by ultrasonic vibration-assisted laser engineered net shaping process, *Materials Letters*. 179 (2016) 61-64.
- [154] J.L. Laborde, A. Hita, J.P. Caltagirone, et al., Fluid dynamics phenomena induced by power ultrasounds, *Ultrasonics*. 38 (2000) 297-300.
- [155] K. Shah, A.J. Pinkerton, A. Salman, et al., Effects of melt pool variables and process parameters in laser direct metal deposition of aerospace alloys, *Materials and Manufacturing Processes*. 25 (2010) 1372-1380.
- [156] H. Wang, Y.B. Hu, F.D. Ning, et al., Ultrasonic vibration-assisted laser engineered net shaping of Inconel 718 parts: Effects of ultrasonic frequency on microstructural and mechanical properties, *Journal of Materials Processing Technology*. 276 (2020) 116395.
- [157] T. Jimma, Y. Kasuga, N. Iwaki, et al., An application of ultrasonic vibration to the deep drawing process, *Journal of Materials Processing Technology*. 80 (1998) 406-412.
- [158] F. Luo, K.H. Li, J.M. Zhong, et al., An ultrasonic microforming process for thin sheet metals and its replication abilities, *Journal of Materials Processing Technology*. 216 (2015) 10-18.

- [159] F. Luo, B. Wang, Z.W. Li, et al., Time factors and optimal process parameters for ultrasonic microchannel formation in thin sheet metals, *The International Journal of Advanced Manufacturing Technology*. 89 (2017) 255-263.
- [160] J.Y. Koo, Y.P. Jeon, C.G. Kang, Effect of stamping load variation on deformation behaviour of stainless steel thin plate with microchannel, *Proceedings of the Institution of Mechanical Engineers, Part B: Journal of Engineering Manufacture*. 227 (2013) 1121-1128.
- [161] W.T. Park, C.K. Jin, C.G. Kang, Improving channel depth of stainless steel bipolar plate in fuel cell using process parameters of stamping, *The International Journal of Advanced Manufacturing Technology*. 87 (2016) 1677-1684.
- [162] P.Y. Li, J. He, Q. Liu, et al., Evaluation of forming forces in ultrasonic incremental sheet metal forming, *Aerospace Science and Technology*. 63 (2017) 132-139.
- [163] R. Cheng, N. Wiley, M. Short, et al., Applying ultrasonic vibration during single-point and two-point incremental sheet forming, *Procedia Manufacturing*. 34 (2019) 186-192.
- [164] C.E. Winsper, D.H. Sansome, Fundamentals of ultrasonic wire drawing, *J Inst Metals*. 97 (1969) 274-280.
- [165] V.P. Severdenko, V.V. Klubovich, A.V.E. Stepanenko, *Ultrasonic rolling and drawing of metals*, Springer, 1972.
- [166] K. Siegert, J. Ulmer, Superimposing ultrasonic waves on the dies in tube and wire drawing, *J. Eng. Mater. Technol.* 123 (2001) 517-523.
- [167] J.J. Buckley, M.K. Freeman, Ultrasonic tube drawing, *Ultrasonics*. 8 (1970) 152-158.
- [168] K. Siegert, A. Möck, Wire drawing with ultrasonically oscillating dies, *Journal of Materials Processing Technology*. 60 (1996) 657-660.
- [169] V.C. Kumar, I.M. Hutchings, Reduction of the sliding friction of metals by the application of longitudinal or transverse ultrasonic vibration, *Tribology International*. 37 (2004) 833-840.
- [170] K. Siegert, J. Ulmer, Superimposing ultrasonic waves on tube and wire drawing, *SAE Transactions*. 109 (2000) 695-701.
- [171] C. Bunget, G. Ngaile, Influence of ultrasonic vibration on micro-extrusion, *Ultrasonics*. 51 (2011) 606-616.
- [172] X.C. Zhuang, J.P. Wang, H. Zheng, et al., Forming mechanism of ultrasonic vibration assisted compression, *Transactions of Nonferrous Metals Society of China*. 25 (2015) 2352-2360.

- [173] X.X. Wang, Z.C. Qi, W.L. Chen, Investigation of mechanical and microstructural characteristics of Ti-45Nb undergoing transversal ultrasonic vibration-assisted upsetting, *Materials Science and Engineering: A*. 813 (2021) 141169.
- [174] M. Jäckisch, M. Merklein, Investigation of thermal effects during ultrasonic-assisted upsetting, *Procedia Manufacturing*. 50 (2020) 220-225.
- [175] M.Y. Cao, H. Hu, X.D. Jia, et al., Mechanism of ultrasonic vibration assisted upsetting of 6061 aluminum alloy, *Journal of Manufacturing Processes*. 59 (2020) 690-697.
- [176] M.K. Choi, H. Huh, N. Park, Process design of combined deep drawing and electromagnetic sharp edge forming of DP980 steel sheet, *Journal of Materials Processing Technology*. 244 (2017) 331-343.
- [177] J.J. Li, L. Li, M. Wan, H.P. Yu, L. Liu, Innovation applications of electromagnetic forming and its fundamental problems, *Procedia Manufacturing*. 15 (2018) 14-30.
- [178] F. Weber, J. Gebhard, R. Gitschel, S. Goyal, M. Kamaliev, S. Wernicke, A.E. Tekkaya, Joining by forming—A selective review, *Journal of Advanced Joining Processes*. 3 (2021) 100054.
- [179] C.F. Li, D.H. Liu, H.P. Yu, Z.B. Ji, Research on formability of 5052 aluminum alloy sheet in a quasi-static–dynamic tensile process, *International Journal of Machine Tools and Manufacture*. 49 (2009) 117-124.
- [180] S. Yan, H. Yang, H. Li, X. Yao, A unified model for coupling constitutive behavior and micro-defects evolution of aluminum alloys under high-strain-rate deformation, *International Journal of Plasticity*. 85 (2016) 203-229.
- [181] Z. Lai, Q. Cao, X. Han, Y. Huang, F. Deng, Q. Chen, L. Li, Investigation on plastic deformation behavior of sheet workpiece during radial Lorentz force augmented deep drawing process, *Journal of Materials Processing Technology*. 245 (2017) 193-206.
- [182] M. Kleiner, C. Beerwald, W. Homberg, Analysis of process parameters and forming mechanisms within the electromagnetic forming process, *CIRP annals*. 54 (2005) 225-228.
- [183] K.I. Mori, N. Bay, L. Fratini, F. Micari, A.E. Tekkaya, Joining by plastic deformation, *CIRP Annals*. 62 (2013) 673-694.
- [184] C.N. Okoye, J.H. Jiang, Z.D. Hu, Application of electromagnetic-assisted stamping (EMAS) technique in incremental sheet metal forming, *International Journal of Machine Tools and Manufacture*. 46 (2006) 1248-1252.
- [185] Z. Shen, M. Peng, D. Zhu, T. Zheng, Y. Zhong, W. Ren, C. Li, W. Xuan, Z. Ren, Evolution of the microstructure and solute distribution of Sn-10wt% Bi alloys during electromagnetic

- field-assisted directional solidification, *Journal of Materials Science & Technology*. 35 (2019) 568-577.
- [186] H. Jiang, N. Li, Z. Xu, C. Yan, D. Wang, X. Han, Non-twinning deformation mechanism of pure copper under high speed electromagnetic forming, *Materials & Design*. 81 (2015) 54-58.
- [187] M. Kamal, G.S. Daehn, A uniform pressure electromagnetic actuator for forming flat sheets, (2007).
- [188] H. Yu, Q. Zheng, S. Wang, Y. Wang, The deformation mechanism of circular hole flanging by magnetic pulse forming, *Journal of Materials Processing Technology*. 257 (2018) 54-64.
- [189] X. Li, Q. Cao, Z. Lai, S. Ouyang, N. Liu, M. Li, X. Han, L. Li, Bulging behavior of metallic tubes during the electromagnetic forming process in the presence of a background magnetic field, *Journal of Materials Processing Technology*. 276 (2020) 116411.
- [190] A. Jäger, D. Risch, A.E. Tekkaya, Thermo-mechanical processing of aluminum profiles by integrated electromagnetic compression subsequent to hot extrusion, *Journal of Materials Processing Technology*. 211 (2011) 936-943.
- [191] C. Weddeling, V. Walter, P. Haupt, A.E. Tekkaya, V. Schulze, K.A. Weidenmann, Joining zone design for electromagnetically crimped connections, *Journal of Materials Processing Technology*. 225 (2015) 240-261.
- [192] Y. Jin, H. Yu, Enhanced formability and hardness of AA2195-T6 during electromagnetic forming, *Journal of Alloys and Compounds*. 890 (2022) 161891.
- [193] Y. Kiliclar, O.K. Demir, M. Engelhardt, M. Rozgić, I.N. Vladimirov, S. Wulfinghoff, C. Weddeling, S. Gies, C. Klose, S. Reese, Experimental and numerical investigation of increased formability in combined quasi-static and high-speed forming processes, *Journal of Materials Processing Technology*. 237 (2016) 254-269.
- [194] X. Cui, J. Li, J. Mo, J. Fang, B. Zhou, X. Xiao, F. Feng, Incremental electromagnetic-assisted stamping (IEMAS) with radial magnetic pressure: a novel deep drawing method for forming aluminum alloy sheets, *Journal of Materials Processing Technology*. 233 (2016) 79-88.
- [195] P. Dong, Z. Li, S. Feng, Z. Wu, Q. Cao, L. Li, Q. Chen, X. Han, Fabrication of titanium bipolar plates for proton exchange membrane fuel cells by uniform pressure electromagnetic forming, *International Journal of Hydrogen Energy*. 46 (2021) 38768-38781.
- [196] H. Li, X. Yao, S. Yan, J. He, M. Zhan, L. Huang, Analysis of forming defects in electromagnetic incremental forming of a large-size thin-walled ellipsoid surface part of

- aluminum alloy, *Journal of Materials Processing Technology*. 255 (2018) 703-715.
- [197] Z. Wu, Q. Cao, J. Fu, Z. Li, Y. Wan, Q. Chen, L. Li, X. Han, An inner-field uniform pressure actuator with high performance and its application to titanium bipolar plate forming, *International Journal of Machine Tools and Manufacture*. 155 (2020) 103570.
- [198] A. Long, M. Wan, W. Wang, X. Wu, X. Cui, B. Ma, Forming methodology and mechanism of a novel sheet metal forming technology-electromagnetic superposed forming (EMSF), *International Journal of Solids and Structures*. 151 (2018) 165-180.
- [199] F.Q. Li, J.H. Mo, J.J. Li, L. Huang, H.Y. Zhou, Formability of Ti-6Al-4V titanium alloy sheet in magnetic pulse bulging, *Materials & Design (1980-2015)*. 52 (2013) 337-344.
- [200] G.N. Chu, G. Chen, B.G. Chen, S. Yang, A technology to improve formability for rectangular cross section component hydroforming, *The International Journal of Advanced Manufacturing Technology*. 72 (2014) 801-808.
- [201] H. Su, L. Huang, J. Li, F. Ma, P. Huang, F. Feng, Two-step electromagnetic forming: a new forming approach to local features of large-size sheet metal parts, *International Journal of Machine Tools and Manufacture*. 124 (2018) 99-116.
- [202] H. Yu, C. Li, Z. Zhao, Z. Li, Effect of field shaper on magnetic pressure in electromagnetic forming, *Journal of Materials Processing Technology*. 168 (2005) 245-249.
- [203] H. Yu, J. Chen, W. Liu, H. Yin, C. Li, Electromagnetic forming of aluminum circular tubes into square tubes: experiment and numerical simulation, *Journal of Manufacturing Processes*. 31 (2018) 613-623.
- [204] S.K. Dond, T. Kolge, H. Choudhary, A. Sharma, G.K. Dey, Determination of magnetic coupling and its influence on the electromagnetic tube forming and discharge circuit parameters, *Journal of Manufacturing Processes*. 54 (2020) 19-27.
- [205] Q. Cao, X. Han, Z. Lai, Q. Xiong, X. Zhang, Q. Chen, H. Xiao, L. Li, Analysis and reduction of coil temperature rise in electromagnetic forming, *Journal of Materials Processing Technology*. 225 (2015) 185-194.
- [206] M. Soni, M. Ahmed, S.K. Panthi, S. Kumar, K.S. Gavel, Influence of compression coil geometry in electromagnetic forming using experimental and finite element method, *The International Journal of Advanced Manufacturing Technology*. 117 (2021) 1945-1958.
- [207] E. Paese, M. Geier, R.P. Homrich, P. Rosa, R. Rossi, Sheet metal electromagnetic forming using a flat spiral coil: Experiments, modeling, and validation, *Journal of Materials Processing Technology*. 263 (2019) 408-422.
- [208] S. Ouyang, X. Li, C. Li, L. Du, T. Peng, X. Han, L. Li, Z. Lai, Q. Cao, Investigation of the electromagnetic attractive forming utilizing a dual-coil system for tube bulging, *Journal*

- of Manufacturing Processes. 49 (2020) 102-115.
- [209] E. Thibaudeau, B.L. Kinsey, Analytical design and experimental validation of uniform pressure actuator for electromagnetic forming and welding, *Journal of Materials Processing Technology*. 215 (2015) 251-263.
- [210] Q. Xiong, H. Tang, M. Wang, H. Huang, L. Qiu, K. Yu, Q. Chen, Design and implementation of tube bulging by an attractive electromagnetic force, *Journal of Materials Processing Technology*. 273 (2019) 116240.
- [211] N. Yan, Z. Li, Y. Xu, M.A. Meyers, Shear localization in metallic materials at high strain rates, *Progress in Materials Science*. 119 (2021) 100755.
- [212] H.K. Zhang, H. Xiao, X.W. Fang, Q. Zhang, R.E. Logé, K. Huang, A critical assessment of experimental investigation of dynamic recrystallization of metallic materials, *Materials & Design*, 193 (2020) 108873.
- [213] H. Su, L. Huang, J. Li, W. Xiao, H. Zhu, F. Feng, H. Li, S. Yan, Formability of AA 2219-O sheet under quasi-static, electromagnetic dynamic, and mechanical dynamic tensile loadings, *Journal of Materials Science & Technology*. 70 (2021) 125-135.
- [214] W.B. Zhou, J.G. Lin, D.S. Balint, T.A. Dean. Clarification of the effect of temperature and strain rate on workpiece deformation behaviour in metal forming processes, *International Journal of Machine Tools and Manufacture*. 171 (2021) 103815.
- [215] J. Fang, J. Mo, J. Li, Microstructure difference of 5052 aluminum alloys under conventional drawing and electromagnetic pulse assisted incremental drawing, *Materials Characterization*. 129 (2017) 88-97.
- [216] B.X. Xie, L. Huang, J.H. Xu, Y. Wang, J.J. Li. Microstructure evolution and strengthening mechanism of Al-Li alloy during thermo-electromagnetic forming process, *Journal of Materials Processing Technology*, 315 (2023) 117922.
- [217] Y. Hashimoto, H. Hata, M. Sakai, H. Negishi, Local deformation and buckling of a cylindrical Al tube under magnetic impulsive pressure, *Journal of Materials Processing Technology*. 85 (1999) 209-212.
- [218] D.H. Liu, C.F. Li, H.P. Yu, Numerical modeling and deformation analysis for electromagnetically assisted deep drawing of AA5052 sheet, *Transactions of Nonferrous Metals Society of China*. 19 (2009) 1294-1302.
- [219] S. Gies, A.E. Tekkaya, Analytical prediction of Joule heat losses in electromagnetic forming coils, *Journal of Materials Processing Technology*. 246 (2017) 102-115.
- [220] C. Weddeling, O.K. Demir, P. Haupt, A.E. Tekkaya, Analytical methodology for the process design of electromagnetic crimping, *Journal of Materials Processing Technology*. 222

- (2015) 163-180.
- [221] B. Kinsey, A. Nassiri, Analytical model and experimental investigation of electromagnetic tube compression with axis-symmetric coil and field shaper, *CIRP Annals*. 66 (2017) 273-276.
 - [222] O. Maloberti, O. Mansouri, D. Jouaffre, et al., Analytical design model of coil parameters for the electro-magnetic forming technology-Case of the 1-turn coil dedicated to tubular parts forming and crimping with 1D approximation, *Journal of Materials Processing Technology*. 266 (2019) 450-473.
 - [223] J. Unger, M. Stiemer, B. Svendsen, H. Blum, Multifield modeling of electromagnetic metal forming processes, *Journal of Materials Processing Technology*. 177 (2006) 270-273.
 - [224] J. Li, W. Qiu, L. Huang, H. Su, H. Tao, P. Li, Gradient electromagnetic forming (GEMF): a new forming approach for variable-diameter tubes by use of sectional coil, *International Journal of Machine Tools and Manufacture*. 135 (2018) 65-77.
 - [225] Q. Cao, L. Li, Z. Lai, Z. Zhou, Q. Xiong, X. Zhang, X. Han, Dynamic analysis of electromagnetic sheet metal forming process using finite element method, *The International Journal of Advanced Manufacturing Technology*. 74 (2014) 361-368.
 - [226] M.A. Bahmani, K. Niayesh, A. Karimi, 3D Simulation of magnetic field distribution in electromagnetic forming systems with field-shaper, *Journal of Materials Processing Technology*. 209 (2009) 2295-2301.
 - [227] X. Cui, J. Li, J. Mo, J. Fang, Y. Zhu, K. Zhong, Investigation of large sheet deformation process in electromagnetic incremental forming, *Materials & Design*. 76 (2015) 86-96.
 - [228] K. Sofi, M. Hamzaoui, H. El Idrissi, A.N.S. Moh, D. Jouaffre, A. Hamzaoui, Electromagnetic pulse generator: An analytical and numerical study of the Lorentz force in tube crimping processes, *CIRP Journal of Manufacturing Science and Technology*. 31 (2020) 108-118.
 - [229] D.A. Oliveira, M.J. Worswick, M. Finn, D. Newman, Electromagnetic forming of aluminum alloy sheet: free-form and cavity fill experiments and model, *Journal of Materials Processing Technology*. 170 (2005) 350-362.
 - [230] A. Long, M. Wan, W. Wang, X. Wu, X. Cui, 3D modeling strategies for simulating electromagnetic superposed forming processes, *International Journal of Mechanical Sciences*. 138 (2018) 409-426.
 - [231] X. Cui, Z. Du, A. Xiao, Z. Yan, D. Qiu, H. Yu, B. Chen, Electromagnetic partitioning forming and springback control in the fabrication of curved parts, *Journal of Materials Processing Technology*. 288 (2021) 116889.

- [232] Q. Cao, X. Li, Z. Li, L. Du, L. Xia, Z. Lai, Q. Chen, X. Han, L. Li, Coil-less electromagnetic forming process with uniform-pressure characteristics for shaping sheet metals, *Journal of Manufacturing Processes*. 70 (2021) 140-151.
- [233] P. Jimbert, I. Eguia, I. Perez, M.A. Gutierrez, I. Hurtado, Analysis and comparative study of factors affecting quality in the hemming of 6016T4AA performed by means of electromagnetic forming and process characterization, *Journal of Materials Processing Technology*. 211 (2011) 916-924.
- [234] H. Park, J. Lee, Y. Lee, J.H. Kim, D. Kim, Electromagnetic expansion joining between tubular and flat sheet component, *Journal of Materials Processing Technology*. 273 (2019) 116246.
- [235] J.Q. Tan, M. Zhan, H.W. Li, Dependence on forming parameters of an integral panel during the electromagnetic incremental forming process, *Chinese Journal of Aeronautics*. 31 (2018) 1625-1634.
- [236] Q. Zhang, L. Huang, J. Li, F. Feng, H. Su, F. Ma, K. Zhong, Investigation of dynamic deformation behaviour of large-size sheet metal parts under local Lorentz force, *Journal of Materials Processing Technology*. 265 (2019) 20-33.
- [237] Z.S. Fan, S.T. Huang, J.H. Deng, Cladding of aluminum alloy 6061-T6 to mild steel by an electromagnetic tube bulging process: finite element modeling, *Advances in Manufacturing*. 7 (2019) 73-83.
- [238] X.H. Cui, J.H. Mo, J.J. Li, J. Zhao, Y. Zhu, L. Huang, Z.W. Li, K. Zhong, Electromagnetic incremental forming (EMIF): a novel aluminum alloy sheet and tube forming technology, *Journal of Materials Processing Technology*. 214 (2014) 409-427.
- [239] F. Feng, J. Li, R. Chen, L. Huang, H. Su, S. Fan, Multi-point die electromagnetic incremental forming for large-sized sheet metals, *Journal of Manufacturing Processes*. 62 (2021) 458-470.
- [240] E. Iriondo, J.L. Alcaraz, G.S. Daehn, M.A. Gutiérrez, P. Jimbert, Shape calibration of high strength metal sheets by electromagnetic forming, *Journal of Manufacturing Processes*. 15 (2013) 183-193.
- [241] W. Liu, X.F. Zou, S.Y. Huang, Y. Lei, Electromagnetic-assisted calibration for surface part of aluminum alloy with a dedicated uniform pressure coil, *The International Journal of Advanced Manufacturing Technology*. 100 (2019) 721-727.
- [242] X. Cui, J. Mo, J. Li, H. Yu, Q. Wang, Reduction of springback in V-shaped parts using electromagnetic impulse calibration, *Procedia engineering*. 207 (2017) 801-806.
- [243] X. Cui, Z. Zhang, Z. Du, H. Yu, D. Qiu, Y. Cheng, X. Xiao, Inverse bending and

- springback-control using magnetic pulse forming, *Journal of Materials Processing Technology*. 275 (2020) 116374.
- [244] Z. Du, Z. Yan, X. Cui, B. Chen, H. Yu, D. Qiu, W. Xia, Z. Deng, Springback control and large skin manufacturing by high-speed vibration using electromagnetic forming, *Journal of Materials Processing Technology*. 299 (2022) 117340.
- [245] X. Cui, J. Mo, J. Li, X. Xiao, B. Zhou, J. Fang, Large-scale sheet deformation process by electromagnetic incremental forming combined with stretch forming, *Journal of Materials Processing Technology*. 237 (2016) 139-154.
- [246] J. Imbert, M. Worswick, Electromagnetic reduction of a pre-formed radius on AA 5754 sheet, *Journal of Materials Processing Technology*. 211 (2011) 896-908.
- [247] J. Imbert, M. Worswick, Reduction of a pre-formed radius in aluminium sheet using electromagnetic and conventional forming, *Journal of Materials Processing Technology*. 212 (2012) 1963-1972.
- [248] V. Psyk, C. Beerwald, W. Homberg, M. Kleiner, Extension of forming limits by using a process combination of electromagnetic forming and hydroforming, in: *Proceedings of the 8th International Conference on Technology of Plasticity (ICTP)*, 2005.
- [249] J. Fang, J. Mo, X. Cui, J. Li, B. Zhou, Electromagnetic pulse-assisted incremental drawing of aluminum cylindrical cup, *Journal of Materials Processing Technology*. 238 (2016) 395-408.
- [250] J.C. Du, J.M. Rimsza, Atomistic computer simulations of water interactions and dissolution of inorganic glasses, *Materials Degradation*. 1 (2017) 16.
- [251] S.T. Zhao, R.P. Zhang, Q. Yu, J. Ell, R.O. Ritchie, A.M. Minor, Cryoforged nanotwinned titanium with ultrahigh strength and ductility, *Science*. 373, (2021) 1363-1368.
- [252] <https://www.compsmag.com/article/factory-monitoring-how-it-works/>
- [253] <https://webinars.sw.siemens.com/en-US/digital-twin-in-manufacturing/#form>
- [254] H. Yang, H. Li, H. Sun, Y.H. Zhang, X. Liu, M. Zhan, Y.L. Liu, M.W. Fu, Anisotropic plasticity and fracture of alpha titanium sheets from cryogenic to warm temperatures, *International Journal of Plasticity*, 156 (2022) 103348.
- [255] H. Li, F.Z. Jin, M.Y. Zhang, J.H. Ding, T.J. Bian, J.H. Li, J. Ma, L.W. Zhang, Y.F. Wang, Decoupling electroplasticity by temporal coordination design of pulse current loading and straining, *Materials Science and Engineering: A*. 881 (2023) 145435.

Declaration of interests

- ☒ The authors declare that they have no known competing financial interests or personal relationships that could have appeared to influence the work reported in this paper.
- ☐ The authors declare the following financial interests/personal relationships which may be considered as potential competing interests: